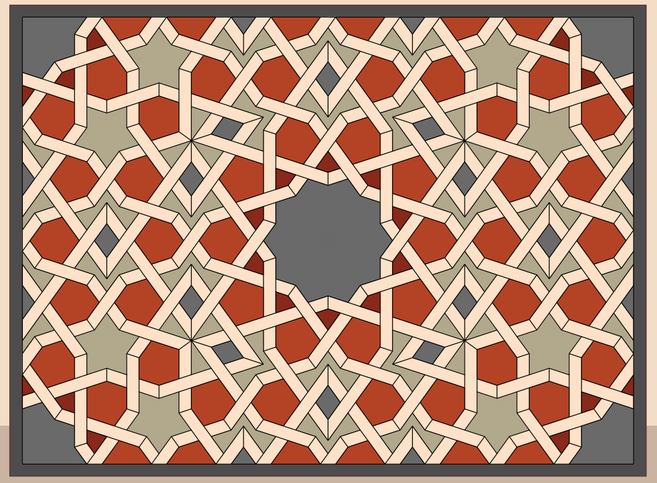

Research Journal of Mathematics and Technology, Volume 15, Number 1, 2026

Research Journal of Mathematics & Technology

ISSN 2163-0380

Vlume 15, Number 1, 2026

Research Journal of Mathematics & Technology

Volume 15, Number 1

ISSN 2163-0380

June 2026

RJMT Editorial Board

Web site: http://rjmt.mathandtech.org/
Published by:

Mathematics and Technology, LLC
PO Box 215
Welcome, NC27374-0215, USA

Foreword

We hope that you, as friends and colleagues, along with your families and your loved ones, are all in good health and good spirits.

The Research Journal of Mathematics and Technology (RJMT) is a printed forum for the publication of selected papers from the Electronic Journal of Mathematics and Technology (eJMT: http://ejmt.mathandtech.org/). One of eJMT's goals is to publish peer-reviewed papers demonstrating how "technology" can be utilized to make mathematics and its applications fun (F), accessible (A), challenging (C), and theoretical (T).

The first four papers of this issue are from the October 2025 eJMT issue. The last two are from the February 2026 eJMT issue. As you read these six papers, you will see discussions of different areas of mathematics using various technologies. There are several papers exploring the innovative use of technological tools in discovering mathematics. We hope these creative ways of experimenting with mathematics will be beneficial to you and your students. As you do so, we encourage you to write about your experiences for future issues of eJMT. Instructions for preparing and submitting papers to eJMT can be found online at https://ejmt.mathandtech.org/SubmissionGuidelines.html.

As this edition of RJMT is being prepared, we are planning the 31st ATCM (Asian Technology Conference in Mathematics: https://atcm.mathandtech.org/) to be held in hybrid format from December 12-15, 2026, which is to be held at the University of Coimbra, Department of Mathematics, Portugal. Thank you all for your continued support of eJMT, RJMT, and ATCM.

Mirosław Majewski
Guest Editor

Wei-Ch Yang
Editor-in-chief

TABLE OF CONTENTS

A Research on the Effects of Using 3D Dynamic Geometry Software as Learning Material of the Cross-Section of a Cube for Junior High School Students

Makoto HANDA
e-mail tjk_handa@tjk.jp
Tokyo Jogakkan Middle & High School, Japan

Abstract

Since 2022, one ICT device per student has been available at junior high schools in Japan. However, the use of ICT in mathematics education in Japan is still low. In this research, we asked first-year junior high school students to consider the cutting plane of a cube using 3D dynamic geometry software in the teaching of spatial figures. We confirmed that the students' knowledge and skills of the cubic cutting plane improved when they operated the 3D dynamic geometry software independently while consulting with each other. On the other hand, regarding students' development of "thinking, judgment, and expression skills" we found that the students were visually misled at the stage of drawing 3-D figures on a flat surface.

1 Introduction

In the research of figures in the mathematics department of junior high schools in Japan, 3-D figures are mainly taught in the first grade of junior high school. The Courses of Study for Junior High Schools published in 2017 demands students to acquire some aims. It defines the aim of knowledge and skills as understanding the positional relationship of lines and planes in space. Also, it defines the aim of thinking ability as finding the nature of 3-D figures and expressing them on the plane by themselves. ([7], p.78)

1.1 Mathematics instruction in a one-student-one-unit environment

The Japanese Ministry of Education, Culture, Sports, Science and Technology (MEXT) initially planned to achieve a goal of one ICT device per student by 2023. Due to the Covid pandemic, the learning environment that promotes achieving this goal was established at all junior high schools nationwide rapidly. ([8], p.4). However, ICT has not been utilized in mathematics classes in Japan.

The first supplementary budget for FY2009 and other measures increased the penetration rate of electronic blackboards in public schools, and "there is an undeniable sense that the improvement of mathematics teachers' instruction using ICT has shifted from the effective use of digital teaching materials such as learning materials and software to the improvement of instruction through the use

of electronic blackboards as presentation devices." ([18], p.2), Yasuno (2019) points out. Even in an environment in which each student has one terminal, the use of ICT by mathematics teachers is still not active.

Tani and Yanagimoto (2017) note that "in Japanese secondary education, there are very few situations in which ICT is used in textbooks, and the types of ICT handled are very few. ([15], pp.18-19). Although, in Japan, practical research on mathematics education using graphing calculators has been conducted since the 1990s. Onishi (2015) points out that "Japan is one of the world's leading countries in the production of ICT equipment, but the reality is that ICT equipment is rarely utilized in mathematics classes."([12], pp.77-78)

However, by 2022, a learning environment where each student has one ICT terminal has been established nationwide. It is about time mathematics teachers in Japan utilized ICT as a material that makes students learn mathematics effectively. Until 2000, it had been hard for students to understand some figures especially 3D figures, by using ICT applications. After 2010, ICT function has improved, and 3D figures are operated easily on ICT. Therefore, this research examines the effectiveness of using ICT, focusing on the instruction of 3D figures.

1.2 Considerations for teaching 3D geometry and the use of ICT

Kinoshita et al. (2020) analyzed the solution strategies of learners who solve 3-D figure tasks using three media (real objects, tablets, and paper), not only through behavioral observation, but also through experiments measuring brain activity and eye movement. As one of the results, they point out that "we need to be very careful about teaching methods that easily use tablet materials as a substitute for real materials" ([4], p.96). However, Kinoshita et al. (2020) did not clarify what kind of tablet materials were used in their research.

Aoki et al. (2021) clarified the process of learners' problem solving when performing a cube cutting task by measuring their eye movement. As one of the results, they revealed that "the wrong answers show difficulty in identifying a point that is not visible" ([1], 2021, p.128). From this point of view, "it is important to combine the enhancement of opportunities for manipulative activities using 3D teaching materials and 3D teaching materials using tablets, etc., depending on the situation" ([1], pp.128-129).

Yamada and Tsukamoto (2012) noted that by utilizing ICT in the teaching of cube floor plans, "the students were able to break free from the biased viewpoint that they had been able to see only from a certain direction by understanding that the viewpoint could be moved by the computer." ([16], p.43) and "the activity to confirm the change of viewpoint by computer was effective" ([16], p.43). However, they do not mention instruction regarding the cutting plane of the cube.

Iijima (2021) states that "when the subject is considered to be the students or a group of students, learning in which ICT is positioned as a tool for activating inquiry and dialogue should be given equal or greater importance than passive learning" ([2],p.22). author think that the aim is to encourage dialogue with others through the use of ICT and to have students explore the nature of mathematics.

Shimizu and Kakihana (1999) stated that teaching students to draw their own diagrams using Cabri, a graphic learning software, "is an effective method that leads to independent learning." ([14], pp.56-58). This is a research of drawing instruction of plane figures, but it does not mention whether the use of ICT in teaching 3-D figures also fosters students' independent learning attitudes.

Juandi et al. (2021) analyzed the effectiveness of Dynamic Geometry Software (hereinafter referred to as the DGS) by reviewing various research papers on mathematics learning. As a result,

Juandi et al. (2021) state ”The results of the analysis reveal that the use of DGS has a high positive impact on students' math abilities.” ([3], p.29). In mathematics education in Japan, the use of ICT to develop lessons that investigate mathematics is still not very active, but it is clear that mathematics learning using DGS is an approach that is needed even from an international perspective.

Marasabessy and Helsa (2024) claim ”This present study has estimated that the utilization of GeoGebra software in geometry lesson provides positive strong effect toward the cultivation of spatial visualization of students. Moreover, it can be justified that significantly GeoGebra-assisted geometry lesson cultivates students' spatial visualization skills.” ([6], pp.11-12). However, if the use of GeoGebra can help to improve spatial visualization capabilities, we believe that it can also be used in the consideration of cubic cut surfaces.

2 Purpose of the research

In Japanese mathematics textbooks, there is a lesson called ”B Figures”. It aims for first-year junior high school students to understand the positional relationship of lines and planes in space and to calculate the surface area and volume of a solid object, (see [9], p.4). Since1998, the treatment of the cutting surfaces of cube was removed.

2.1 Purpose of this research

In the Courses of Study published in 2017, the content for the first grade lists ”knowing the positional relationship of lines and planes in space” in terms of knowledge and skills as one of the matters to be acquired through mathematical activities related to spatial figures ([7], p.78). As part of this ”knowing the positional relationships of lines and planes in space”, students are required to ”know the positional relationships of lines and planes in space”. we focused on considering the cutting plane of a cube. Cutting cubes is not covered in the 2017 Courses of Study. Although it was once considered too difficult to handle and was reduced in the past, the author thought that it would be possible to study the cutting plane of a cube using ICT.

In this research, ICT is used in the mathematics classroom to encourage students to intuitively grasp numbers and perform exploratory activities related to the cutting plane of a cube. Specifically, first-year junior high school students are taught about cubic cutting planes using DGS. ICT is used instead of relying on manipulative activities with 3D models when thinking about cubic sectional planes. If the learning effect can be demonstrated in a class using GeoGebra Classic Ver.6.0718(hereinafter referred to as GeoGebra) as a 3D-DGS, ICT can be used in mathematics education in Japan. If we can demonstrate the learning effects of teaching using 3D-DGS, we can show the necessity of using ICT in mathematics education in Japan for further exploration and consideration of mathematics. We believe that the importance of this research can be demonstrated.

Before conducting this activity, we will conduct a pre-survey to assess students' understanding of the section plane of a cube. Then, a post-survey will be administered after the class has practiced using 3D-DGS. In the post-survey, students will be asked to work on problems similar to those in the pre-survey to see if their understanding of cubic cutting planes has deepened. The results of the pre-survey and post-survey are compared quantitatively. The purpose of this comparison is to see if students' understanding of the cubic section plane is improved by having them manipulate the 3D-DGS independently. In addition, we will qualitatively examine whether there was a change in

students' attitudes toward learning about the cubic section plane, based on students' presentations through the mathematical activities and their impressions after the class.

3 Research Methods

This research was conducted from late September to early October 2023 for approximately two weeks, five hours per week. The school where the research was conducted mainly used a non-examined textbook, "Systematic Mathematics 1 Geometry" (hereafter referred to as "Systematic Mathematics"). In this practice, the latter two hours were used for worksheets (hereinafter referred to as "WS").

3.1 Target students

The target students were a total of 77 students in two first-year junior high school classes at a private integrated girls' junior and senior high school in Tokyo, Japan. Both classes were organized so that there would be no bias in academic ability based on the results of an entrance examination. When students enroll in the school, their parents or guardians give written consent for them to participate in the recording and presentation of their learning activities. Therefore, there are no ethical problems.

Each year, an iPad is purchased for each student as they enter their first year of junior high school. In the year 2023 students who entered the school purchased an Apple iPad, 9th Generation Wi-Fi model A2602. The iPads are kitted out with the necessary applications installed and configured for easy use within the school. Each student who will be using the dynamic geometry software also owns one of these iPads. Microsoft Teams (hereinafter referred to as "Teams") and GeoGebra are installed on them. In this practice, we will use GeoGebra as the 3D dynamic geometry software. In addition, author will use Teams to share files of teaching materials and to encourage students to respond to questionnaires.

3.2 Class Flow

In the class, "Systematic Mathematics" was used. Chapter 2, "Spatial Figures," was taught in the following order: Section 1, "Various solids," Section 2, "Planes and lines in space," and Section 3, "Various ways of looking at solids. Section 3 deals with the cross-section of a cube. In the text of the textbook, it is only described in half of a page.

Before beginning the instruction on the cross-section of a cube, the students are asked to answer six questions on the cross-section of a cube in a quiz. This was a pre-survey, and the students had about 10 minutes to answer the questions. The teacher then gave explanations and had the students grade their own answers, and collected them. In the WS, author shared the GeoGebra file (Figure 1) prepared by the author in advance on Teams, and each student downloaded the file and manipulated it on her own terminal to examine it. After the WS instruction, a quiz (6 similar questions about the cross-section of a cube) was given again. This was a post-survey, and the students had about 10 minutes to answer the questions. The teacher gave explanations and allowed the students to grade themselves, and then collected the answers. Finally, the students were asked to give their impressions of the class on cubic sections. The students were asked to fill in their impressions by answering a questionnaire on Teams during class time.

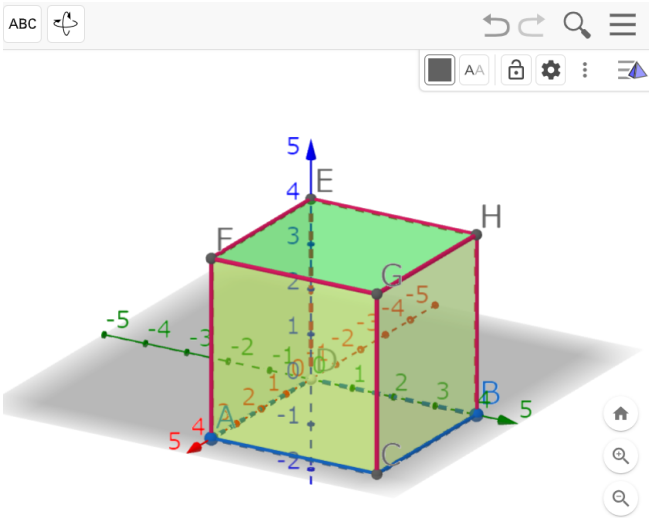

Figure 1: Cube shared in Teams

3.3 Methods of Verification

The purpose of this research is to verify the objectives of Chapter 2 by comparing the results of the pre-survey and the post-survey. We will quantitatively confirm whether the number of correct answers in the pre- and post-survey quizzes increases. In addition, author will analyze the questionnaires administered after the exercise. The questionnaire was developed based on the one used in a previous research by Shimizu and Kakihana (1999), which asked for responses to 1 to 12 items using a five-item method. Students' self-evaluations of "independent learning attitude," "thinking, judging, and expressing," and "knowledge and skills" were examined. By examining the average of the students' self-evaluations, author can verify their "independent learning attitude", "thinking, judgment and expression", and "knowledge and skills".

At the end of the questionnaire, the students were asked, "Please tell me what you think was good and what you regret about studying the cubic section." The results of the free-response section of the questionnaire, as well as the statements made by the students during the lessons using the WS, will be qualitatively verified. The GeoGebra files submitted by the students will also be referenced where appropriate.

The questionnaire was distributed through Forms, an application on Teams, with the questions shown in the attachment at the end of this document, and participants were instructed to answer the questions individually.

4 The worksheet in practice

In this practice, after teaching the aforementioned Chapter 2 of "Systematic Mathematics" in the order of Sections 1 and 2, we prepared and conducted a workshop on the cross-section of a cube in Section 3.

In the pre- and post-survey questions and the WS questions, the students were asked to specify the three points through which the cut plane passes, based on the cube treated in the previous research by Aoki et al. A research by Aoki et al. (2021) revealed that "misrespondents show difficulty in

identifying points in invisible positions" ([1], p. 128). In the WS, Question 1, which was used as an example, did not include a question that required the identification of a point located in an unseen position. The cross-section of [Q3] is the same as the one in the textbook. The cross-section in [Q3] is an applied question that is not covered in textbooks. Therefore, author did not ask a question that requires the identification of a point located in an unseen position because author considered it difficult to predict the cross-section. In addition, three questions were prepared for each of the WS questions [Q1] to [Q3], (1) to (3), respectively. The shape (1) is drawn in GeoGebra, and the shape (2) and (3) appear by dragging and moving the three points through which the cut plane passes. This was also explained as an example in [Q1].

4.1 Activities with GeoGebra (Part 1)

The first pre-survey question was explained in the form of a self-assessment. The explanation was given with chalk on the blackboard, without using ICT. Next, the explanation was given using the 3D application function of GeoGebra with WS. [Q1] explained how to draw a plane passing through the three points P, Q, and R based on the file shown in Figure 1. After explaining (1), (2) and (3) showed how the cutting plane changes by dragging and moving the three points P, Q, and R. However, (3) was not shown. However, (3) was explained in the form of sharing the screen that the students were exploring in Figure 2. We used a projector that could be projected on the side of the blackboard in the classroom, and the students' screens were shared using an AppleTV installed in the classroom, displaying the students' terminal screens. Figure 2 shows that the students changed their viewpoints to confirm the shape of the cross-section, and also made efforts to make the colors easy to see. The following is the interaction with the students during the sharing: T is the teacher's question, S_i is the student's comment, and the operation of the application is shown in parentheses.

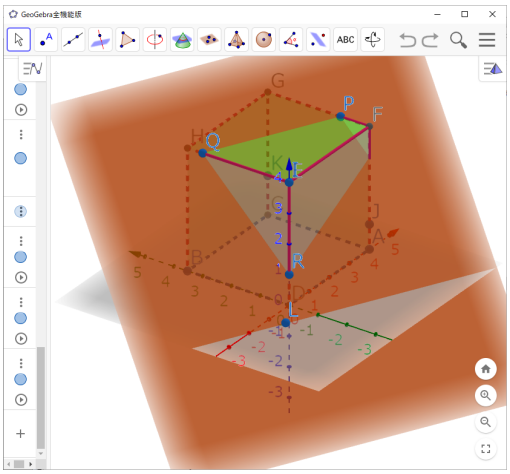

Figure 2: Student's work file for [Q1] (3)

T： What shape is this cross-section?
S_1： It is a trapezoid.
T： What kind of trapezoid is it?
S_1： It is an isopod trapezoid.
T： Which side is equal to which side?

S_1： (moves GeoGebra to change the viewpoint of the cross-section)
T： The lengths of the sides extending from PQ and R are equal.

4.2 Activities with GeoGebra (Part 2)

The students were asked to investigate [Q2] and [Q3] using the 3D application feature of GeoGebra. They consulted with other students and taught each other during their investigations. We aimed for the kind of learning that activates inquiry and dialogue as claimed by Iijima (2021) by considering the student group as the main subject and using ICT as a tool. However, we were not able to confirm [Q2] and [Q3] in one class period, so we decided to continue the work in the next class period.

The following is an exchange with a student who shared the screen of [Q2].

T： What shape is this cross-section?

S_2： It is a hexagon.

T： What kind of hexagon is it?

S_2： (Adjust the position of points P, Q, and R to the midpoints of the sides and change the viewpoint to a position that is easier to see)

T： It looks like a regular hexagon. The visible edges on each side are the same length. Can you transform it into (2)?

S_2： (The position of P does not seem to move well. The student will open another file and show her classmates.)

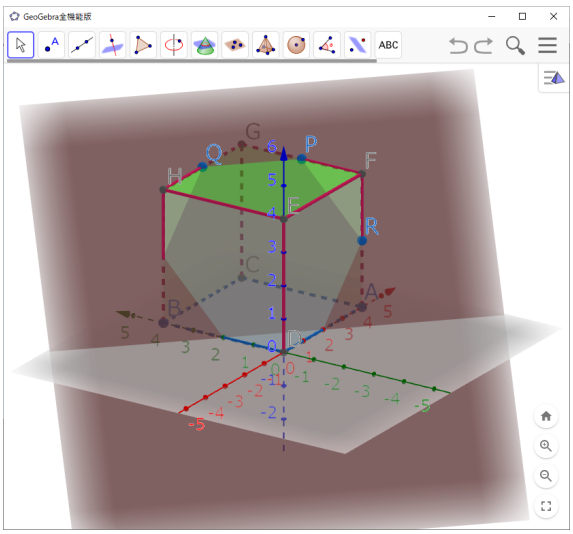

Figure 3: Student's work file for [Q2] (1)

The teacher also shared the students' screenshots of [Q3] and reviewed them, and a post-assessment quiz was given at the end of the second period. The teacher also explained the post-survey quiz to the students and had them grade their own answers and then collected them. Both the pre-survey and post-survey quizzes were administered without the use of ICT. The schools in which author conducted the tests did not require the use of ICT, so author did not use ICT for the quizzes in this practice either.

5 RESULTS

This section reports the results of the pre- and post-survey questions, as well as the classroom situation and the results of the questionnaire.

5.1 Pre and Post Survey Results

The pre-survey and post-survey questions are listed in the Appendix at the end of this report. ”Cutting planes of a cube (Part 1)” is the pre-survey question and ”Cutting planes of a cube (Part 2)” is the post-survey question. Each survey consists of six questions. Each question asks the participants to draw a cutting plane through the three points P, Q, and R on the edge of the cube (hereinafter referred to as the Fig.) and to name the shape of the cutting plane (hereinafter referred to as the C-S). The author thought that questions (1) to (5) would be improved in the later part of the test, since the tendency of the questions is the same in the pre- and post-tests. Question (6) was asked to see if it could be applied to the pre- and post-tests since the tendency of this question was different between the pre- and post-tests. Of the 77 students, 73 students who took both the pre- and post-tests were analyzed. Scoring was based on a binary score of 1 correct or 0 incorrect, with no subscores. The percentage of correct answers for each of these questions is shown in Figure 4. Table 2 shows the 2×2 crosstabulations and odds ratios of correct and incorrect answers for each question, pre- and post-test. The numbers in the ”Number of correct/incorrect answers” column indicate the number of respondents, and the percentages are shown in parentheses. Although the total number of samples exceeded 50, many of the samples in each cell were less than 50, so Fisher’s exact test was performed in R. 4.1.2.([13]) The coefficient of correlation (V) was also examined as an effect size. The table 1 of Yanagawa (2023) was used as the index for determining Cramer’s coefficient of correlation. ([17], p.126).

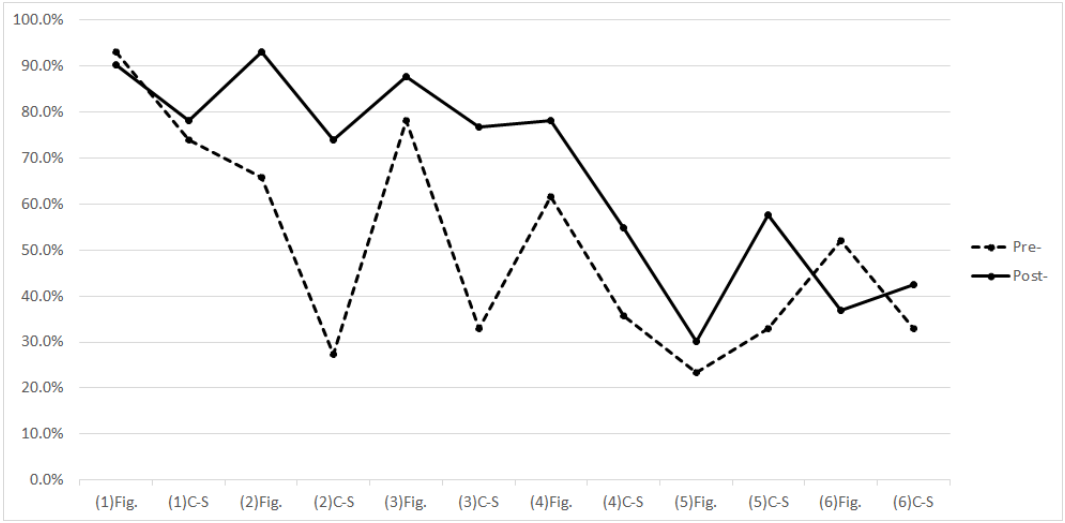

Figure 4: Scoring results of pre- and post-survey questions

Table 1: Index for determining Cramer's linkage coefficients

Cramer's V	Strength of a linkage
0〜0.1	Very weak
0.1〜0.25	Weak
0.25〜0.5	Medium
0.5〜1.0	Strong

Table 2: Crosstabulation Tables and Odds Ratios

Question	pre-responses		post-responses		Odds ratio	Odds 95% CI
	Correct	Incorrect	Correct	Incorrect		
(1)Fig.	68(93.2%)	5(6.8%)	66(90.4%)	7(9.6%)	1.442	[0.436 , 4.773]
(1)C-S	54(74.0%)	19(26.0%)	57(78.1%)	16(21.9%)	0.798	[0.372 , 1.709]
(2)Fig.	48(65.8%)	25(34.2%)	68(93.2%)	5(6.8%)	0.141	[0.050 , 0.395]
(2)C-S	20(27.4%)	53(72.6%)	54(74.0%)	19(26.0%)	0.133	[0.372 , 1.709]
(3)Fig.	57(78.1%)	16(21.9%)	64(87.7%)	9(12.3%)	0.501	[0.205 , 1.221]
(3)C-S	24(32.9%)	49(67.1%)	56(76.7%)	17(23.3%)	0.149	[0.072 , 0.309]
(4)Fig.	45(61.6%)	28(38.4%)	57(78.1%)	16(21.9%)	0.451	[0.218 , 0.934]
(4)C-S	26(35.6%)	47(64.4%)	40(54.8%)	33(45.2%)	0.456	[0.235 , 0.887]
(5)Fig.	17(23.3%)	56(76.7%)	22(30.1%)	51(69.9%)	0.704	[0.336 , 1.472]
(5)C-S	24(32.9%)	49(67.1%)	42(57.5%)	31(42.5%)	0.362	[0.184 , 0.709]
(6)Fig.	38(52.1%)	35(47.9%)	27(37.0%)	46(63.0%)	1.850	[0.955 , 3.582]
(6)C-S	24(32.9%)	49(67.1%)	31(42.5%)	42(57.5%)	0.664	[0.338 , 1.302]

Table 3: Results of Fisher's exact test

Question	Cramer's V	p-value	95% CI
(1)Fig.	.050	.765	[0.372 , 6.053]
(1)C-S	.048	.699	[0.345 , 1.831]
(2)Fig.	.339	$< .01^{**}$	[0.040 , 0.416]
(2)C-S	.466	$< .01^{**}$	[0.060 , 0.293]
(3)Fig.	.127	.187	[0.181 , 1.321]
(3)C-S	.440	$< .01^{**}$	[0.067 , 0.327]
(4)Fig.	.179	$.047^{*}$	[0.202 , 0.989]
(4)C-S	.193	$.030^{*}$	[0.222 , 0.934]
(5)Fig.	.077	.455	[0.313 , 1.567]
(5)C-S	.248	$.005^{**}$	[0.174 , 0.747]
(6)Fig.	.152	.096	[0.908 , 3.780]
(6)C-S	.099	.306	[0.320 , 1.373]

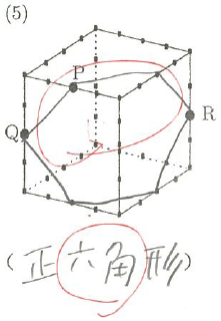

Figure 5: Example 1 of the incorrect answers in the post-survey (5)

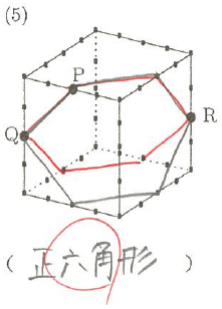

Figure 6: Example 2 of the incorrect answers in the post-survey (5)

Table 4: Number of correct and incorrect answers for (5) figure

	pre-	post-
correct answer	17(23.3%)	22(30.1%)
wrong answer 1	18(24.7%)	23(31.5%)
wrong answer 2	38(52.1%)	28(38.4%)
計	73	73

(2)Fig. shows the effect size ($V = .339$), which is moderately correlated. The odds ratio was 0.141 (95% CI [0.050, 0.395]), and the Fisher's test showed a significant difference ($p < .01$). Similar results were found for (2)C-S and (3)C-S. Although the effect sizes ($.179, .193, .248$, respectively) were weak for (4)Fig, (4)C-S, and (5)C-S, the odds ratios were 0.451 (95% CI [0.218, 0.934]), 0.456 (95% CI [0.235, 0.887]), and 0.362 (95% CI [0.184, 0.183 CI [0.184, 0.709]), respectively, and the Fisher's test showed a significant difference ($p < .05$).

As for (5), a significant difference ($p < .05$) in the percentage of correct responses was observed for the (5)C-S, but no difference was observed for the (5)Fig., and even in the post-survey, such incorrect responses as in Figure 5 and Figure 6 were noticeable. The student in Figure 5 did not even notice her error when she scored herself and gave the correct answer. The table 4 summarizes the results of the responses in (5)Fig. The numbers in brackets indicate the number of respondents, and the percentages are given in brackets. Incorrect answer 1" in the table refers to the incorrect answers such as "Figure 5" and "Figure 6". "Incorrect answer 2" represents other incorrect answers.

5.2 Comparing Worksheet Practice with Pre and Post Surveys

Problems like the pre- and post-survey problem (5) are addressed in WS Q2(1), as introduced in the 4.2 section. The fact that the cross-section is a regular hexagon was confirmed by the fact that the lines on each side are diagonals of a right-angled isosceles triangle. Correct answers were checked by moving the viewpoint while sharing the work files of the correct answers (Figure 3). The students who were able to confirm that the cross-section was a regular hexagon using GeoGebra, as shown in Figure 3, were 38 out of 77 students, or about half.

When the students in Figure 5 were asked to consider Question 2(1) of the WS, they were also able to check the cross-section in the file, as in Figure 7, and sketched the correct cross-section. However, in the post-test question, she wrote ”Wrong Answer 1”. Thus, there were several students who sketched ”Wrong Answer 1” on the post-question, even though they were able to check the correct cross-section in the file. in the post-survey question, even though they were able to check the correct cross-section of WS Q2(1) using GeoGebra. This was the case for 9 out of 73 students.

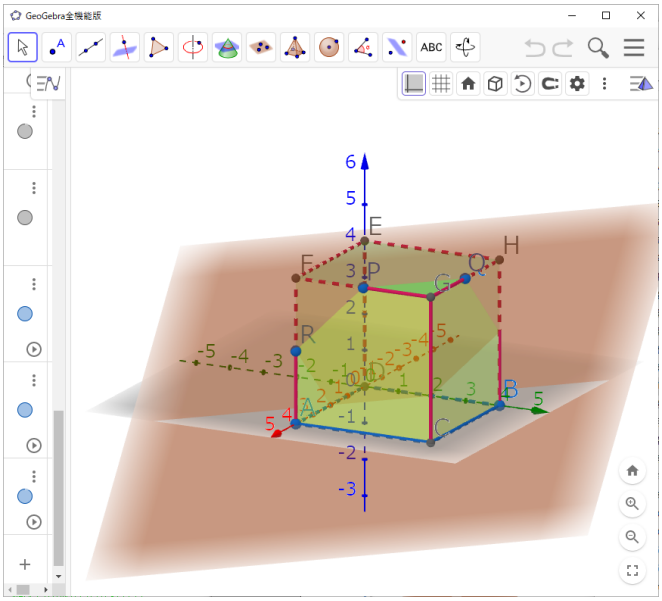

Figure 7: WS Q2(1)

5.3 Results of the Questionnaire

The questionnaire was administered to 77 target students in the form of a questionnaire with their names written on it and answered from Forms. The response period was from October 2 to October 11, 2023, after the second period of this practice. 68 students responded (93.2% response rate) within this period.

5.3.1 Multiple Choice Questionnaire Results

In the multiple-choice questionnaire, students self-rated their attitudes toward ”independent learning,” ”thinking, judging, and expressing,” and ”knowledge and skills” on a 5-point scale from 1 to 5, where the higher the number, the more they self-rated that they had achieved the goals of the class. The average rating for each item is shown in Table 5. The correspondence between the perspectives of ”independent learning attitude,” ”thinking, judging, and expressing,” and ”knowledge and skills” and the question items is shown in Table 6. The results of the questionnaire are shown in Figure 8

Table 5: Means for each question

No.	Mean of evaluation	No.	Mean of evaluation
1	4.29	7	4.50
2	4.12	8	4.24
3	4.25	9	4.65
4	4.44	10	4.44
5	2.63	11	4.47
6	4.40	12	4.01

Table 6: Correspondence between perspectives and questions

Perspective	Item No.	Mean
independent learning	1,4,5,6,11,12	4.04
thinking, judgment, and expression	7,8,9	4.46
knowledge and skills	2,3,10	4.27

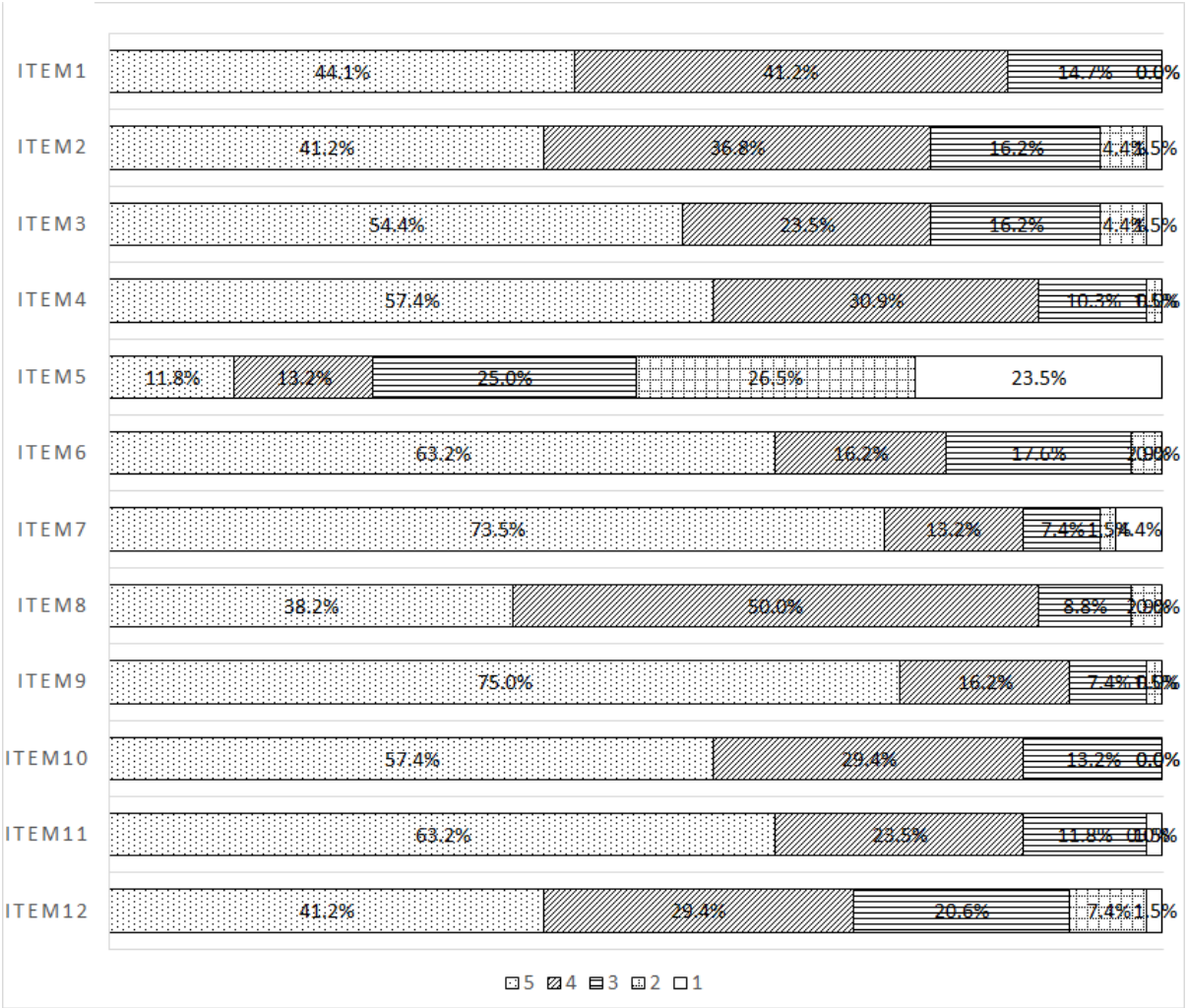

Figure 8: Results of the multiple-choice questionnaire

5.3.2 Results of Descriptive Questionnaire

Question 13 asked students to write free-response answers to the question, ”Please tell me what you think was good and what you regret about the study of cubic section planes.” The results were analyzed using R ver. 4.1.2. ([13]) with the RMeCab package ver. 1.07 ([10]). 68 responses were analyzed using morphological analysis to break them down into word units, and the following four nouns were noted as frequently used by the author. The noun ”GeoGebra” was used in 40 cases, ”cutting plane” in 24 cases, ”understanding” in 19 cases, and ”friend” in 17 cases. The most frequently used adjectives were ”easy” (29), ”good” (19), and ”fun” (7). As verbs, ”can” and ”understand” were used in 47 and 23 cases, respectively. This analysis was conducted using Kobayashi’s (2020) function for creating a KWIC concordance ([5], pp.123-124). Based on these words that we focused on, the following are examples of how students may have collaborated with others and considered them through a trial-and-error process.

- I had a lot of fun learning by thinking creatively with my friends, and I gained a deeper understanding of cross-sections and was very happy when I completed the figure.
- I was able to understand the diagrams while looking at the printouts, but I couldn’t present them, so I will have the courage to do so next time.
- I was able to concentrate on the work in cooperation with my friends. Even if I didn’t know how to do spatial graphics, I could understand by listening to my friends’ presentations and we were able to teach each other.

In addition, several impressions were mentioned that showed an improvement in students’ motivation to learn through ICT-supported instruction. The important ones are listed below.

- It was easier to understand when I practiced with GeoGebra than when I explained orally, so I would like to continue to use GeoGebra for problems involving figures.
- It was fun to use GeoGebra for cross-sectional drawings, as if I was doing crafts. I also wanted to review it by myself because I was interested in it.
- It was convenient to use GeoGebra because I could easily see the cut surface. I would like to try many other things.
- GeoGebra was easy to solve because I could see the figure from various angles. However, I could not fully remember how to operate it, and I had to ask my friend many times.

Finally, several students commented that their understanding of the cross-section of a cube was deepened. The important comments are listed below.

- I have always had a hard time understanding 3-D cutting. However, thanks to the teacher’s clear explanations, I was able to understand it. I was able to deepen my understanding further by studying with GeoGebra.
- This time, I was not good at cutting cross-sections, but I was able to deepen my understanding by listening to my friends and the teacher.

- I could not see the actual cube from many angles just from the textbook, so GeoGebra allowed me to see it from above and below, and I could color the cross-sectional shapes so I could learn more about the shapes of the cut surfaces.
- Using the iPad, I was able to move the figure freely and see the cut surface, which was something I couldn't understand just by writing it in my notebook, so it became very easy to imagine.

6 Considerations

6.1 Discussion of the Pre and Post Surveys

Half of the 12 questions showed a learning effect in 6 of the 12 questions. Based on the results of the 5.1 section, it is assumed that the learning effect was observed in the understanding of (2)Fig. and (2)C-S. The same is true for (3)C-S, (4)Fig. It can be considered that the 3D-DGS is useful for improving students' understanding of the cross-section of a cube.

The following is a discussion of the questions for which no significant differences were found. The percentage of correct answers to question (1) in Figure 4 indicates that both the pre and post difficulty levels of Figure 4 and C-S were similarly superior to each other. (3)Fig., the only difference was the orientation of the cut surface. Therefore, author do not believe that there was any difference between the pre and post test. Question (6) was an applied problem with a different trend between pre and post, and therefore there was no significant difference in the percentage of correct answers.

The percentage of correct answers in (5)Fig. increased after the test. However, the number of incorrect answers, as in Figure 5 and Figure 6, is about the same as the number of correct answers, as shown in the Table 4. This may be due to students being visually confused. To solve this problem, it is possible to consider teaching materials other than ICT. For example, it may be necessary to consider using a 3D printer to produce 3D model materials.

6.2 Considerations from the Questionnaire

The results of the multiple-choice questionnaire in Table 5 show that the average score for all items is 4.00 or higher, except for question 5. The answer to question 5, "Were you willing to make a presentation in class about the drawing?", which asked about "independent learning attitude", had a mean of 2.63, which was lower than the other items. Therefore, the mean of the overall rating of "independent learning attitude" in the table was 4.04, which was slightly lower than the other two perspectives.

From the comments in the descriptive questionnaire in the comments in section 5.3.2 such as "Listening to my friends' presentations was very good because I could understand them and we could teach each other" and "I felt a sense of accomplishment by discussing opinions with my friends and creating a cross-section" indicate that the use of ICT, as pointed out by Iijima (2021), promoted dialogue with others and allowed students to explore the properties related to mathematics. author believe that the use of ICT, as pointed out by Iijima (2021), promoted dialog with others and allowed students to explore the nature of mathematics. In addition, there were some reflections on question 5, "Did you try to present your drawings willingly in class?". Students were encouraged to explore the nature of mathematics through the use of ICT. The students' comments such as "I would like to have

the courage to make a presentation in the next class" indicate that they would like to improve their attitudes towards learning in the future.

The comments in section 5.3.2 also show an increase in students' motivation to use ICT in their future studies. The comments in the descriptive questionnaires show that students are actively using ICT to think through trial and error and to develop new ways of expressing themselves.

The word "understanding" was used positively in 19 of the comments in the descriptive questionnaire, including the one presented here. Comments such as "Studying with GeoGebra helped me deepen my understanding" and "Being able to move the figure freely and see the section plane made it much easier for me to imagine" were representative of these comments. The students' impressions also confirmed the reason for the improvement in the percentage of correct answers in the post-survey questions.

7 CONCLUSIONS

This research was conducted by having students independently manipulate the 3D-DGS to investigate cubic cutting planes. The goal was to confirm that students' understanding of and attitudes toward learning about cubic sectional planes improved as a result of this activity.

7.1 Effects of Using the 3D-DGS

The results of the pre- and post-surveys (2) to (4) show that the number of correct answers increased significantly for 6 out of 12 questions (Table 3), which was half of the total. This result quantitatively confirms that the learning activity using 3D-DGS by WS was effective in deepening students' understanding of the cubic section plane. While there was no difference between the pre- and post-assessment for simple questions such as (1), students were able to develop the ability to identify points located in invisible positions as in questions (2) to (4).

In question (5), there was no significant difference in the increase in the number of correct answers. The reason for this is that, as discussed in section 5.2, there were several participants who gave incorrect answers, such as Figure5 and Figure6, even though they could identify the correct cross-section in 3D-DGS, as shown in Figure7 (see Table 4). These errors may be due to the fact that students were visually misled at the stage of drawing the 3-dimensional figure on the plane, even though they were able to correctly observe the cross-sectional view using ICT. Aoki et al. (2021) pointed out that "the enhancement of opportunities for manipulative activities using 3D learning materials and the combination of 3D learning materials using tablets, etc., depending on the situation" ([1], p.129) should also be considered. In the future, we would like to consider developing 3D learning materials using 3D printers, etc., which have recently become more convenient to use.

7.2 Teaching Practice and Students' Impressions

In the WS, students exchanged opinions with each other using the 3D-DGS and changed the viewpoints and color of the cross-sections through a trial-and-error process. The use of ICT, as pointed out by Iijima (2021), encouraged dialog with others and allowed students to explore the nature of mathematics. Several student comments such as "I was able to deepen my understanding" and "It became easier to imagine the cutting plane" were also noted. The results of the pre- and post-surveys

confirm that the students themselves felt that their understanding of the cutting plane of the cube had improved.

7.3 Conclusion

The use of ICT to examine the cross-section of a cube in the study of spatial geometry was found to improve students' understanding, and the use of ICT in mathematical activities was found to be effective in stimulating students to interact with others and to explore the properties of spatial geometry. In addition to the quantitative improvement in performance on the survey questions, several students indicated that their understanding had deepened. Changes in motivation to learn were also observed, such as "I am more interested" and "I want to try other things". The importance of using ICT as a tool for exploring mathematics was confirmed in the research of the cross-section of a cube in the study of spatial figures. It can be said that ICT is a useful tool to deepen students' understanding and improve their motivation to learn. Therefore, ICT should be more actively incorporated into the daily teaching of mathematics in Japan as a tool for exploring and thinking about mathematics on a daily basis.

While these effects were observed, some problems were found in the activity of drawing the cross-section confirmed by ICT on a plane, suggesting that not only ICT but also other activities such as showing real models are necessary. In the future, author would like to consider the use of 3D materials using a 3D printer. In addition, since the target students were limited to first-year junior high school students, author would like to consider conducting the survey for high school students in the future.

References

[1] Aoki, S., Okamoto, N., and Kuroda, K. (2021)：Characteristics of learners' eye movement when performing a cube-cutting task: Analysis of eye-movement measurement experiments, *Mathematics Education Society of Japan, Japan Journal of Mathematics Education and Related Fields*, 62, 1 & 2, pp.121-129.

[2] Iijima, Y. (2021)：Mathematical Inquiry Changing with ICT: Seven Conditions for Successful Learning in the Next Generation, *Meiji Tosyo*, p.22.

[3] Juandi, D., Kusumah, Y.S., Tamur, M., Perbowo, K.S., Siagian, M.D., Sulastri, R., & Negara, H.R.P. (2021)：The Effectiveness of Dynamic Geometry Software Applications in Learning Mathematics: A Meta-Analysis Study. *International Journal of Interactive Mobile Technologies (iJIM)*, 15(02).
https://doi.org/10.3991/ijim.v15i02.18853
(2025.2.10.accessed)

[4] Kinoshita,T., Okamoto,N., Kuroda, K. (2020)：Characteristics of strategy for perception and learning of three-dimensional shapes using a real object, a tablet tool, and a paper medium: Physiological data analysis, *Mathematics Education Society of Japan, Japan Journal of Mathematics Education and Related Fields*, 61, 1 & 2, pp.89-97.

[5] Kobayashi, Y. , Hamada, A., Mizumoto, A.(2020)：Introduction to Educational Data Analysis with R, *Ohmsha*, pp.121-124

[6] Marasabessy, R., & Helsa, Y. (2024)：Fostering spatial visualization in GeoGebra-assisted geometry lesson: A systematic review and meta-analysis. *Eurasia Journal of Mathematics, Science and Technology Education*, 20(9), em2509, pp.18-37.
https://doi.org/10.29333/ejmste/15170
(2025.2.10.accessed)

[7] MEXT(2017)：Courses of Study for Junior High Schools (Notification in 2017) Commentary, *Nippon Bunkyo Publishing Co.*

[8] MEXT(2022)：Results of the 2021 Survey on the Actual Status of Informatization of Education in Schools (as of March 1, 2022)
https://www.mext.go.jp/content/20220830-mxt_jogai02-000023485_1.pdf
(2022.10.8.accessed)

[9] Ministry of Education (1998)：Courses of Study for Junior High Schools (December 1998) Explanation - Mathematics -, *Osaka Syoseki*, pp.1-24

[10] Motohiro Ishida (2021). RMeCab: interface to MeCab. R package version 1.07.

[11] Okabe,T. Kitajima,S. (2022)：Systematic Mathematics 1 Geometry, *Suuken Shuppan*, pp.38-56.

[12] Onishi,T. (2015)：Non-Euclidean Ggeometry with Dynamic Geometry Software, *Research Report, Journal of Science Education in Japan*, 29, 9, pp. 77-82.

[13] R Core Team (2021). R: A language and environment for statistical computing. R Foundation for Statistical Computing, Vienna, Austria. URL https://www.R-project.org/.

[14] Shimizu, K. and Kakihana, K. (1999)：Computer-assisted student activities, *Meiji Tosyo*, pp.5-117.

[15] Tani,A. Yanagimoto, A. (2017)：Development of teaching materials by using acomparison study between Japan and Germany in order to improve the understanding of a function and its meaning: From a present knowledge survey with german students, *Mathematics Education Society of Japan, Japan Journal of Mathematics Education and Related Fields*, 58, 3 & 4, pp.18-19.

[16] Yamada,K. ,Tsukamoto, Y,(2012)：An improvement on the teaching of sketch of a cube by using ICT, *Research Bulletin of the Faculty of Education, Niigata University*, 5, 2, pp.34-45.

[17] Yanagawa, K. (2023)：Introduction to Data Science for Education, Language, and Psychology with R, *Ohmsha*, p.126.

[18] Yasuno, F. (2019)：Developing skills in creating teaching materials through the use of dynamic mathematics software and other tools, National Institute for Educational Policy Research (as of 2019).
https://www.edu.sugiyama-u.ac.jp/math/file-kaken/yasuno.pdf
(accessed October 8, 2022)

Appendix 1

GeoGebra Cubic Cutting Plane Questionnaire

① Were you interested in learning more about cubic cut surfaces using GeoGebra?

② Did you learn anything new about cubic cut surfaces through your observations with GeoGebra?

③ Did you learn anything new through this GeoGebra study?

④ Do you think you were self-motivated to learn about cubic cut surfaces?

⑤ Did you willingly give a presentation in class about cubic cutting planes?

⑥ Did you listen attentively to your friends' ideas and opinions about the cutting plane of a cube?

⑦ Did you discuss the solution of the problem of the cutting plane of a cube with your friends?

⑧ Were you able to think in different ways about the cutting plane of a cube?

⑨ Did you have enough time to think about solving the problem of a cubic cutting plane?

⑩ Was your teacher's explanation easy to understand?

⑪ Did you enjoy this lesson on cubic sections?

⑫ Did you want to learn more about cubic figures?

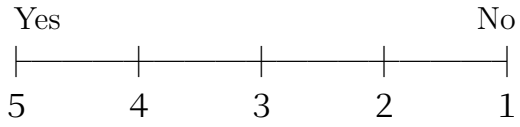

⑬ Please tell me what you thought was good and what you regret about learning about cubic section surfaces.

Appendix 2

Cutting plane of a cube (Part 1)
Your Name（　　）

[Question] Draw the shape of the cut surface of the cube below when it is cut in the plane passing through the three points P, Q, and R. Note the symbols in the drawing to indicate which lines are parallel and which lines are equal in length. Also, name the shape of the cut surface in parentheses below.

(1)

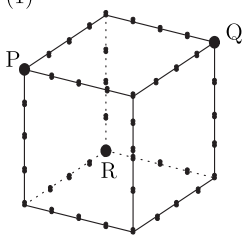

(　　)

(2)

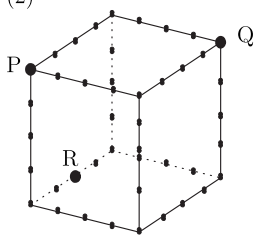

(　　)

(3)

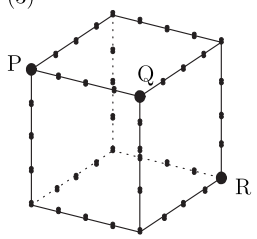

(　　)

(4)

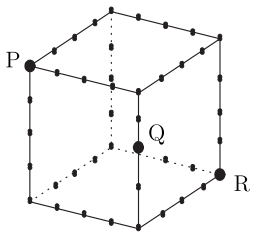

(　　)

(5)

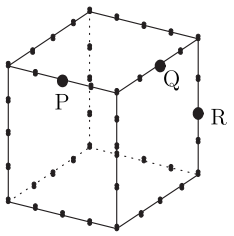

(　　)

(6)

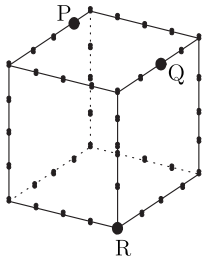

(　　)

Cutting planes of a cube (Part 2)
Your Name（　　）

[Question] Draw the shape of the cut (cutting plane) of the cube below when it is cut by a plane passing through the three points P, Q, and R. In the drawing, draw symbols to indicate which lines are parallel and which lines are equal in length. Also, name the shape of the cut surface in parentheses below.

(1)

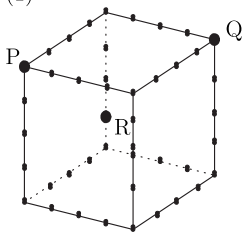

(　　)

(2)

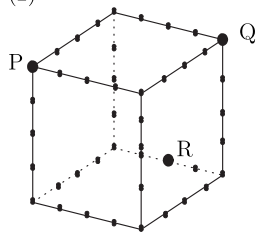

(　　)

(3)

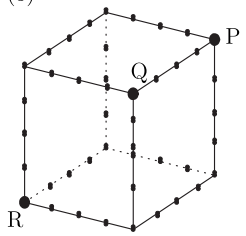

(　　)

(4)

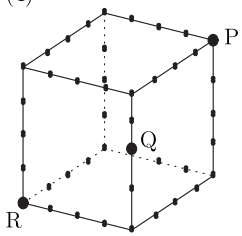

(　　)

(5)

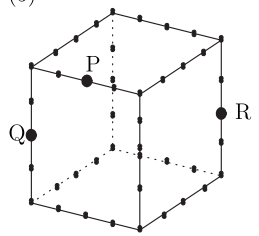

(　　)

(6)

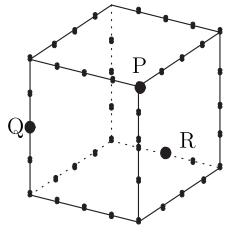

(　　)

The Research Journal of Mathematics and Technology, Volume 15, Number 1

Observing the cut surface of a cube with GeoGebra

[Q1] Let's examine the cut plane in the figure on the right using GeoGebra. Follow the steps below to operate GeoGebra.

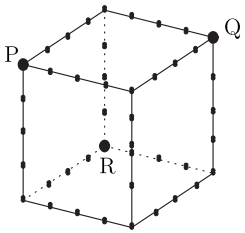

1. Open the "cube cross section.ggb" uploaded to Teams.
2. Select the menu "Point on Object" in GeoGebra, and draw a point P on the edge EF. (If it is not P, rename it.)
3. Next, take a point Q on the edge EH and a point R on the edge OE.
4. Check if you can move points P, Q, and R on the edge by dragging them.
5. Select the menu "Plane through 3 points" in GeoGebra and specify the points P, Q, and R.
6. Change the color of the plane to make it easier to see the shape of the cut plane. In the following operations, change the viewing direction as necessary.
7. Check the shape of the plane when point P is placed at vertex F, point Q is placed at vertex H, and point R is placed at vertex O.
8. For the figures (1) to (3) below, use the GeoGebra file you have created to examine the shape of the cut plane. Also, write the names of the shapes of the cut surfaces in parentheses below.
9. Save your GeoGebra file as a "$\cdots$ Download" file, rename the file to your number and name, and submit it via Teams.
10. Check out the other forms besides (1) through (3) below.

(1)

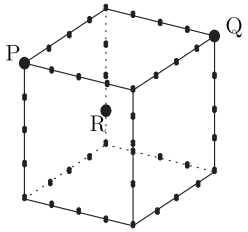

(　　)

(2)

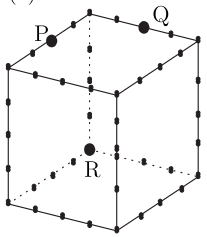

(　　)

(3)

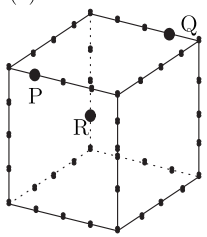

(　　)

Your Name (　　)

[Q2] Use GeoGebra to examine the cut plane of the cube below when cut by a plane passing through the three points P, Q, and R, and draw the result in the figure below. Note the symbols in the figure to indicate which lines are parallel and which lines are equal in length. Also, name the shapes of the cut surfaces in parentheses below.

Finally, save the GeoGebra file used in the discussion as a "Download in ... format," rename the file to your own name, and submit it via Teams.

(1)

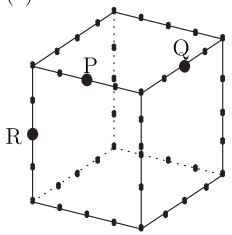

(　　)

(2)

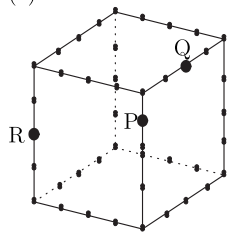

(　　)

(3)

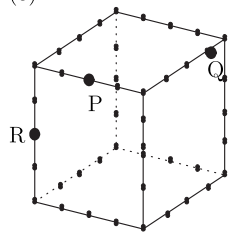

(　　)

[Q3] Use GeoGebra to examine the cut plane of the cube below when cut by a plane passing through the three points P, Q, and R, and draw the result in the figure below. Note the symbols on the figure to indicate which lines are parallel and which lines are equal in length. Also, name the shapes of the cut surfaces in parentheses below.

Submit the GeoGebra file used in the discussion, renaming the file to your own name, via Teams.

(1)

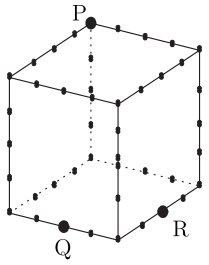

(　　)

(2)

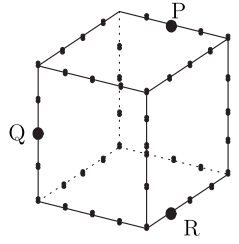

(　　)

(3)

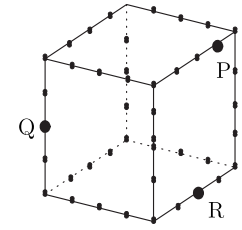

(　　)

Please share your thoughts and impressions about using GeoGebra to examine a cube's cut surfaces.

A half-automated study of a 2-parameter family of integrals

David G. Zeitoun
ed.technologie@gmail.com
Talpiot College of Education
Holon, Israel

Thierry N. Dana-Picard
ndp@jct.ac.il
Jerusalem College of Technology
Jerusalem, Israel

Abstract

The study of some parametric integrals is presented with a combined approach of analytical development, the usage of a Computed Algebra System (CAS) and of the Online Encyclopedia of Integer Sequences. The paper runs around the analysis of the 2-parameter definite integral

$$I_n^{(p)} = \int_0^{\pi/4} x^p \tan^n x \; dx.$$

The methodology for the solution includes a) an analytical investigation for the study of the parametric integral, b) computations with a CAS of the integral for specific values of the parameter, c) investigation of the connection between the integral and special functions or mathematical constants, and d) derivation of a general algorithm for the complete computation of the parametric integral. Comparing the outputs of different kinds of software yields useful remarks about the understanding of the outputs, an important issue in mathematics education in a technology-rich environment.

1 Introduction.

The computation of parametric definite integrals is an interesting mathematical field (e.g. see [27, 7]). On the one hand, parametric integrals help students to grasp more abstract situations than in the cases without parameters. On the other hand, in domains such as Physics and Engineering, numerous phenomenons have a mathematical translation into such integrals; for example, see [17]. Moreover, such computations may lead to formula for indefinite series, and also to derive combinatorial identities and integral representations for combinatorial objects; for example, see [12, 15, 6, 16, 28, 29, 32] and the papers in reference there. In the specific case of Catalan numbers, different presentations and applications are given in [24].

Computing the integrals by hand may be unilluminating. The usage of technology has been analyzed and discussed for a long time, not only for the domain that we are interested in here. Buchberger [9] says that a Computer Algebra System (CAS) should be used only where the user knows how to perform the computations by hand, not as a black box where the user has no knowledge on what are

the processes at work inside. A good example of this approach is in the book [2] where the described algorithms are first "run by hand", and then applied with their version implemented in software[1]. With a black box usage, the CAS is a facilitator to obtain a result, not to develop more mathematical knowledge. For a short presentation of this *White-Box / Black-Box Principle*, we refer to [10].

Nevertheless, but as already seen in [13], it happens that the CAS is used to bypass a lack of theoretical knowledge, then proceeding backwards the gap can be filled. In [19], Drijvers notes that generally a CAS works as a black box, it does not provide insight into the algorithms. Advanced versions of a CAS may provide some insight, either as a step-by-step command, as in the Derive software (in version 6.1, released a long time ago, which was the last release), or via tutorials such as Maple's tutorials. These tutorials work in an interactive way, providing hints for every single step, sometimes more than one. The user then chooses and checks the efficiency of the proposed step. A suitable usage of such a tutorial provides a good scaffolding to the user, which has to be gradually faded. These tutorials are a kind of intelligent tutoring systems, an interesting AI application which can propose hints, analyze the user's answer, monitor and guide students (Kock et al. [23] compare this with the generative AI systems which became popular since year 2023 with the first launch of ChatGPT). Note that the same tutorials have a shortcut giving the final answer immediately; this is a black box usage. Anyway, this usage is highly personal , and each user will develop his/her own instrumental genesis [3, 31]. A good balance between paper-and-pencil and CAS assisted work is crucial. As we will see, "the computer offers to provide scaffolding both to enhance mathematical reasoning and to restrain mathematical error" (J. Borwein in[8]).

In this paper, we study a 2-parameter family of definite integrals. For small values of the parameters, computations may be performed by hand, but this is time-consuming. A CAS can be used after a few computations, without contradicting Buchberger's point of view. This may be a partial solution only, as we will see in Section 2. In certain cases, the output of an automated computation shows an integral which cannot be computed analytically. From that point, either numerical methods should be used, or an induction formula has to be looked for, as in [15, 16] and other cases referenced there.

The numerical results obtained with a CAS have to be exploited. The investigation made a strong usage of the Online Encyclopedia of Integer Sequences (OEIS)[2]. This proved a really efficient approach, enabling to enounce conjectures, which have then to be proven.

The integral

$$I_n = \int_0^{\pi/4} \tan^n x \, dx$$

and an application to soil mechanics have been described in [17]. Here we study a generalization of it, namely the 2-parameter integral defined by:

$$I_n^{(p)} = \int_0^{\pi/4} x^p \tan^n x \, dx, \tag{1}$$

where the parameters p and n are non negative integers.

A motivation has been provided by students of the 2nd author in an engineering curriculum, who came to him from time to time to ask for additional exercises, beyond the official syllabus. It is

[1]The book is devoted to Gröbner bases and their applications. This is not the topic of our work here, but the didactic methodology is similar to what we claim

[2]http://www.oeis.org.

valuable to be prepared to answer requests by highly motivated students; the authors had opportunities to propose such extensions of the syllabus. They are involved both in mathematics teachers education and in engineering education. Even when the syllabi do not mention explicitly teaching and working in a technology-rich environment, they think that this is what has to be done nowadays, inciting students to develop their own technological skills, preparing them also for lifelong learning. Such exercices have been included in practice sessions of a Calculus course at JCT.

First, we derive by hand an induction formula, then we try to have more insight into the 2-parameter sequence of integrals. For this we use a Computer Algebra System, here the Maple package and its tutorials, and the Online Encyclopedia of Integer Sequences.

Automated methods have been analyzed and documented for questions in Geometry, Analytic Geometry and in Differential Geometry (for example, see the survey [14]). The important novelty here is that, for parametric integrals no visual intuition is afforded. This is not rare with integrals, recall the example of $\int x \ln x \ dx$ for which the choice of the functions for an integration by parts is counter-intuitive. The present study requests more abstract thinking. After all, parametric integrals are already a more abstract object than "ordinary" definite integrals.

2 An induction formula

For integrals where the integrand contains a power of the tangent function, it is natural to look for an induction with an increment of 2 in the power. We have:

$$\begin{aligned} I_n^{(p)} + I_{n-2}^{(p)} &= \int_0^{\pi/4} x^p \tan^n x \ dx + \int_0^{\pi/4} x^p \tan^{n-2} x \ dx \\ &= \int_0^{\pi/4} x^p (\tan^n x + \tan^{n-2} x) \ dx \\ &= \int_0^{\pi/4} x^p (\tan^2 x + 1) \ \tan^{n-2} x \ dx \end{aligned}$$

Integration by parts of the last expression, using the functions:

$$f(x) = x^p \text{ and } g(x) = \frac{\tan^{n-1} x}{n-1} \tag{2}$$

whence

$$f'(x) = px^{p-1} \text{ and } g'(x) = \tan^{n-2} x(\tan^2 x + 1) \tag{3}$$

This leads to the following recurrence relation:

$$I_n^{(p)} + I_{n-2}^{(p)} = \frac{1}{n-1}\left(\frac{\pi}{4}\right)^p + \frac{p}{n-1} I_{n-1}^{(p-1)}, \ p \geq 1; \ n \geq 1. \tag{4}$$

We can also derive general recurrence formulas for both the sum $\sum_n I_n^{(p)}$ for a given p, and for $I_n^{(p)}$.

Proposition 1 *When n is even, we denote $n = 2l$, and the following holds:*

$$I_{2l}^{(1)} = \frac{\pi}{4} \sum_{k=1}^{2l-1} \frac{(-1)^k}{k} + \sum_{k=1}^{2l-1} \frac{(-1)^k I_k}{k} - \frac{1}{2} \left(\frac{\pi}{4}\right)^2 \tag{5}$$

2.1 The case of even n

2.1.1 Analytic work

For a given integer $p \geq 1$ and if n is even:

$$I_n^{(p)} + 2(I_{n-2}^{(p)} + I_{n-4}^{(p)} + \cdots + I_2^{(p)}) + I_0^{(p)} = \left(\frac{\pi}{4}\right)^p \sum_{k=1}^{n-1} \frac{1}{k} + p \sum_{k=1}^{n-1} \frac{I_k^{(p-1)}}{k}$$
$$= (\Psi(n) + \gamma) \left(\frac{\pi}{4}\right)^p + p \sum_{k=1}^{n-1} \frac{I_k^{(p-1)}}{k}.$$

By addition and substraction of the iterative formula in Equation (4), we derive the following formula:

$$I_n^{(p)} + I_0^{(p)} = \left(\frac{\pi}{4}\right)^p \sum_{k=1}^{n-1} \frac{(-1)^k}{k} + p \sum_{k=1}^{n-1} \frac{(-1)^k I_k^{(p-1)}}{k}. \tag{6}$$

The first integral in the sequence is

$$I_0^{(p)} = \frac{1}{p+1} \left(\frac{\pi}{4}\right)^{(p+1)}, \tag{7}$$

therefore, the following holds:

$$I_n^{(p)} = \left(\frac{\pi}{4}\right)^p \sum_{k=1}^{n-1} \frac{(-1)^k}{k} + p \sum_{k=1}^{n-1} \frac{(-1)^k I_k^{(p-1)}}{k} - \frac{1}{p+1} \left(\frac{\pi}{4}\right)^{(p+1)} \tag{8}$$

Equation (8) means that $I_n^{(p)}$ is a linear function of the previous integrals $I_n^{(k)}$, for $k < p$.

If n is even and $p = 0$, we obtain the following identity:

$$I_n^{(0)} + I_0^{(0)} = \sum_{k=1}^{n-1} \frac{I_k}{k}. \tag{9}$$

Using the previous derivation, we obtain $I_0^{(0)} = \frac{\pi}{4}$, whence:

$$I_n^{(0)} = \sum_{k=1}^{n-1} \frac{I_k}{k} - \frac{\pi}{4}. \tag{10}$$

If n is even and $p = 1$, we obtain:

$$I_n^{(1)} + 2(I_{n-2}^{(1)} + I_{n-4}^{(1)} + \cdots + I_2^{(1)}) + I_0^{(1)} \tag{11}$$

Also a general expression of $I_n^{(1)}$ may be derived:

$$I_n^{(1)} = \frac{\pi}{4} \sum_{k=1}^{n-1} \frac{(-1)^k}{k} + \sum_{k=1}^{n-1} \frac{(-1)^k I_k}{k} - \frac{1}{2} \left(\frac{\pi}{4}\right)^2 \tag{12}$$

2.1.2 Analysis with a CAS

Using a Computer Algebra System, we obtain the following values for small even values of the parameter n:

$$
\begin{aligned}
I_0^{(1)} &= \frac{\pi^2}{32} \\
I_2^{(1)} &= -\frac{\pi^2}{32} + \frac{\pi}{4} - \frac{\ln 2}{2} \\
I_4^{(1)} &= \frac{\pi^2}{32} - \frac{\pi}{6} - \frac{1}{6} + \frac{2}{3}\ln 2 \\
I_6^{(1)} &= -\frac{\pi^2}{32} + \frac{13\pi}{60} + \frac{13}{60} - \frac{23}{30}\ln 2 \\
I_8^{(1)} &= \frac{\pi^2}{32} - \frac{19\pi}{105} - \frac{29}{105} + \frac{88}{105}\ln 2 \\
I_{10}^{(1)} &= -\frac{\pi^2}{32} + \frac{263\pi}{1260} + \frac{2333}{7560} - \frac{563}{630}\ln 2 \\
I_{12}^{(1)} &= \frac{\pi^2}{32} - \frac{1289\pi}{6930} - \frac{3578}{10395} + \frac{3254}{3465}\ln 2 \\
I_{14}^{(1)} &= -\frac{\pi^2}{32} + \frac{36979\pi}{180180} + \frac{397753}{1081080} - \frac{88069}{90090}\ln 2
\end{aligned}
$$

Remark 2 *Look at the coefficient of π in this output. It determines 2 sequences of integers, a sequence of numerators 1,-1,13,-19,263, ... and a sequence of denominators 4,6,60,105,1260, ... The database OEIS does not have an entry for the sequence of denominators, but proposes to consider two subsequences according to the index being either odd or even. Starting from this database searching, some non trivial connections can be found between the integrals studied here and other mathematical objects, with an approach similar to [12, 15]. Such a study is not in the scope of the present paper, we leave it as an open question for a later study.*

2.2 The case of odd n

2.2.1 Analytic work

For a given integer $p \geq 1$ and odd n, we have:

$$
I_n^{(p)} + 2\left(I_{n-2}^{(p)} + I_{n-4}^{(p)} + \cdots + I_3^{(p)}\right) + I_1^{(p)} = \left(\frac{\pi}{4}\right)^p \sum_{k=2}^{n-1} \frac{1}{k} + p \sum_{k=2}^{n-1} \frac{I_k}{k}
$$

By addition and substraction of the iterative formula (i.e., Equation (4)), we obtain:

$$
-I_n^{(p)} + I_1^{(p)} = \left(\frac{\pi}{4}\right)^p \sum_{k=2}^{n-1} \frac{(-1)^k}{k} + p \sum_{k=2}^{n-1} \frac{(-1)^k I_k^{(p-1)}}{k}
$$

For $p = 0$, we find the previous expression. For even n and $p = 1$, we obtain:

$$
I_n^{(1)} + 2(I_{n-2}^{(1)} + I_{n-4}^{(1)} + \cdots + I_3^{(1)}) + I_1^{(1)} = \frac{\pi}{4} \sum_{k=2}^{n-1} \frac{1}{k} + \sum_{k=2}^{n-1} \frac{I_k}{k}
$$

Then we derive a general expression for $I_n^{(1)}$ and $n = 2l + 1$:

Proposition 3

$$I_{2l+1}^{(1)} = \frac{\pi}{4}\sum_{k=2}^{2l}\frac{(-1)^k}{k} + \sum_{k=2}^{2l}\frac{(-1)^k I_k}{k} - I_1$$

2.2.2 Analysis with a CAS

Using a Maple, we obtain the following values for small odd values of the parameter n:

$$\begin{aligned}
I_1^{(1)} &= \frac{\pi}{8}\ln 2 + \int_0^{\pi/4}\ln(\cos x))\ dx \\
I_3^{(1)} &= -\frac{\pi}{8}\ln 2 - \int_0^{\pi/4}\ln(\cos x))\ dx + \frac{\pi}{4} - \frac{1}{2} \\
I_5^{(1)} &= \frac{\pi}{8}\ln 2 + \int_0^{\pi/4}\ln(\cos x))\ dx - \frac{\pi}{4} + \frac{2}{3} \\
I_7^{(1)} &= -\frac{\pi}{8}\ln 2 - \int_0^{\pi/4}\ln(\cos x))\ dx + \frac{\pi}{3} - \frac{73}{90} \\
I_9^{(1)} &= \frac{\pi}{8}\ln 2 + \int_0^{\pi/4}\ln(\cos x))\ dx - \frac{\pi}{3} + \frac{284}{315} \\
I_{11}^{(1)} &= -\frac{\pi}{8}\ln 2 - \int_0^{\pi/4}\ln(\cos x))\ dx + \frac{23\pi}{60} - \frac{3103}{3150} \\
I_{13}^{(1)} &= \frac{\pi}{8}\ln 2 + \int_0^{\pi/4}\ln(\cos x))\ dx - \frac{23\pi}{60} + \frac{54422}{51975} \\
I_{15}^{(1)} &= -\frac{\pi}{8}\ln 2 - \int_0^{\pi/4}\ln(\cos x))\ dx + \frac{44\pi}{105} - \frac{10459489}{9459450} \\
I_{16}^{(1)} &= \frac{\pi}{8}\ln 2 + \int_0^{\pi/4}\ln(\cos x))\ dx - \frac{44\pi}{105} + \frac{5452712}{4729725}
\end{aligned}$$

The following remarks can be made:

1. Two subsequences appear, for even indices and for odd indices.
2. The integral $\frac{\pi}{8}\ln 2 + \int_0^{\pi 4}\ln(\cos x))\ dx$ appears for an index $n \equiv 1 \mod 4$, and its opposite for $n \equiv 3 \mod 4$. The sign change comes from the $(-1)^k$ factor in the two first terms in Proposition (3).
3. The integral $\int_0^{\pi 4}\ln(\cos x)\ dx$ is left in closed form and cannot be evaluated analytically.

With Maple, the following result is obtained:

$$\int_0^{\pi/4}\ln(\cos x)\ dx = \frac{\pi}{4}\ln 2 + \frac{1}{2}G, \tag{13}$$

where G denotes the Catalan constant[3].

In [1], the integral presentations of the Catalan constant are given, but without analytic proofs. There, computations have been performed with Mathematica. Note that this is a black-box usage of the CAS, in contradiction to Buchberger's point of view. Nevertheless, we can follow a path in reversed direction and note that

$$G = \sum_{r=0}^{\infty} \frac{(-1)^r}{(2r+1)^2}. \tag{14}$$

3 Study of the influence of the parameter p

In this section we investigate the dependence of the parameter p on the 2-parameter integral $I_n^{(p)}$. The fundamental iterative formula (4) connects $I_n^{(p)}$ with the terms $I_{n-2}^{(p)}$ and $I_{n-1}^{(p-1)}$ and this for a given p.

The influence of p may be checked in two ways.

First, in the given integration interval, i.e. for $0 \leq x \leq \frac{\pi}{4} < 1$, we have $0 < x^p < 1$. It follows that $I_n^{(p)} < I_n$, where

$$I_n = \int_0^{\pi/4} \tan^n x \, dx. \tag{15}$$

3.1 The tangent power integral

This last equation has been studied by the authors in [17]. In this reference , we derived closed combinatorial formulas for the tangent-power integral , according to the congruence class modulo 4 of the parameter m. We presented three different forms of the definite integral:

1. A finite series formula: for even indices, the following holds:

$$I_{2k} = (-1)^k \frac{\pi}{4} + \sum_{l=1}^{k} \frac{(-1)^{(l+k)}}{2l-1}. \tag{16}$$

   For odd n, we have:

$$I_{2k+1} = (-1)^k \frac{\ln 2}{2} + \sum_{l=1}^{k} \frac{(-1)^{(l+k)}}{2l}$$

2. An equivalent formula using double factorials:

$$\begin{aligned} I_{4k-2} &= -\frac{\pi}{4} + \frac{k}{(2k-1)!!} \\ I_{4k-1} &= \frac{\ln 2}{2} + \frac{1}{2} + \frac{k}{(2k-1)!!} \\ I_{4k} &= \frac{\pi}{4} + \frac{k}{(2k-1)!!} \\ I_{4k+1} &= \frac{\ln 2}{2} + \frac{1}{2} + \frac{k}{(2k)!!} \end{aligned}$$

[3] See the sequence https://oeis.org/A006752

These different expressions have different physical meanings leading to different types of understandings and teaching:

3.2 An iterative algorithm for $I_n^{(p)}$ for n and $p = 1, ..., k$

In the previous section we derived a general iterative equation for fixed n between $I_n^{(p)}$ and the terms $I_k^{(p-1)},\ k < n$:

- If n is even:

$$I_n^{(p)} = \left(\frac{\pi}{4}\right)^p \sum_{k=1}^{n-1} \frac{(-1)^k}{k} + p \sum_{k=1}^{n-1} \frac{(-1)^k I_k^{(p-1)}}{k} - \frac{1}{p+1} \left(\frac{\pi}{4}\right)^{(p+1)}$$

- If n is odd:

$$-I_n^{(p)} + I_1^{(p)} = \left(\frac{\pi}{4}\right)^p \sum_{k=2}^{n-1} \frac{(-1)^k}{k} + p \sum_{k=2}^{n-1} \frac{(-1)^k I_k^{(p-1)}}{k}$$

As a consequence, we may compute iteratively any integral $I_n^{(p)}$. The method consists in:

(i) Check if n is even or odd

(ii) If n is even, compute $I_k^{(0)} = \int_0^{\pi/4} \tan^n x\ dx$ for $k < n$.

(iii) Then use the above formula to compute $I_n^{(1)}$

(iv) Then compute $I_k^{(1)}$ for $k < n$.

(v) Compute $I_n^{(2)}$ and so on until $I_n^{(p)}$

(vi) If n is odd, compute $I_k^{(0)} = \int_0^{\pi/4} \tan^n x\ dx$ for $1 < k < n$.

(vii) Then use the above formula to compute $I_n^{(1)}$

(viii) Then compute $I_k^{(1)}$ for $k < n$.

(ix) Compute $I_n^{(2)}$ and so on ....until $I_n^{(p)}$

3.3 Analysis of an integral using a power series

We consider the integral

$$J_n = \int_0^{\pi/4} \frac{\tan^n x}{1-x} dx. \tag{17}$$

For any integer $n > 0$, we were unable to obtain a direct analytic computation of this integral using a CAS. Only numerical values have been obtained. Nevertheless, the integral J_n may be computed

using the integral $I_n^{(p)}$ studied earlier. The domain of integration is the interval $\left[0, \frac{\pi}{4}\right]$, therefore $|x| < 1$ and we have

$$\frac{1}{1-x} = \sum_{i=0}^{\infty} x^i,$$

and it follows that

$$J_n = \int_0^{\pi/4} \frac{\tan^n x}{1-x}; dx = \sum i = 0^{\infty} \int_0^{\pi/4} x^i \ \tan^n x \ dx = \sum_{i=0}^{\infty} I_n^i.$$

The computation of J_n requires the computation of the integrals I_n^i for all i. In the previous section, we presented an iterative method to compute I_n^i from the different $I_n^{i-1}; i \geq 1$. Now we present an approximate method to compute J_n.

We have:

$$\forall n \geq n_0, \ I_n^{(i)} \approx (\frac{\pi}{4})^i) \int_0^{\frac{\pi}{4}} \tan^n(x) \ dx.$$

It follows that:

$$J_n = \sum_{i=0}^{\infty} I_n^{(i)} = \sum_{i=0}^{n_0} I_n^i + \sum_{i=n_0}^{\infty} I_n^{(i)}.$$

Using the above approximation, we obtain:

$$J_n = \sum_{i=0}^{n_0} I_n^{(i)} + \left[\sum_{i=n_0}^{\infty} (\frac{\pi}{4})^i)\right] \left[\int_0^{\frac{\pi}{4}} \tan^n(x) \ dx\right].$$

Therefore, we obtain:

$$J_n = \sum_{i=0}^{n_0} I_n^i + \left[(\frac{\pi}{4})^{n_0} \frac{1}{1-\frac{\pi}{4}}\right] \ \cdot \ \left[\int_0^{} \tan^n(x) \ dx\right].$$

The index n_0 may be chosen by using an error level ϵ and require that $x^{n_0} < \epsilon$.

3.4 Analysis of the integral $L_n = \int_0^1 \arctan^n(x) \ dx$

Note first that this integral is a particular case of the integral $I_n^{(p)}$ studied above. When asked to compute this integral for small values of the parameter, a CAS returns only the closed from of the integral. Only in numerical form, some other output can be obtained, but this is irrelevant to our purpose here..

Consider the change of variable: $u = \arctan(x)$; then $x = \tan(u)$ for $0 \leq u \leq \frac{\pi}{4}$. Note that $dx = (1 + \tan^2 u) \ du$. With this change of variable $L_n = \int_0^{\pi/4} \ u^n \ (1 + \tan^2 u) \ du$, whence:

$$L_n = \int_0^{\pi/4} u^n \ du + I_2^{(p)} \tag{18}$$

Finally, we have the following proposition:

Proposition 4 *For every non negative integers n and p, the following holds:*

$$L_n = \frac{1}{n+1} \left(\frac{\pi}{4}\right)^{n+1} + I_2^{(p)}.$$

4 Some thoughts in the aftermath

Previous explorations of parametric definite integrals, no matter how many parameters were involved, opened for us various ways to build bridges between mathematical domains. In many cases, integral presentations of combinatorial objects have been derived. In other cases, they provided an opportunity to prove combinatorial identities [15, 16, 28, 29]. A CAS is an important tool for such an exploration and proofs. Nevertheless, it is sometimes hard to conjecture such an identity and another technology can be useful. This was the case for the mentioned works, and using the Online Encyclopedia of Integer Sequences revealed efficient. Of course, it helped to have a conjecture, but this conjecture had to be proven by more theoretical means.

For the examples of the present work, the situation is somehow different. We could try various inputs for searching the database, but none provided a ready-to-use answer. For all our trials, the database proposed a modified version of the input, and understanding the proposed sequences was non-trivial. This is a good illustration that exploring mathematical objects in a technology-rich environment does not follow a predefined path.

The OECD defined the so-called 4 C's of 21st century education: Communication, Collaboration, Critical Thinking and Creativity. These are crucial in various settings (see for example [30]. Here, the collaboration can be between humans, but also between man and machine. Collaboration with technology, i.e. human and machine together, requires strong Critical Thinking in order to analyse the outputs of the CAS and of the interactive database. We shall mention that collaboration with a generative AI requires this still more; see [4, 23]. Critical Thinking and Creativity are central skills, opposite to Black-Box usage of technology. Further, Creativity leads to the possible conjectures. This is a modern way to deal with mathematics, with a scheme exploration-conjecture-proof. It request also the understanding that the new technological skills are an integral part of the new mathematical knowledge, and that a new technological discourse has to be developed [3, 26]. Such exploration can be initiated by a 5th C, namely Curiosity; a kind of exploration has been proposed in Remark 2. This has been the basis of [17], where mathematical curiosity and communication and collaboration between researchers yielded an interesting application.

Nowadays, curiosity can push in new directions. We asked an AI for references about parametric definite integrals. Most answers gave general chapters in Calculus books, the only relevant to *parametric* definite integrals was a presentation in a conference [18].

Finally, we wish to recall what we wrote in Section 1. Parametric definite integrals enable students to step forwards towards more abstract understanding than what is offered in a first Calculus course. But they are not always a pure mathematical exercise. They have numerous applications in science, in particular in Physics; [22] provides an insight into students' difficulties to translate the knowledge acquired in definite integrals in a Calculus course into the needed skills for Physics. Nevertheless, the topics is quite rare in Calculus textbooks, and also in the classical syllabus; we found a subchapter in [25] (subchapter 7.4). Despite the fact that these applications are not an integral part of teh official syllabus, the authors try to give by that way some motivation to the students asking "what is this good for?". Regarding the mental schemes that they require, these are parallel to what is required in Linear Algebra for solving parametric systems of linear equations; see [11], where some problems are analyzed, such as the lack of investigation of special values of the parameters[4].

[4]Such problems, when working with AI for mathematics education, are analyzed in [4].

Appendix: the work with mathematical software The exploration of the sequence of parametric integrals on subsubsections 2.1.2 and 2.2.2 has been performed using two different softwares. As mentioned above, we used Maple 2024, but also Derive[5]. This last is not available anymore, but the community of users still exists. Even if all of the members use now other packages, they still share applications during conferences, and/or use it in class.

The formulas displayed in subsubsections 2.1.2 and 2.2.2 have been obtained with Derive, as shown in Figure 1. The 2-parameter family of integrals is defined, then it is computed for small values of the parameters. For this, the **Vector** command is applied. Its syntax is ***Vector(parametric formula, parameter, starting value, end value, step)*** . The choice of the starting value and the step enables to distinguish what happens with odd (resp. even) values of the parameter. A noticeable feature of the output is the presence of a closed integral, namely $\int_0^{\pi/4} \ln(\cos x)\ dx$.

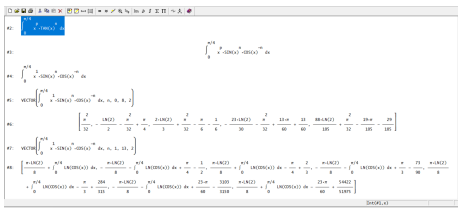

Figure 1: A session with Derive

We are ware that a software discontinued 20 years ago cannot be recommended. Maybe the example here (as in previous published works [**?**]) will incite development of such an output and make it available in existing software.

In parallel, we used the following Maple code (of course, with different choices for the values of the parameter and step):

```
restart:
f := x*tan(x)^n;
for i from 0 by 2 to 14 do
    n := i;
    int(f, x = 0 .. Pi/4);
end do;
```

In order to take into account the 2 parameters, we used nested ***for*** loops. The output appears different from above.For odd values of the parameter, it involves the so-called *Catalan constant*, as shown in Figure 2. Actually, the answers by the two packages are equivalent, as explained by Equation (13). It has been checked also with Maple, as shown in Figure 3.

This is a good opportunity to draw students' attention to the fact that they should not relate to the output as THE answer, but rather as a representation of the answer. It is well known that mathematical objects cannot be grasped with hands, but are dealt with using various representations. A rich knowledge is developed when switching between different representations, which can reveal different aspects of the same mathematical object; see [20]. Here we have, on the one hand, a representation

[5]We have this opportunity to evoke Josef Böhm's memory, a good friend devoted to education and to the Derive community; he was the editor of the Derive Newsletter.

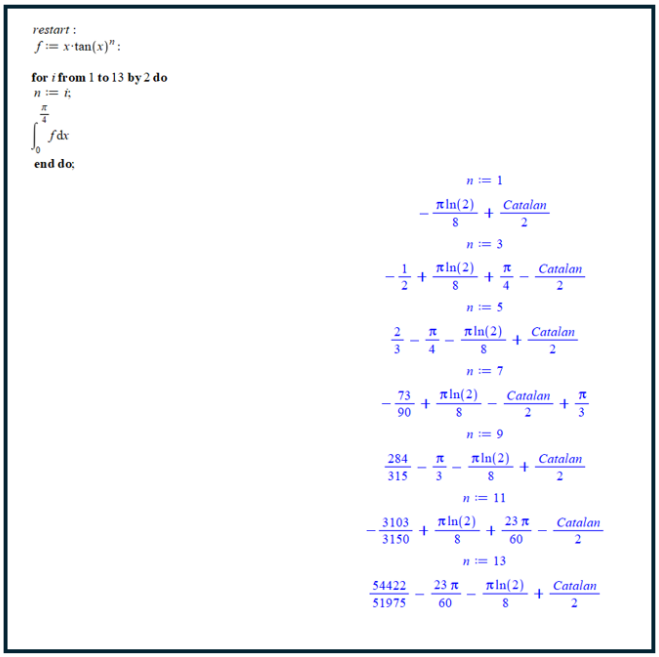

Figure 2: A session with Maple

Figure 3: Verification that the two outputs are equivalent

using an implicit form for a definite integral, in a situation where the integrand has no primitive being described by a closed formula. Generally, the registers of representation mentioned for mathematical objects are graphical, numerical, symbolic, etc. The objects under study in this work belong to Calculus, and the representations that we dealt with may be explained as belonging to a symbolic registers, but their appearances are different. Of course, engineers may wish to have a numerical representation, which can be more easily applied in concrete situations. Maybe we should speak here about subregisters of representation. Such a situation is not rare, and students meet them quite early. On the other hand, we have a representation involving the Catalan constant, an object which is rarely met by undergraduates. This provides an opportunity for a small extension of the curriculum.

Finally we wish to mention that the reflections about the different roles of technology usage for helping humans address mathematical issues do not need to apply only to students, they are equally useful for researchers.

Acknowledgements: The authors wish to thank the reviewers for useful comments and sugges-

tions.The 2nd author has been partially supported by the CEMJ Chair at JCT.

Declaration: The authors declare no conflict of interest.

References

[1] Adamchik, V. (2002). *A certain series associated with Catalan's constant*, Zeitschrift für Analysis und ihre Anwendungen **21 (3)**, 1-10.

[2] Adams, W., Loustaunau, P. (1994). *An Introduction to Gröbner Bases*, Graduate Studies in Mathematics **3**, American Mathematical Society.

[3] Artigue, M. (2002). *Learning Mathematics in a CAS Environment: The Genesis of a Reflection about Instrumentation and the Dialectics between Technical and Conceptual Work*, International Journal of Computers for Mathematical Learning **7(3)**, 245-274.

[4] Bagno,E., Dana-Picard, Th., Reches,S. (2024). *ChatGPT in Linear Algebra: Strides Forward, Steps to Go*, Open Educational Studies 6 (1), 20240031. DOI: https://doi.org/10.1515/edu-2024-0031.

[5] Bailey, D.H., Borwein, J.M., Mattingly, A., Wightwick, G. (2013). T*he Computation of Previously Inaccessible Digits of p^2 and Catalan's Constant*, Notices of the AMS 60 (7), 844-854.

[6] Bernstein, D.S. (2018). *Scalar, Vector, and Matrix Mathematics: Theory, Facts, and Formulas*, Princeton University Press.

[7] Boros, G., Moll V.H. (2006). *Irresistible Integrals: Symbolic, Analysis and Experiments in the Evaluation of Integrals,* Cambridge University Press.

[8] Borwein,J.M. (2012). *Exploratory Experimentation: Digitally-Assisted Discovery and Proof*, in (G. Hanna and M. de Villiers, edts) Proof and Proving in Mathematics Education - The 19th ICMI Study, 69- 96, Springer.

[9] Buchberger, B. (1989). *Should students learn integration rules?*, Risc-Linz Series no. 89-07.0, Linz: University of Linz.

[10] Buchberger, B. (2024). The White-Box / Black-Box Principle for Using Symbolic Computation Systems in Math Education, https://www3.risc.jku.at/people/buchberger/white_box.html. (retrieved December 2024).

[11] Dana-Picard,Th. (2001). *Matricial Computations: Classroom Practice with a Computer Algebra System*, European Journal of Engineering Education **26 (1)**, 29-37.

[12] Dana-Picard, Th. (2005). *Parametric integrals and Catalan numbers*, International Journal of Mathematical Education in Science and Technology **36 (4)**, 410-414.

[13] Dana-Picard, Th. (2005). *Technology as a bypass for a lack of theoretical knowledge*, International Journal of Technology in Mathematics Education 11 (3), 101-109.

[14] Dana-Picard, Th. (2023). *Computer Assisted Proofs and Automated Methods in Mathematics Education*, in (P. Quaresma et al., edts), Proceedings of ThEdu'22 - 11th International Workshop on Theorem Proving Components for Educational Software, Electronic Proceedings in Theoretical Computer Science, 2-23..

[15] Dana-Picard, Th., Zeitoun, D.G. (2012). *Sequences of definite integrals, infinite series and Stirling numbers*, International Journal of Mathematical Education in Science and Technology **43 (2)**, 219-230.

[16] Dana-Picard, Th. and Zeitoun, D.G. (2011). *Parametric integrals, Wallis formula and Catalan numbers*, International Journal of Mathematical Education in Science and Technology **43 (4)**, 515-520.

[17] Dana-Picard, Th., Zeitoun, D.G. (2017). *Exploration of Parametric Integrals related to a Question of Soil Mechanics*, International Journal of Mathematical Education in Science and Technology **48 (4)**, 617-630. DOI: https://doi.org/10.1080/0020739X.2016.1256445

[18] Dana-Picard, Th. and Zeitoun, D.G. (2019). *Parametric integrals, combinatorial identities and applications*, Book of Abstracts, ACA 2019 Conference (Applications of Computer Algebra), Montréal, Canada, July 16-20. https://math.unm.edu/~aca/ACA/2019/Education/Dana-Picard_integrals.pdf

[19] Drijvers, P. (2000). Students encountering obstacles using a CAS, International Journal of Computers for Mathematical Learning **5(3)**, 189-209.

[20] Duval, R. (2018). *Understanding the Mathematical Way of Thinking – The Registers of Semiotic Representations*, Springer. DOI: http://dx.doi.org/10.1007/978-3-319-56910-9

[21] Gradshteyn I.S., Ryzhik I.M. (1965). *Table of Integrals, Series and Products* 4e, A. Jeffrey (ed.), Academic Press.

[22] Hu, D., Rebello, S. (2013). *Using conceptual blending to describe how students use mathematical integrals in physics*, Physical Review Physics Education Research 9, 020118. DOI: https://doi.org/10.1103/PhysRevSTPER.9.020118

[23] Kock, Zj., Salinas-Hernández, U., Pepin, B. (2025). *Engineering Students' Initial Use Schemes of ChatGPT as an Instrument for Learning*. Digital Experiences in Mathematics Education 11, 192–218. DOI: https://doi.org/10.1007/s40751-025-00169-w

[24] Koshy, T (2009). *Catalan Numbers with Applications*, Oxford University Press.

[25] Lax, P.D., Terell, M.S. (2014). Calculus with Applications 2e, Springer..

[26] Mann, G., Dana-Picard, Th., Zehavi, N. (2007). *Technological Discourse on CAS-based Operative Knowledge*, International Journal of Technology in Mathematics Education **14 (3)**, 113-120.

[27] Moll V.H. (2002). *The Evaluation of Integrals: A Personal Story*, Notices of the A.M.S. **49 (3)**, 311-314..

[28] Qi, F., Akkurt, A., Yildirim, H. (2017). *Catalan Numbers, k-Gamma and k-Beta Functions, and Parametric Integrals*, Journal of Computational Analysis and Applications **25(6)**, 1036-1042.

[29] Qi, F. (2017). *Parametric integrals, the Catalan numbers, and the beta function*, Elemente der Mathematik **72**, 103-110. DOI: https://doi.org/10.4171/EM/332.

[30] Saimon, M., Lavicza, Z., Dana-Picard, Th. (2022). *Enhancing the 4 C's among College Students of a Communication Skills Course in Tanzania through a project-based Learning Model*, Education and Information Technologies **28(6)**, 6269-6285. DOI: https://doi.org/10.1007/s10639-022-11406-9

[31] Trouche, L. (2005). *Instrumental Genesis, Individual and Social Aspects*. In: Guin, D., Ruthven, K., Trouche, L. (eds) The Didactical Challenge of Symbolic Calculators. Mathematics Education Library, vol 36. Springer, Boston, MA. DOI: https://doi.org/10.1007/0-387-23435-7_9

[32] Yin, L., Qi, F. (2018). *Several series identities involving the Catalan Numbers*, Transactions of A. Ramadze Mathematical Institute **172**, 466-474.

Enhancing Mathematical Understanding Through Visual Representations in a Hungarian University

Vanda Fülöp[1]
fulopv@math.u-szeged.hu

Miklós Tekeli[1,2]
tekeli.miklos@gmail.com

[1] Bolyai Institute, University of Szeged
Aradi vértanúk tere 1, 6720 Szeged, Hungary

[2] GAMF Faculty of Engineering and Computer Science, John von Neumann University
Izsáki út 10, 6000 Kecskemét, Hungary

Abstract

For university students of the 2020s, visual experiences play a central role in their daily lives and learning habits. Our experience suggests that traditional teaching methods, such as using lengthy texts, are less effective for this generation. We hypothesize that a curriculum incorporating visual elements, diagrams, and dynamic teaching materials enables more efficient education. Spectacular, interactive learning tools not only make teaching engaging but also facilitate the acquisition of new knowledge through direct experiences and active participation.

To test this, we conducted an experiment at the University of Szeged, comparing two introductory mathematics courses: the Mathematics Teacher Training Program (experimental group) and the Mathematics BSc Program (control group). Our findings indicate that the use of visual and interactive tools significantly improved students' performance. This article presents opportunities for applying visual teaching aids in various topics aiming to enhance the learning process's efficiency and the experiment's results.

To our knowledge, this is the first study in Hungary that comprehensively examines the impact of visual tools on university-level mathematics education over an entire semester, rather than focusing on a short specific topic.

1 Introduction

Today's university students are accustomed to the immediate feedback and visual stimuli of the digital world [12]. Their learning habits significantly differ from traditional approaches, posing new challenges to the education system. Due to the continuous influx of visual stimuli on their smartphones, they are accustomed to receiving and requiring a sequence of short, successive stimuli. A 90-minute lecture, or even a 45-minute class focusing predominantly on textual information, tends to be felt overly long, difficult to follow, monotonous, and fails to maintain their attention.

Taking these challenges into account, we believe that integrating visual elements, diagrams, and interactive teaching aids into the curriculum is necessary to enhance learning efficiency and sustain

attention. These types of teaching materials not only make learning enjoyable but also help students acquire new knowledge through direct experiences and active engagement [19], [7].

Numerous studies support the benefits of using visual aids. The role of visualisation is relevant from an early age, as it facilitates conceptual understanding and problem-oriented thinking [4]. However, this impact is not limited to early childhood; later, in higher education, it aids in comprehending abstract concepts while also boosting motivation [11], [14], [17]. The use of diagrams and graphical tools is especially beneficial in mathematics education, particularly when solving complex, multi-step problems. Fortunately, many examples in mathematics education lend themselves to visual representation [6], [3], [7], [19].

This article presents instruction supplemented with visual aids and analyzes its effectiveness in university mathematics teaching. Specific tasks and proposals for utilizing visual aids are discussed in [20].

We tested the effectiveness and applicability of our method through an experimental program at the University of Szeged. During the research, we compared two similar introductory mathematics courses: in the experimental group (Mathematics Teacher Training Program; MT, 16 students), we integrated visual aids into the teaching process, while in the control group (Mathematics BSc Program; BSc, 22 students), traditional teaching methods were applied.

In analyzing the results, we aimed to determine the extent to which visual tools contribute to improving students' performance and how these methods enhance the learning experience. In the following sections, we briefly outline the teaching method, present the methodology and results of the study in detail, and conclude with future plans and tasks.

2 Teaching Strategies and Approaches

The course is a compulsory first-semester subject for both the Mathematics Teacher Training Program (MT; experimental group) and the Mathematics BSc Program (BSc; control group), with content in the two being nearly identical. The course aims to deepen and practice the high school-level intermediate mathematics curriculum while laying the foundation for the advanced knowledge required for university studies. Based on years of experience, we have observed that students entering the BSc program typically possess deeper initial knowledge and have four weekly hours for the course, compared to two in the MT. This additional time allowed the control group to engage in more practice with both a higher quantity and difficulty of problems, enabling them to explore certain issues in greater depth. To address this disparity, we developed visual aids specifically for the MT group, aiming to bridge the knowledge gap and mitigate its impact.

For the experimental group, we created various simple graphics, animations, dynamic, and interactive resources. At least half of the tasks in each topic were supplemented with such visual aids, whether for in-class exercises, homework, or assignments. In this section, we demonstrate, through specific examples, how dynamic visuals and visual aids were integrated into high school mathematics problems for the experimental group. These tools not only added visual appeal but also effectively supported the development of problem-solving and modeling skills while improving text comprehension and problem-solving abilities.

While the control group also made use of traditional visualization tools—such as algebraic tables or graphs drawn on the board—they did not use any digital or interactive tools. The range and intensity

of visual methods applied in the experimental group went significantly beyond this baseline.

The experimental group was taught by the second author of the paper, so there was no need to train an external teacher in the methodology associated with the developed approach. The control group was instructed by another qualified high school mathematics educator with a similar professional background and enthusiasm. This ensured consistency in course quality and methodological approach, helping to mitigate potential teacher-related biases.

2.1 Simple Algebraic Visualizations

To address common algebraic errors observed in previous years, we created simple graphics aimed at making algebraic calculations more engaging. Studies (e.g., [17]) confirm that students can more easily organize their knowledge with the help of such visuals, leading to better retention and easier recall of concepts and methods. Our own experiences support these findings as well.

Unfortunately, many students struggle with understanding and correctly applying the Balance Method, and this also presents a challenge for them. To aid their comprehension, we created the following diagram, which visually illustrates the preservation of equality through equivalent transformations.

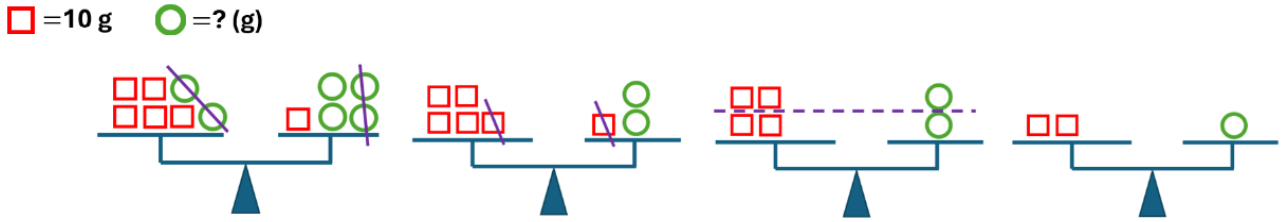

Figure 1: Visual Representation of the Balance Method

2.2 Simple Graphs

When analyzing inequalities, as well as equations and systems of equations, we find the function-based approach highly beneficial. Students often solve problems algebraically, as this is the method they were primarily taught in high school. However, representing the function's graph in a coordinate system not only makes the solution process shorter but also more intuitive (Figure 2), helping to clarify why a problem has no solution, a single solution, or multiple solutions.

Combining graphical and algebraic approaches enhances understanding, serves as a tool for verifying steps, reduces errors, and strengthens conceptual grasp. This integration encourages students to critically assess their solutions and gain deeper insights into mathematical relationships.

2.3 Animations, Dynamic and Interactive Teaching Materials

2.3.1 Developing a New Perspective

We created numerous visual teaching aids, primarily using the GeoGebra and MS PowerPoint. Unlike static diagrams, dynamic resources help students interpret and understand the role of parameters and

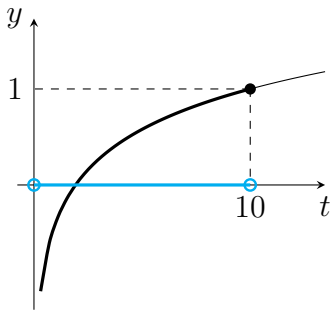

$$\lg(2x+1) < 1$$

$$\lg(t) < 1$$

$$0 < t < 10$$

Figure 2: Graphical Representation of Logarithmic Inequality

solve parameter-based problems correctly. They enable us to present mathematical concepts through novel and illustrative approaches.

The dynamic GeoGebra teaching aid shown in the Figure 3 and accessible via [9] was designed for the topic of inequalities involving absolute values.

In this application, the inequality

$$|x - a| \leq b$$

is examined through the analogy of illuminating with a flashlight. This representation visualizes the solution set of the inequality and its geometric interpretation for different parameter values. The direction of the inequality can also be reversed in the aid, and the right side of the diagram dynamically displays the standard graphical analysis.

This vivid representation of inequalities involving absolute values helps students grasp the concept of distance, which is essential for understanding abstract topics in calculus and avoiding incorrect algebraic solutions, such as $3 < x < -1$.

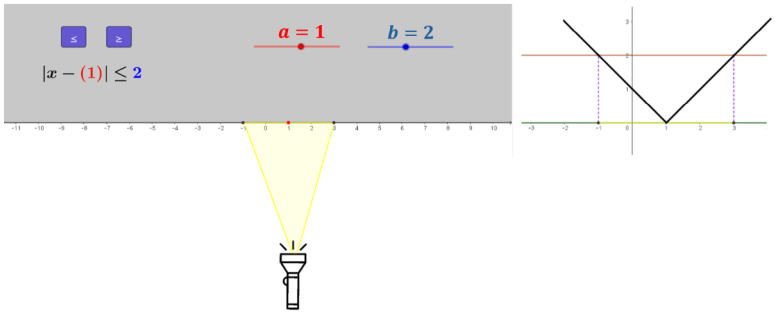

Figure 3: Graphical Analysis of Absolute Value Inequalities

Absolute value problems of this type are traditionally taught using case analysis. When appropriate, the graphical interpretation is drawn on the board by the instructor.

2.3.2 Word Problems

Word problems in mathematics are becoming increasingly challenging not only for high school students, but also for university students. This can be attributed, among other reasons, to the strong

correlation between problem-solving processes and reading comprehension skills [18], [3], which, according to PISA studies, are rapidly deteriorating [15]. We employed two alternative methods:

- Word Problem → Visual Aid → Model

It was particularly important to create animations and digital teaching aids for various word problems, as visual representation of the information-such as graphical depiction of the scenarios described in the tasks-significantly aids students in understanding the text. Students can independently interpret the mathematical problems underlying the word problems. Furthermore, dynamic, interactive teaching aids allow students to formulate hypotheses and solution ideas through individual experiments and observations (Figure 4).

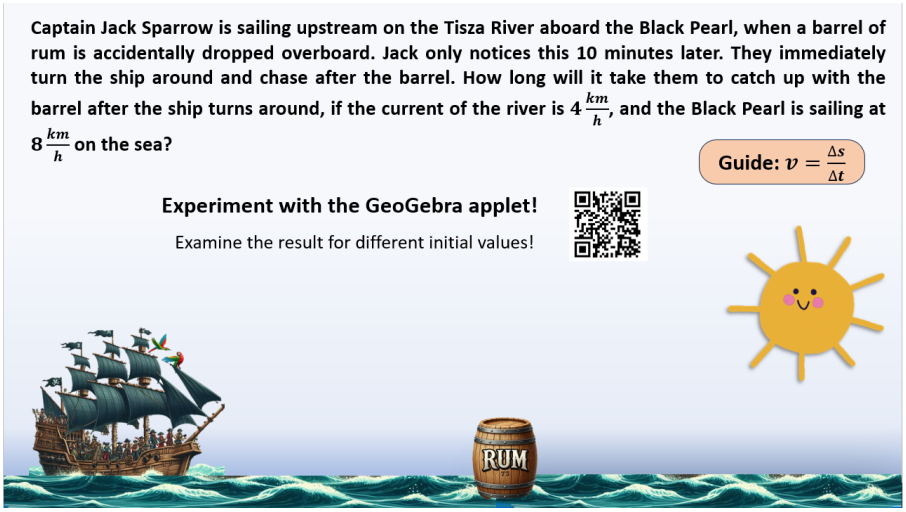

Figure 4: Digital Teaching Aid for a Motion Problem

In this learning environment, the instructor acts as a facilitator who supports students in using the program and helps them organize their solution ideas without dominating the educational process. This approach to word problems greatly encourages independent learning and fosters critical thinking through experimentation [2].

In traditional teaching approaches, word problems are typically processed in a linear sequence, following the Word Problem → Model steps, without the use of visual aids.

- Visual Aid → Word Problem → Model

In traditional instruction, the Visual Aid → Word Problem → Model approach to solving word problems is not applied at all. In relation to word problems, we incorporated creativity-demanding tasks into the teaching process of the experimental group. These tasks required students to create solvable word problems based on an image or animation (Figure 5).

In these types of tasks, students need to formulate and solve mathematical questions based on visual information. This develops their spatial imagination and abstract thinking [1], while also strengthening reading comprehension skills, as describing the problem they devised demands precise and clear text creation [8]. Additionally, visual-based tasks can increase students' motivation

[10], as they create an experiential learning environment that actively involves them not only in the solution process but also in problem creation.

As a homework assignment, students were tasked with formulating and solving a word problem based on the image and data shown in Figures 5 and 6 below.

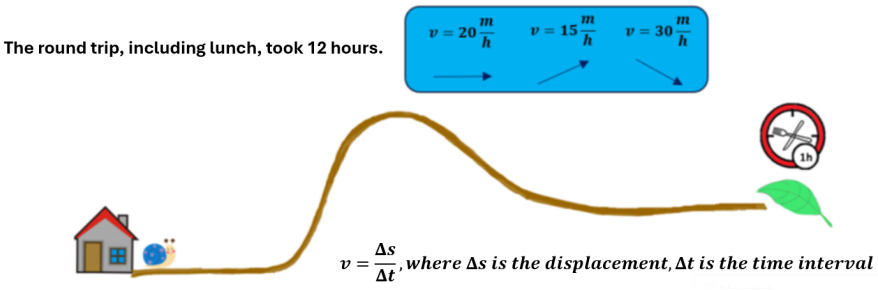

Figure 5: Creating a Word Problem Based on an Image

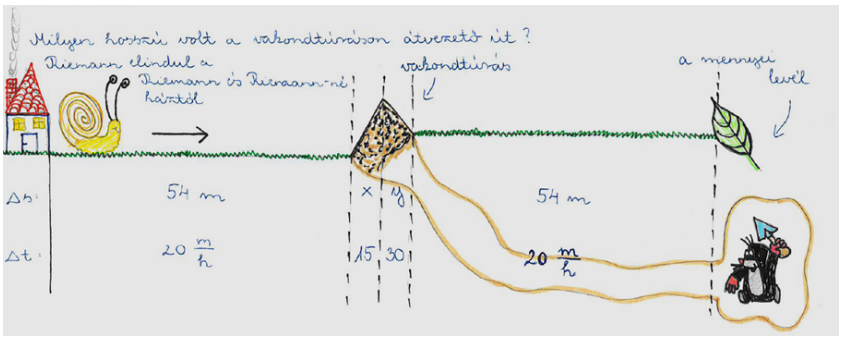

Figure 6: A solution detail submitted by an MT student for the task above

We observed that this processing approach encouraged interest even in more complex motion problems.

3 Experimental and Control Groups

All students from the respective programs participated in the study, with no selection process involved. Although advanced-level mathematics exams are not required for admission to either the MT or the BSc Programs, 5 out of 16 students in the experimental group (31%) and 13 out of 22 students in the control group (59%) had completed advanced-level exams. Therefore, we expected the MT students to have a significant initial disadvantage compared to the BSc students.

The curriculum for both groups followed the same problem book [13]. However, the experimental group had only 2 weekly hours compared to 4 weekly hours for the control group. Additionally, the BSc group's deeper mathematical subjects provided better opportunities to develop problem-solving, abstraction skills, and mathematical reasoning. Hence, we considered it a success of our method if the gap between the two groups did not widen.

4 Methodology of the Study

The experimental group engaged with the material using the proposed teaching method, whereas the control group was taught through conventional approaches. Our aim was to determine how visualization affects student performance, measured through a diagnostic test at the beginning of the semester, a final test at the end, and midterm assignments.

The initial test primarily included tasks from the intermediate-level high school curriculum, while the final test incorporated advanced-level tasks studied during the course. The initial test was completed by 16 students from the experimental group and 22 from the control group, while the final test was taken by 15 students (4 with advanced-level high school mathematics) in the experimental group and 14 students (10 with advanced-level mathematics) in the control group.

Both groups took the same test under identical conditions without the use of any aids. Motivation to perform well was equally encouraged by incorporating test results into the final course grade.

5 Results of the Study

5.1 Comparison of Diagnostic Test Results

The comparison of the initial and final tests is illustrated using bar charts to display the percentage of completely correct answers. The width of the bars corresponds to the group size. The magenta horizontal line indicates the average performance of the respective group, while the blue bars show the averages for students with intermediate-level exams, and the green bars represent the averages for students with advanced-level exams.

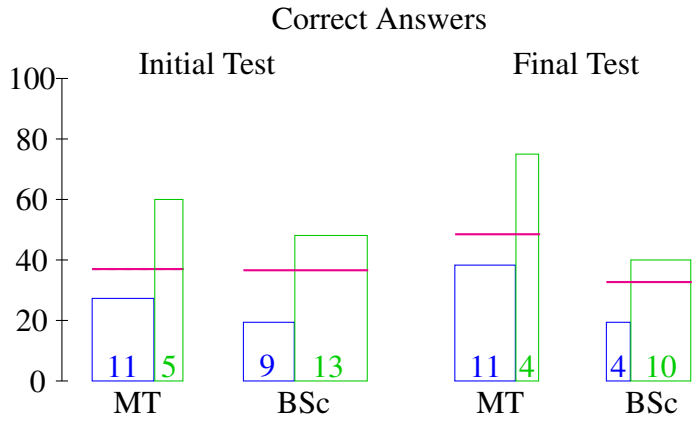

Several noteworthy and unexpected results emerged:

1. At the beginning of the semester, the diagnostic test results showed a minimal advantage for the MT group over the BSc group, based on average performance. However, this difference was minimal because the ratio of intermediate- to advanced-level exams varied significantly between the groups. When comparing students with the same level of high school exams, the MT group's performance was noticeably better.

2. By the end of the semester, despite fewer BSc students taking the final test, and with the ratio of advanced-level students improving (from 13–9 to 10–4), the MT students achieved significantly better average results. Not only did they match the overall average of the BSc group, but their performance clearly exceeded it.

3. Comparing the two tests, the final test was naturally more challenging. This is evident from the weaker average performance of BSc students with advanced-level exams. In contrast, MT students showed significant improvement among both intermediate- and advanced-level exam holders, demonstrating the success of our method.

4. The diagnostic test also confirmed that students with intermediate-level high school exams generally arrive with inadequate calculation skills. This was already noted in the need to create a visualization for the Balance Method (Figure 1). It is clear that greater emphasis on fundamental calculation skills is necessary at the intermediate level.

A similar conclusion can be drawn if we evaluate the tests using the traditional grading guide applied to national high school exams:

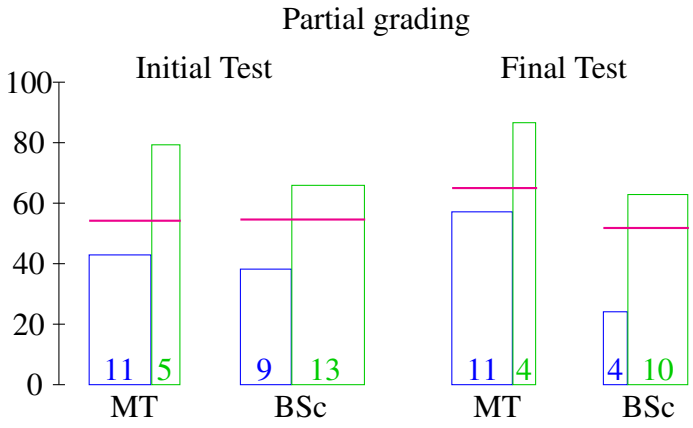

For students who completed both the pre-test and post-test (N=29), we examined the effectiveness of the method using non-parametric statistical tests. First, we used the Wilcoxon signed-rank test to determine whether there was a statistically significant difference between the pre-test and post-test scores of individual students. In the MT group, we found a significant improvement ($p=0.0045$), indicating that students' performance improved in a statistically verifiable manner over the semester. In contrast, no significant change was observed in the BSc group ($p=0.5749$), meaning that their results did not show a statistically detectable shift compared to the pre-test.

Next, we used the Mann–Whitney U test to compare the two groups, first in terms of post-test performance and then in terms of the degree of improvement. We found no statistically significant difference in post-test scores between the groups ($p=0.1538$), suggesting that their final performance levels were similar. However, the difference in improvement was statistically significant ($p=0.0415$), indicating that students in the MT group demonstrated a significantly greater degree of progress over the semester than those in the BSc group. The effect size measured by Cliff's delta (Cliff's delta = 0.45) indicates a medium effect, suggesting that the instructional method applied in the MT group had a meaningful impact on student development.

These findings suggest that the method used in the MT group supported student learning more effectively than the traditional instructional approach used in the BSc group. While no significant difference was found in the final performance between the two groups, students in the MT group exhibited statistically verifiable greater improvement throughout the semester.

While partial scoring resulted in higher percentages, it masked the severity of the problem. Therefore, in subsequent analyses, we focused exclusively on the percentage distribution of completely correct answers to highlight shortcomings.

5.2 Comparison of Common Tasks in Midterm Tests

Due to the differing number of contact hours and, consequently, the varying depth of content coverage, it was not feasible to fully align the midterm tests, which formed the basis for the students' grades.

Only three common tasks were included, allowing for their comparative analysis.

The percentage distribution of completely correct answers is as follows:

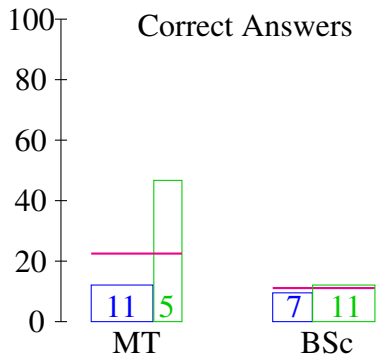

Despite the control group being allowed to use the standard mathematical table during the test, the complexity of the tasks and the aforementioned deficiencies in calculation skills resulted in very poor performance in both groups. Nevertheless, it is evident that the average performance of students with intermediate-level final exams in the MT group matches that of students with advanced-level final exams in the BSc group. In our opinion, this is due to the effectiveness of the visual method, as we will substantiate in the following section.

6 Relevant Examples

Due to space constraints, we will detail only the three most illustrative tasks to demonstrate the positive impact of visualization. Alongside the percentage of correct solutions, we will also present the frequency of diagram usage. Furthermore, we will briefly address problem-solving errors and include a selection of diagrams created by students.

6.1 Task: *Solve the following inequality:*

Initial test	Final test
$x^2 - 9 \geq 0$	$x^2 + 2 \geq x$

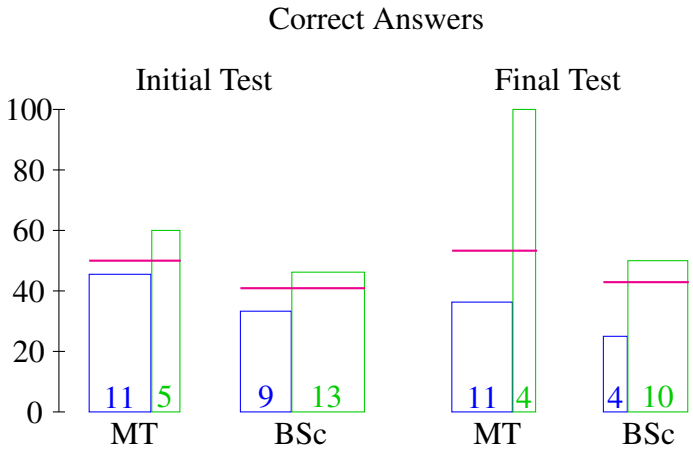

Since solving the second task requires more complex reasoning, we neither expected nor observed better average performance. A small portion of the errors stemmed from calculation mistakes, while the majority resulted from incorrect square root extraction, reflecting a reliance on algebraic methods.

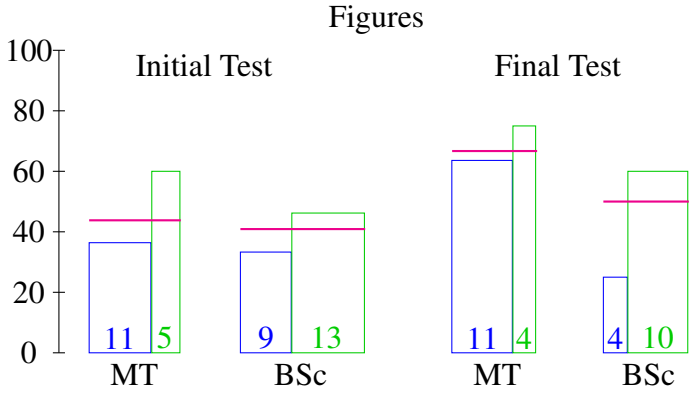

By the end of the semester, the proportion of students in the experimental group who created diagrams increased significantly, with nearly 70% of them producing some form of visualization for the task. The visualizations took various forms, indicating that the students did not simply replicate a single solution type (Figure 7).

6.2 Task: *How many solutions does the following equation have?*

$$|x + 3| + 1 = x + 4$$

This type of problem appeared only in the final test. The following results were obtained:

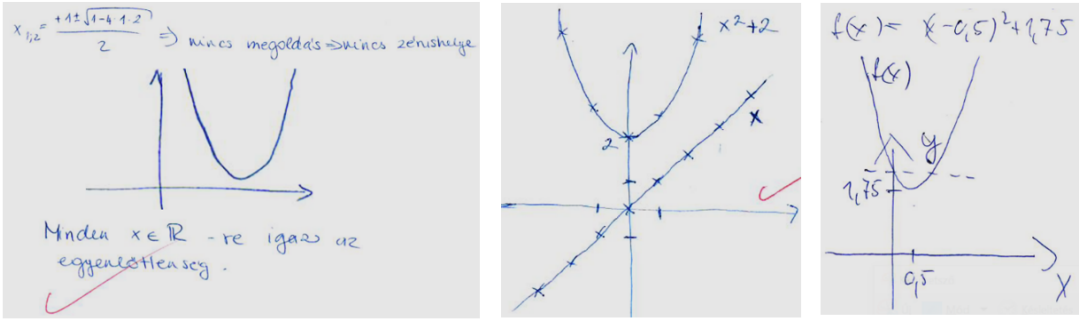

Figure 7: Diagrams created by the experimental group for Task 6.1

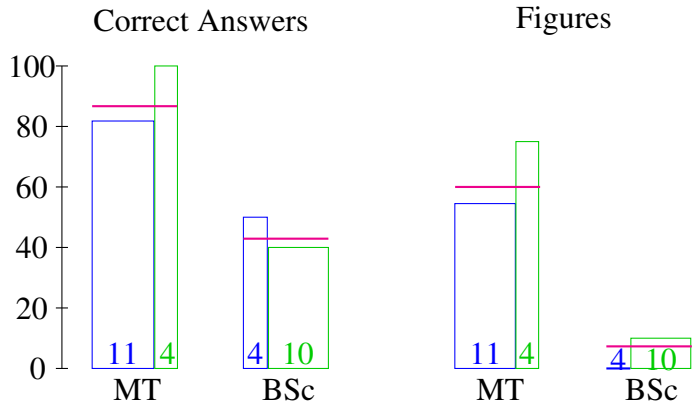

The experimental group achieved significantly better and outstanding results compared to the control group, with a much higher proportion of diagrams created. The errors stemmed from the incorrect use of the algebraic method of case separation. Based on this example, the role of graphical representation in providing the correct final result is convincing (Figure 8).

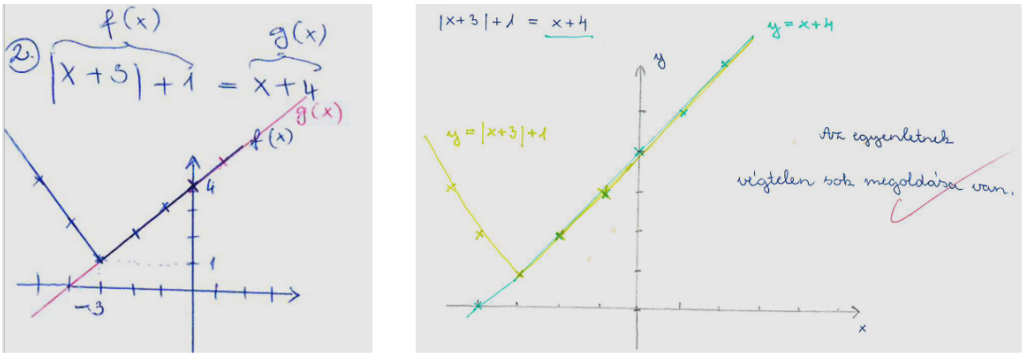

Figure 8: Diagrams created by the experimental group for Task 6.2

6.3 Task: *Solve the following inequality:*

$$2\cos^2 x - 5\sin x - 4 \leq 0$$

Finally, we analyze in detail the task from the mid-term test on which students performed very poorly, in order to better understand which steps posed difficulties and where visualization provided support. For this purpose, the solution of the task was divided into two parts.

- **Part 1:** Based on the trigonometric identity $\cos^2 x = 1 - \sin^2 x$, the formulation of the quadratic inequality by introducing a new variable, followed by the correct solution of the equation and then the inequality.

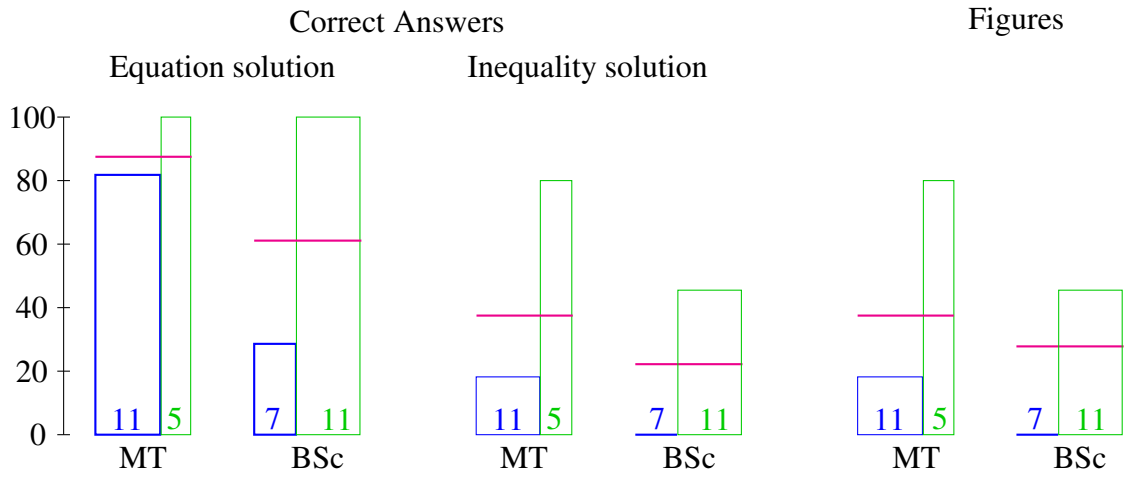

The experimental group performed better even in the first part of the task. Both groups were able to correctly formulate the quadratic inequality at a similar rate; however, the use of the quadratic formula posed slightly more problems for the control group. It was evident that transitioning from the equation to the inequality remained a challenge for students, and unfortunately, no BSc student with an intermediate-level high school graduation exam managed to complete this step successfully. Furthermore, it is crucial to note that all students who created diagrams solved the inequality flawlessly.

- **Part 2:** The correct solution of the trigonometric equation and inequality.

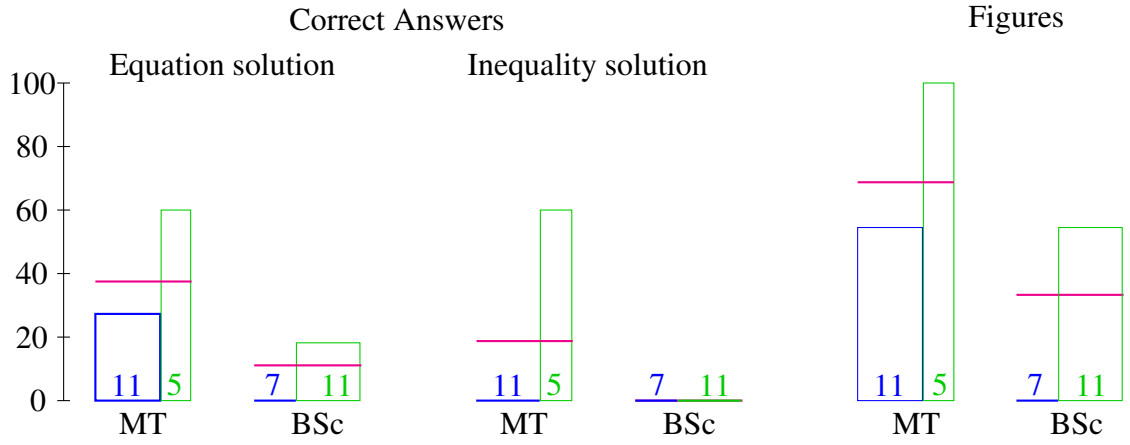

The experimental group not only created visualizations for the task at a significantly higher rate, but, presumably with the help of the diagrams, were also able to solve the trigonometric equation at

a higher rate. The solution to the trigonometric inequality was successfully achieved only by the MT group, who either read it off from the unit circle or from the graph of the function (Figure 9). This again demonstrates that graphical representation plays a key role in providing the correct final result.

The most common mistake resulted from incorrect diagram or graph creation, but several students also made errors when converting the angle from degrees to radians. Unfortunately, some students from the MT group, despite providing the correct graphical solution to the inequality, incorrectly wrote the interval of the solution set. These were naturally not included in the correct solutions, though it was simply a minor oversight.

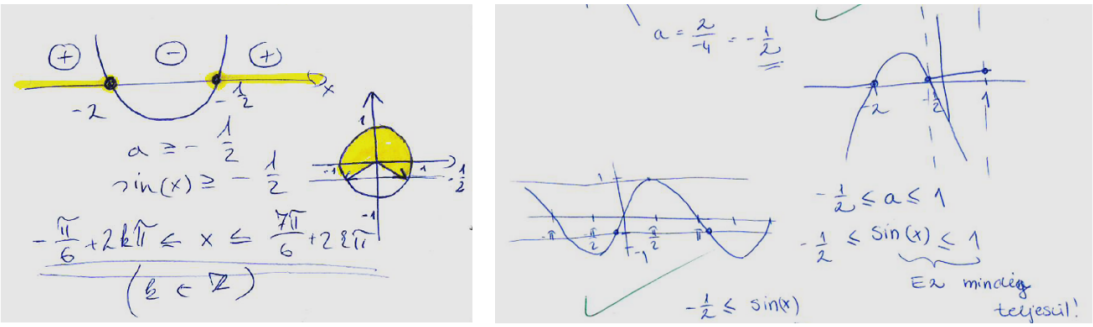

Figure 9: Diagrams created by the experimental group for Task 6.3

7 Student feedback

We assessed the impact of visualization on student attitudes based on classroom work, as well as through assignments and homework, and students were also able to provide anonymous written feedback about the course at the end of the semester.

The attitude change was clearly indicated not only by the significantly better classroom engagement than usual, but also by the fact that even those students who otherwise struggled to follow the solution process began to think through the problems using graphs and diagrams. This suggests that the method stimulated creative problem-solving, and the students focused not only on traditional algebraic solutions. It is particularly important to note that by the third lesson, every student in the experimental group started tasks independently, without exception. In contrast, the control group still left several tasks incomplete in the last test.

The quality and detail of the submitted tasks and homework clearly showed that students effectively and enthusiastically used the supplementary materials. After the class, they were already interested in what visual materials they would receive or what they would need to prepare themselves. They looked forward to the upcoming tasks with sincere anticipation. The effectiveness of the supplementary materials is further supported by assignment data: the average submission rate for the five mid-semester assignments was 88.75%, and students achieved an average accuracy of over 70% based on partial scoring.

The above conclusions were also reflected in the end-of-semester feedback:

"The classes were good, especially the GeoGebra animations were really cool."

"The idea is great, and it would be good to have a course like this in several semesters."

"The course helps expand and deepen high school material."

"Very important course, it helped bring students with different levels of prior knowledge to the same level."

"It was my favorite class."

"Very enjoyable, we made good progress, clear and fair expectations."

8 Conclusion

Surprisingly, the average of the pre-semester assessment showed a minimal advantage for the experimental group over the control group. In the case of the experimental group, we supported the review and expansion of high school knowledge with visual aids and new presentation methods. This engaging, visually appealing approach not only made learning more motivating but also encouraged students to engage in independent learning. Our primary goal was achieved: the experimental group's results, due to the differing number of lessons and the varied depth of mathematics subjects, did not fall short of the control group's level.

Despite the small sample size, the presented data clearly demonstrate that we not only met the minimal expectations but also achieved results far surpassing our goals. The performance of the experimental group significantly increased, further extending its advantage over the control group. Furthermore, the increased use of visualizations clearly demonstrates that students in the experimental group adopted a new, creative approach to problem-solving, confirming the method's validity, practicality, and effectiveness, along with its positive influence on student attitudes.

While we did not find studies specifically addressing the impact of visualization over a full-semester university course, particularly in the context of mathematics teacher education versus mathematics training, several studies have demonstrated the significant effect of GeoGebra in comparison to traditional teaching methods at the university level [5] [16]. These findings are in line with our own observations, which show that visual tools, such as GeoGebra, not only have a significant impact on academic results but also positively influence student attitudes.

9 Future Directions

Following the completion of the article, we plan to further revise the curriculum of the Practical Courses, adapting it to the lower knowledge level of students studying under the 2020 National Core Curriculum. Based on the results of the research, the aim is to further develop and align the methods so that future students can apply visual tools and methods more effectively in their mathematical studies.

Later this year, we aim to repeat the testing of our method within a larger course of over 100 students. We plan to refine the methods, such as expanding the types of visualizations and tailoring them to meet students' individual needs.

Last but not least, a key task is the detailed description of the teaching methodology, which we believe is an essential part of the method's success, alongside the tasks equipped with visualizations. This will also help our colleagues successfully adapt our method to their own teaching fields.

References

[1] Arcavi, A. (2003). The role of visual representations in the learning of mathematics. *Educational Studies in Mathematics*, 52(3), 215–241.

[2] Atnafu, M., & Zergaw, D. (2020). Availability of resources, mathematics teachers' knowledge, and attitude towards mathematics visualization as predictors of the development of students' visualization in mathematics. *Bulgarian Journal of Science and Education Policy*, 14(2), 382–416.

[3] Boonen, A. J., de Koning, B. B., Jolles, J., & van der Schoot, M. (2016). Word problem solving in contemporary math education: A plea for reading comprehension skills training. *Frontiers in Psychology*, 7, 191. https://doi.org/10.3389/fpsyg.2016.00191

[4] Csíkos, C., Szitányi, J., & Kelemen, R. (2012). The effects of using drawings in developing young children's mathematical word problem solving: A design experiment with third-grade Hungarian students. *Educational Studies in Mathematics*, 81, 47–65.

[5] Diković, L. (2009). Applications GeoGebra into teaching some topics of mathematics at the college level. *Computer Science and Information Systems*, 6(2), 191–203.

[6] Dockendorff, M., & Solar, H. (2018). ICT integration in mathematics initial teacher training and its impact on visualization: the case of GeoGebra. *International Journal of Mathematical Education in Science and Technology*, 49(1), 66–84.

[7] Engelbrecht, J., Llinares, S., & Borba, M. C. (2020). Transformation of the mathematics classroom with the internet. *ZDM*, 52, 825–841.

[8] Fischer, F., et al. (2010). Deep-level comprehension of science texts: The role of visualizations and self-explanation prompts. *Learning and Instruction*, 20(6), 465–475.

[9] GeoGebra (2024). GeoGebra Teaching Aid. https://www.geogebra.org/m/dumgtbkf

[10] Goldin, G. A. (2014). Perspectives on emotion in mathematical engagement, learning, and problem solving. *International Journal of Mathematical Education in Science and Technology*, 45(1), 75–88.

[11] Lin, C. (2022). Use Progressive Visualization Teaching Method to Improve Learning Motivation of Calculus Courses. *The European Journal of Social & Behavioural Sciences*, 31(2), 92–110. https://doi.org/10.15405/ejsbs.315

[12] Marin, K. A., & White, S. J. (2023). Generation Z goes to math class: How the effective mathematics teaching practices can support a new generation of learners. *School Science and Mathematics*, 123(1), 31–37.

[13] Máder, A., & Bogya, N. (2019). *Matematikai alapismeretek, Egyetemi példatár*. Szegedi Tudományegyetem, Bolyai Intézet.

[14] Nurhajarurahmah, S. Z. (2021). Students' multiple intelligences in visualization of mathematics problem solving. *Journal of Physics: Conference Series*, 1752(1), 1–7.

[15] OECD. (2022). *PISA 2022 Results (Volume I and II): Country Notes*. https://www.oecd.org/en/publications/pisa-2022-results-volume-i-and-ii-country-notes_ed6fbcc5-en/hungary_3df2ae68-en.html

[16] Pattanapiboon, W., & Nishizawa, H. (2024). Impact on Student Learning Outcomes in Mathematics Using GeoGebra. *Asian Technology Conference in Mathematics (ATCM 2024)*, KOSEN-KMITL, Thailand.

[17] Presmeg, N. (2020). Visualization and learning in mathematics education. *Encyclopedia of Mathematics Education*, 900–904.

[18] Pongsakdi, N., Kajamies, A., Veermans, K., et al. (2020). What makes mathematical word problem solving challenging? Exploring the roles of word problem characteristics, text comprehension, and arithmetic skills. *ZDM Mathematics Education*, 52, 33–44. https://doi.org/10.1007/s11858-019-01118-9

[19] Seemiller, C., & Grace, M. (2017). Generation Z: Educating and engaging the next generation of students. *About Campus: Enriching the Student Learning Experience*, 22(3), 21–26.

[20] Tekeli, M., & Fülöp, V. (2024). Látvány, élmény, ismeret. *Gradus*, 11(1). https://doi.org/10.47833/2024.1.CSC.003

Revealing the secrets of the number pi and copper number algorithms

Adrián Silva Ulloa
e-mail: adrian.silva@uft.cl
Faculty of Civil Engineering
University Finis Terrae, Santiago, Chile

Abstract

The present text constitutes a compilation of humanity's fervour to ascertain the enigmatic number pi, entitled "Revealing the secrets of the number pi and the algorithms of the copper number". In this essay, we seek to illuminate the hidden intricacies of this number, explore its potential connections with other numerical entities, investigate the alleged falsehoods associated with its proponents, and delve into more complex subjects by employing calculus, series, and contemporary technologies. The document's intention is to demonstrate the methods and justify the interesting procedures that lead to the solution of numerical problems, with a particular focus on the number pi. It is a valuable resource for mathematicians, computer scientists, and anyone with an interest in formulas or the human ingenuity behind their discovery. The author posits that each contribution of knowledge leads to a subsequent step, and the discovery of the so-called "absolutely convergent series" will allow the reader to devise an algorithm to find all the digits of pi.

Introduction

We provide the reader with basic instructions to deepen the topics of classical geometry, use of freely available computational tools and the background of the most relevant concepts of numerical calculus such as series and limits, which will allow us to contextualize theoretical foundations to unravel the enigmatic number pi. From the perspective of mathematical authors, in history, we can perceive the longing and inspiration that lead to the discovery of an emblematic problem defined by Archimedes as “The squaring of the circle” and later named by Euler with the Greek letter (pi) (π). A problem that existed long before and that apparently in all ages unified wise men in a common purpose. All these authors wrote about it, committed themselves to obtaining it, motivated by being the first to see what others had not been able to, and then, in the face of failure and resignation, they gave way to future generations.

One of the most important numbers in mathematics is the number pi, probably not a common or necessary number for many people. However, this number is present in a large number of equations and is part of the solution of many scientific statements. Some important examples, it is present in Albert Einstein's famous equations of general relativity, in the cosmological constant of the gravitational curvature tensor $G_{\mu v} = \frac{8\pi G}{c^4} T_{\mu v}$. It is also present in the Heisenberg uncertainty principle, which introduces a fundamental limit of particle theory and where the energy of a photon with angular frequency $\omega = 2\pi f$, can be expressed as $E = \bar{h}\omega$, which is one of the most important formulas of quantum mechanics **[8]**. The number pi is found in many other formulas and equations, in probability theory, in more tangible matters, perhaps, such as in the geometry of space, and it is because of this that some scientists distinguish it with a metallic name of “copper”, since it is in many cases the essence of things.

The challenge associated with the number pi is to find more and more of its decimals, since it is irrational, transcendent and to get to it will have to pass first through infinite limits and Euler's e number. Obtaining its digits became a kind of competition among scientists and computer scientists in the world. The current record is held by a data storage company called Solidigm **[10]**, who announced it in March of this year 2024, before 2023 the record belonged to Google Cloud. The company announced on March 15 (date that celebrates the day of the number pi within the year) that they had managed to reach the mark of 105 trillion digits of this number, but this

changes very fast and it seems to me that already in August this year is around 300 trillion decimals discovered, using computational methods, which demands large amount of memory and large amount of processes. This may be crazy, but Akira Haraguchi, a Japanese engineer and mental therapist, is known for breaking the world record for memorizing digits of the number pi, which he managed to remember 100,000 digits and demonstrated it on October 3, 2006. Akira started reciting the decimals of pi in the plenary hall of the city hall of Kisarazu, Japan, and it took him a total of 16.5 hours to recite all the digits he had memorized without making any mistakes **[9]**. Could this be another obsession of the human fervor for discovery? What could be obtained if we achieve more decimals of pi, some believe that something can happen, and the fact of being able to work with infinitely large numbers such as Graham's number or others incredibly accurate as pi, could perhaps open doors to unexplored areas of knowledge.

In this essay, we will develop background issues that lead to obtaining these decimals of pi and knowing that computers are capable of so much more, we will be able to see the digits of pi and help Akira recite the decimals to count from 100,001 onwards. We will explain motivations, use tools and give an account of some secrets, which are kept in patents of those who have made this work a professional activity. We will explain the most famous methods and describe how to arrive at a new algorithm, of our authorship in Python, which we will call Algorithm ASS.

The devastating problem of squaring a circle

It is imperative to note that in order to approach geometric structures, the utilization of Geogebra is strongly recommended.

Throughout history, mathematicians and geometers, whether amateurs or seasoned professionals, have consistently endeavored to explore these concepts.

The objective is to derive a square with an area equivalent to that of a circle through a finite mechanical sequence of steps. In antiquity, this process entailed the repeated use of a compass, transforming a square into a circle and vice versa.

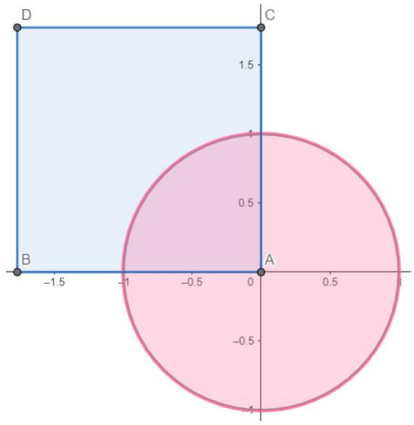

Figure 1. Graphic relationship of the same area, expressed in a square and a circumference.

The crux of the challenge lies in the intractability of obtaining a segment of length equal to the irrational number pi, approximately $\pi \approx 3.141592653589794$. However, it is possible to obtain a segment that measures an irrational number of a similar nature, such as the numbers:

The graphical relationship of the same area, expressed in a square and a circumference, is the same for $\sqrt{2}$ (the diagonal of a square with a side length of 1) or $\sqrt{5}$ (the hypotenuse of a triangle with legs of lengths 2 and 1), or in general for $\sqrt{2}$. This revelation, however, was previously unknown, and throughout history, the same problem persisted, prompting mathematicians to engage with it repeatedly. Perhaps because this kind of problem did not seem too complex for a somewhat experienced geometrician, many claimed its solution, like the root of 2, was possible.

Part 1. What you need to know before knowing pi

This part is intended to investigate foundational aspects of mathematical thinking and to recognize geometric and mathematical representations that establish numerical regularities. Processes that occurred in the history of mankind and are closely related to the number pi.

1.Perimeter and area of a circle

The Egyptians are credited with many of the primary geometric and mathematical concepts that the Greeks used in their writings. It is evident that Egyptian, Mesopotamian, and Indian mathematics inspired Greeks such as Thales of Miletus (between 624 B.C. - 546 B.C.) and Pythagoras (582 B.C. - 507 B.C.), who gave the initial start to Greek mathematics, or Hellenic mathematics, after the time of Alexander the Great and before the Roman Empire, around 27 B.C.

The Egyptians, using an approximation of the number pi, made their calculations evident when they tried to roll a circle with a drop of ink on papyrus, with which they had an excellent approximation of the perimeter $2\,\pi\,r$, applying proportions showed regularities that showed signs of possessing a secret factor implicit in the operation with $2\,\pi$, which was related to the perimeter of the circle of radius 1.

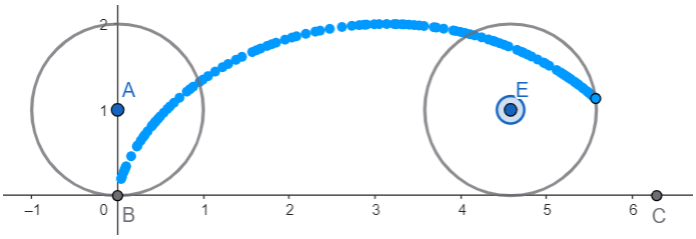

Figure 2. Rotational displacement of a wheel starts from a mark until its circumference is reached.

The Rhind Papyrus (or Ahmes Papyrus, its author dates from about 1650 B.C.) to how to find the value of π by approximating the area of a square with sides 4 and then 8 to that of a circle with diameter 4 and then 8. The area of the circle is approximately equal to the area of an octagon (irregular) of 12 and 24 sides. More details are in the publication of **[18]** Beckmann P. (1971) Publishes A History of Pi.St. Martin's Press.

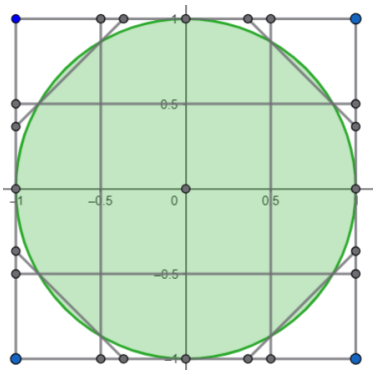

Figure 3. Circle inscribed in a Square. The Square is divided to establish an approximate measurement of each side of the irregular polygon, approximating the perimeter.

$$3+\frac{1}{9}+\frac{1}{27}+\frac{1}{81}=\frac{256}{81}\approx 3.16$$

2. Archimedean Polygons

It was Archimedes (Archimedes of Syracuse ac. 287 - ac. 212, with an astronomer father) who formalized the problem and managed to have a good approximation of the area of a circumference. He also managed to do many other things, he was a renowned mathematician of the time and was very advanced with his ability to perform physical, mechanical, hydrostatic and other applications, in almost all areas of science. In particular, when he needed the area or perimeter of a circle, he knew that a constant was implicit here, since when modifying the size of the radius in the formulas of the area $Pi\,\cdot\,r^2$ and the perimeter $Pi\,\cdot\,2r$ (of his own authorship), it was only necessary to multiply by this constant Pi. Then he proposed to approximate the perimeter of a circumference of radius equal to 1 (where the unit could be the customary one in Greek times, **1 palame**, which was the width of the palm of the hand without the thumb) and he was aware that then he only had to

divide it in half. He considered from the center the 360 degrees of the complete angle, dividing it into equal parts depending on the number of sides of an inscribed polygon and another circumscribed to the circumference. He used trigonometry on each concentric triangle to obtain the lengths of the sides of each polygon and increased the sides of each polygon to "enclose" or bound the value of the perimeter length measure **[5]**.

Thus, depending on the number of sides of the polygon, the cosine of the angle is determined. This task was undertaken by Archimedes with a polygon of 96 sides. Let us recall that r=1, and $\frac{360}{96} = \frac{15}{4} = 3^o45' = 3.75^o$ **[2]**

$$2\pi \approx 96 \cdot \sqrt{2 - 2\cos(3.75^o)} \approx 6.282 = \frac{3141}{500} \quad \text{So:} \quad \pi \approx \frac{3141}{1000} = 3.141$$

He succeeded in bounding pi from below with the inscribed polygon [6], and then from above with the circumscribed polygons of 96 sides, thereby obtaining bounds for the value of pi.:

$$3.141 < \pi < 3.142$$

$\alpha = 360/N$ central angle of each concentric triangle starting from one of the sides of the N-sided polygon.
Lc will be the side of the circumscribed polygon.
Li will be the side of the inscribed polygon.
r will be the radius of the circumference, which will be 1.
N = 6 is the case of the figure on the right. Then:

$$\frac{Li/2}{r} = \sin\left(\frac{\alpha}{2}\right) \quad y \quad \frac{Lc/2}{r} = \tan\left(\frac{\alpha}{2}\right)$$

If we look only at the situation of the inscribed polygon, it is deduced by trigonometric identity of the mean angle **[1]**:

$$Li = 2r\sin\left(\frac{\alpha}{2}\right) = 2r\sqrt{\frac{1-\cos(\alpha)}{2}} = r\sqrt{2 - 2\cos\alpha}$$

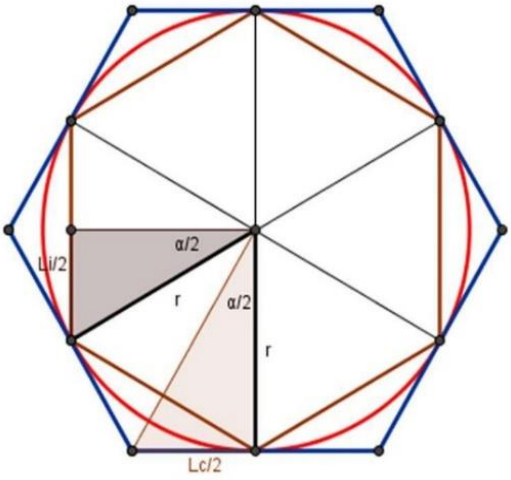

Figure 4. By regular polygons inscribed and circumscribed to the circumference of radius 1.

Then, according to the number of sides of the polygon, the cosine of the angle is determined. Archimedes did this task with a 96-sided polygon. Recalled that $r = 1$, and $\frac{360}{96} = \frac{15}{4} = 3^o45' = 3.75^o$ **[2]**

$$2\pi \approx 96 \cdot \sqrt{2 - 2\cos(3.75^o)} \approx 6.282 = \frac{3141}{500} \quad \text{Thus: } \pi \approx \frac{3141}{1000} = 3.141$$

He was able to bound below pi with the inscribed polygon **[6]** and then above the value with circumscribed 96-sided polygons, obtaining dimensions for the value of pi:

$$3.141 < \pi < 3.142$$

3. Fractional representation of real numbers by Euclid's algorithm

Approximation of a decimal.

Let a, b be any positive integers, with $a \neq b$ and $a < b$. What we want is to obtain an approximation of the fraction $\frac{a}{b}$. By the division algorithm we know that there always exists $q_0 \in \mathbb{Z}$ such that we can write: $b = aq_0 + r_0$ with $0 \leq r < a$. Graphically, the situation is:

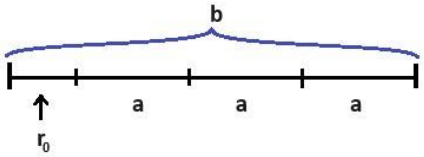

For the case in which $q = 3$
also exists $q_1 \in \mathbb{Z}$ and r_1 such that:

$$a = r_0q_1 + r_1 \text{ with. } 0 \leq r_1 < r_0$$

This is interpreted with the graph:

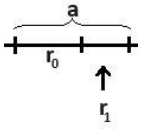

For the case in which $q_1 = 1$

Thus, we summarize that:

$$\frac{a}{b} = \frac{a}{aq_0 + r_0} = \frac{1}{\frac{aq_0 + r_0}{a}} = \frac{1}{q_0 + \frac{r_0}{a}} = \frac{1}{q_0 + \frac{r_0}{r_0q_1 + r_1}} = \frac{1}{q_0 + \frac{1}{\frac{r_0q_1 + r_1}{r_0}}} = \frac{1}{q_0 + \frac{1}{q_1 + \frac{r_1}{r_0}}}$$

As you can see, a convenient stepwise decomposition occurs. Now if the purpose is to have as good an approximation as we want and we will get to one of the finites $\frac{r_{n+1}}{n}$, we will replace them with a value like 1.

For example, let's obtain by this algorithm a reasonable fractional approximation for the decimal number 0.5555 and use all the decimals that the calculator gives us. We start by first asking how many times the unit can be contained in 0.5555 and since it is not, then: $0.5555 \approx 0 + \frac{1}{b}$. We decompose b asking ourselves how many times the first remainder 0.5555 is contained in the unit, from the question $\frac{1}{0.5555} = 1.80018\cdots$, the answer is 1, and we say: $0.5555 \approx \frac{1}{1+\frac{1}{c}}$. We continue decomposing c with remainder $r_1 = 1 - 0.5555 = 0.4445$, and ask ourselves how many times is contained in 0.5555, the operation is $\frac{0.5555}{0.4445} = 1.24971\cdots$, and the answer is 1 again. We already have: $0.5555 \approx \frac{1}{1+\frac{1}{1+\frac{1}{d}}}$. Now, we continue with the next remainder $r_2 = 0.5555 - 0.4445 = 0.111$

And we answer how many times it is contained in 0.4445, with the operation $\frac{0.4445}{0.111} = 4.0045$, the answer is 4.

If we leave the algorithmic approach up to this point, we obtain: $0.5555 \approx \frac{1}{1+\frac{1}{1+\frac{1}{4}}} = \frac{5}{9}$.

You can confirm that this fractional approach is of very good quality.

Decimal approximation of the root of 2. Let's try with another number, let's get a fractional approximation of the number $\sqrt{2}$, which we know is irrational and use Geogebra to recognize with the compass when one segment is contained in the other **[4]**.

Let's start with a segment that measures this value I am referring to the diagonal of the square, of side one unit. You can verify by the Pythagorean Theorem this statement, being the hypotenuse of one of the halves of the square and being right triangles, the measure of the diagonal is exactly $\sqrt{2}$. Now we can have a geometric representation, using a compass. We start with a circle with center at the lower left vertex and radius 1, it responds to the idea that how many times the side of the square is contained in its diagonal, it digs only once. The excess of the diagonal (outside this first circle) ED, is taken up by the radius of another circle, which, with another of equal size, indicates that this excess is contained twice on the other part of the diagonal FE and GF. Continuing, AG is contained twice over the other component.

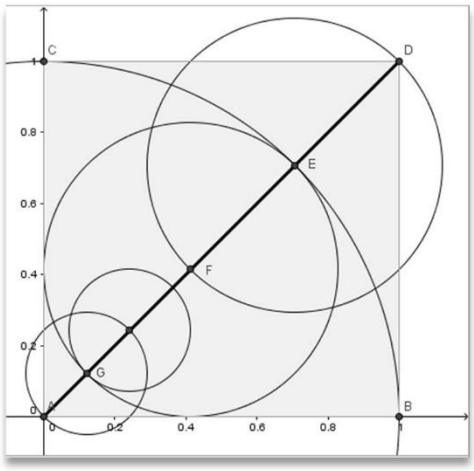

Figure 5. Subdivision of the diagonal of a square with the Geogebra digital compass.

This process is recorded as follows, the times that one segment is contained over the other is in dark color:

$$\mathbf{1}+\frac{1}{\mathbf{2}+\frac{1}{\mathbf{2}+d_3}}=\mathbf{1}+\frac{1}{\mathbf{2}+\frac{1}{\mathbf{2}+\frac{1}{\mathbf{2}+\frac{1}{\mathbf{2}+d_6}}}}=\frac{99}{70}=1.414285714$$

As you can see this compass procedure is exactly Euclid's algorithm. Thus, we obtain a reduced fraction, which has a very good approximation to the fourth decimal place. $\sqrt{2}$ = 1.414213562…

Euclid's algorithm allows us to obtain the decimals with the desired precision, as it is a nomenclature, modern science calls it "continuous fractional form" and has a presentation format, which in this case is $[1;\overline{2}]$.
Some scholars took this very seriously and you can see how an amateur mathematician defined a method that repeatedly included the root of 2, with which he managed to calculate the exact perimeter of a circumference, see **[7]**.

4. Hippocrates lunula area

While the central problem of the "squaring of the circle" remained unsolved more than 240 years before Archimedes, other equally important issues were still around, and the news of the demonstration of the lunula of Hippocrates [Greek mathematician Hippocrates of Chios, 470 BC] spreads. This argumentation came to create hope also in the squaring of areas of a part of the circumference, which could serve to continue the work with the entire circumference.

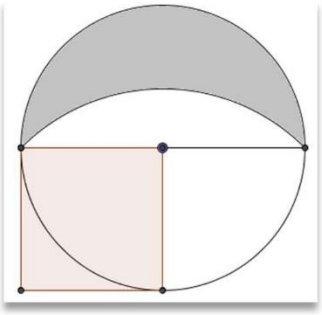

Figure 6. Square of the Hippocrates lunula. The area of the square and the lunula are equal.

The figure on the left corresponds to the squaring of the lunula, a fact that highlights the fervor of this type of theme at the time.

These demonstrations were made with operations similar to the famous Pythagorean Theorem (published around 510 BC), by which the Pythagorean school was created in Magna Graecia, a school of thought that combined philosophical, mystical and scientific aspects. It is that the Pythagorean Theorem was judged by history and it seems to have been discovered much earlier, the Babylonians already used it.

Later, in another part of the world, the Arab mathematician Alhacen (945-1040 AD), recovered the same statement from the Lunulas. Perhaps he found the source, but at that time traveling was very difficult, the publications were handmade and possibly the temptation to be the author of these subjects in another region allowed to be valued among his peers, all limited to know the source. He tried with these arguments of the lunulae to square the circumference and admitted to having failed. Whatever the outcome, the lesson prompted others to rethink these issues. Alhacen had more virtues, he was a precursor of other trends in non-Euclidean geometry by exploring and proposing to modify the "5th Euclidean postulate of parallels" (the fifth postulate of Euclid's Elements).

5.The Fibonacci series

Leonardo of Pisa, better known as Fibonacci (1170-1250 AD), in 1202 AD wrote his book "Liber abbaci" which means "the book of calculation". He explains in his publication about a sequence of the breeding and reproduction of rabbits, which in a few rules could estimate the number of rabbits that there would be in a certain time. The series is generated by the reproductive characteristics of the rabbits in an idealized environment, so that from a pair of rabbits they only reach reproductive maturity after three months. Thus, in the third month they have a pair of offspring (another pair of different sexes), and when these reach maturity in the third month they will be able to add another pair and so it would agree with the sequence counting the pairs of rabbits. Of course, rabbits are not born this way, but that does not matter as long as we describe a special phenomenon and as if things were this way. Fibonacci poses in his book the problem: how many pairs of rabbits are there after one year (12 months)?
Following the series:

Fibonacci Series. This is the count of pairs of rabbits that would be in each month

1	1	2	3	5	8	13	21	34	55	89	144
1	2	3	4	5	6	7	8	9	10	11	12

Answer: 144 pairs of rabbits completed the year. The curious thing about the exercise is that in order to know how many pairs of rabbits there will be next month, it consists of adding those of the two previous months. That is to say, at the 12th month 144 pairs were completed, when at the 10th and 11th month there were 55 and 89 respectively, it is confirmed 55+89=144.

This series was not exactly invented by Fibonacci, but he made it very popular in his book, rather all the rest of his work was devoted to making popular other Arabic methods of calculation that we all know today. It happens that Fibonacci's example became more and more known, because some followers rescued his legacy and collected different examples from nature, as if this series was a very probable sequence of the growth in various natural developments: the petals of flowers, stems of plants and leaves of cobs, etc. What is more, this seemed to relate strongly to another number in vogue in antiquity, a special number used by the architects of the time and referred to as the golden number, namely the number fi ϕ.

$$\phi = \frac{1+\sqrt{5}}{2}$$

$$= 1,618033988749894848204586834365638117720309179805762862135448622 7$$

Interestingly, an incredible relationship was noticed between ϕ and the convergence of a limit that included the Fibonacci series: $\lim_{n\to\infty} \frac{F_{n+1}}{F_n} = \phi$ That is, if we divide two consecutive numbers of the Fibonacci series and do it ¡$es\ el$ 144!

progressively, we obtain the limit that is the golden number

$$\frac{F_5}{F_4} = \frac{5}{3} = 1.66\cdots \quad ; \quad \frac{F_6}{F_5} = \frac{8}{5} = 1.6 \quad ; \quad \frac{F_7}{F_6} = \frac{13}{8} = 1.625$$

It is anecdotal how does one get to the other? It was one more of these discoveries and the appeal of mathematics. The relationship between the Fibonacci sequence with the number fi would also allow us to find any number in the sequence. It can be shown that, for a large number in the position of the Fibonacci series, the relationship is established:

$F_n \approx \frac{1}{\sqrt{5}}\phi^n$ This is deduced from Binet's formula (explained below).

For example, what number will be in position 12 of the Fibonacci series, which we already know, but we will be able to confirm it..., it is calculated: $\frac{1}{\sqrt{5}}(1.618)^{12} \approx 143.96$ and we say then, when rounding, ¡$es\ el$ 144! As you can confirm in the rule above, this is true!

6.The gold number, the metallic numbers and out of this category the numbers: platinum and copper

The golden number is the category that receives numberϕ (also number of God). It was used by a Greek sculptor named Phidias, who was said to have a secret to establish the proportions of his works that made them especially attractive to the eye and it was this proportionϕ . Phidias' fame derived from the creation of the statue of Olympian Zeus, installed in the temple of Zeus at Olympia near Athens in the ancient Graces and considered one of the seven wonders of the ancient world.

The principle consisted of a proportion that was apparently considered whenever it was required to draw the design of the human body and this was extrapolated to all objects in the scene. It was also used by Leonardo Da Vinci. But this secret hovered among the scholars who collected these curiosities of mathematics. It was described as a number that squared equals the same number plus 1.

Euclid defines it in his work "The Elements" as "two numbers a and b are at golden ratio if and only if $a/b = (a+b)/a$, which also indicates that it cannot be written between the division of two integers, it is an irrational. That is to say:

$$\frac{a}{b} = \frac{a+b}{a}$$

$$\frac{a}{b} = \frac{(a+b) \ : b}{a \quad : b}$$

If we collect the latter, we obtain:

$$\frac{a}{b} = \frac{a/b \ + 1}{a/b}$$

$$\phi = \frac{\phi + 1}{\phi}$$

Then, it is a number such that when squared it is equal to the same number plus 1:

$$\phi^2 = \phi + 1$$

This condition coincides with the quadratic equation: $x^2 - x - 1 = 0$, which we can solve with the general formula:

$$x = \frac{1 \pm \sqrt{5}}{2}$$

Now, if it is a geometric solution we should consider only the positive result: $x = \frac{1+\sqrt{5}}{2}$ number that we already showed as irrational. Moreover, the other solution of the equation is $\frac{1-\sqrt{5}}{2} = \frac{-1}{x}$ check it by rationalizing $\frac{-1}{\frac{1+\sqrt{5}}{2}}$, the latter could be a coincidence? Interestingly this number can be expressed in a segment of the Euclidean plane, explained below in Geogebra. Note that this number Fi, has an incredible reduced Euclidean representation, with continuous fractional form [1; 1]. Doesn't this representation seem idealized to you?

As if it were the definition of "unit" for Euclid's algorithm.

$$\phi \approx \mathbf{1} + \frac{1}{\mathbf{1} + \frac{1}{\mathbf{1} + \frac{1}{\mathbf{1} + \frac{1}{\mathbf{1}+1}}}} = \frac{13}{8} = 1.625$$

Achieving this number with the compass is very simple. Use Geogebra.

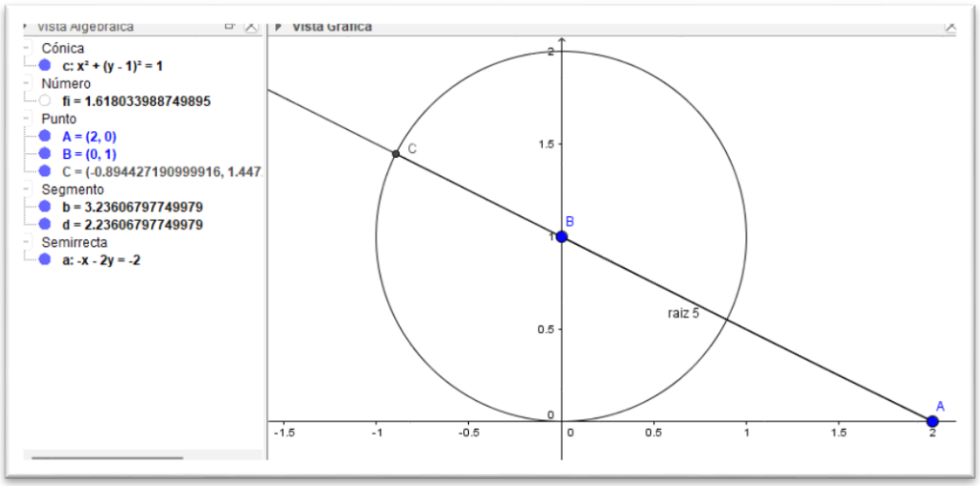

Figure 7. We obtain sqrt(5) in the hypotenuse of the triangle with legs 1 and 2.

Proceed by creating a right triangle, where the square sqrt(5) is located on the triangle's hypotenuse, and the legs measure 1 and 2. Then, subtract 1 from this hypotenuse segment. The excess length is exactly the number phi.

When the representation in Euclid's algorithm of this numberϕ became known, some mathematicians considered it pertinent to give them a name. Argentine mathematicians led by Vera G. de Spinadel (1929 -) in 1994, called them "metallic number family" **[12]**, these are positive quadratic irrational numbers, which correspond to the positive solutions of the quadratic equation: $x^2 - bx - c = 0$ where both b and c are natural numbers. The number ϕ was called the golden number, of course the metallic number family is larger and its name has an explanation related to Euclid's algorithm.

At the time it was believed that this number could be the precursor of a new numeration and could be like the much sought after number pi, but clearly they were of different natures. The number ϕ was more related to a class of geometric and proportional numbers that were used as geometric series, in the context of arts and nature. With these quadratic equation solutions, we can explain the relationship it has with the Fibonacci series.

We have already said that: $\frac{F_{n+1}}{F_n} = \phi$ when n is very large, and by the related property of Fibonacci:

$$F_n + F_{n+1} = F_{n+2}$$

Then:

$$\frac{F_{n+2}}{F_{n+1}} = \frac{F_{n+1} + F_n}{F_{n+1}} = 1 + \frac{F_n}{F_{n+1}}$$

We collect the extremes of this equality:

$$\frac{F_{n+2}}{F_{n+1}} = 1 + \frac{1}{\frac{F_{n+1}}{F_n}}$$

Thus this will happen again for another n+1, and we are presented with a Euclidean reduction as n grows, in identical form of ϕ.

$$\frac{F_{n+3}}{F_{n+2}} = 1 + \frac{1}{1 + \frac{1}{\frac{F_{n+1}}{F_n}}} \qquad \frac{F_{n+4}}{F_{n+3}} = 1 + \frac{1}{1 + \frac{1}{1 + \frac{1}{\frac{F_{n+1}}{F_n}}}}$$

In addition, the French mathematician Jacques Philippe Marie Binet (1786), defines the well-known Binet formula, which uses the two solutions of the quadratic equation already mentioned, and expresses something difficult to believe:

$$F_n = \frac{1}{\sqrt{5}}\left(\left(\frac{1+\sqrt{5}}{2}\right)^n - \left(\frac{1-\sqrt{5}}{2}\right)^n\right)$$

In this case, when n is very large we can eliminate part of the expression since $\lim_{n\to\infty}\left(\frac{1-\sqrt{5}}{2}\right)^n \to 0$

Other numbers were classified among the family of "metallic number family" **[12]**, but none came from the numbers that motivate us, since the family was limited only to those that fulfilled the condition of being solutions of quadratic equations, which neither$e$ or pi do.

There are no official associations of metals with the numbers$e$ (Euler) or pi, but some mathematicians have proposed: The number $\boldsymbol{e}$ (Euler) is associated with platinum, because of its rarity and value in mathematics; the number $\boldsymbol{\pi}$ is associated with copper, because of its importance in geometry and circumference (or because it connects everything like electrical wiring).

7. Calculating numerical accuracy, relationship between old and new methods

The representation of decimal numbers in a computer is called floating point. This representation has a finite decimal point which under a robust numerical framework can be extended so that the computer considers more decimals. The usual numerical packages such as MatLab, SciLab, Mathematics; maintain a standard precision level of 15 decimal places, the rest are filled with zeros, depending on the number of operations required, since the numerical control algorithms maintain precision in iterated multiplications and divisions. The compensation of the decimal representation further away from the range is achieved with algebraic expressions such as fractions and Euclid's algorithm. So these structures are not dismissed out of hand, as if they were discontinued or obsolete. By no means, these old structures are used in large computational processes and operations. Today there are powerful tools available on the Internet, Wolfram Alpha: Computational Intelligence **[11]**, which we will use to query numerical services without getting into the complications of representation.

Imagine that decimals can be stored in a vector of digits, so that they are treated as large numbers instead of tenths. The purpose will be to operate and update the results with long vectors of digits, where position is relevant.

The square root of 3 or sqrt(3) with the digital compass in Geogebra

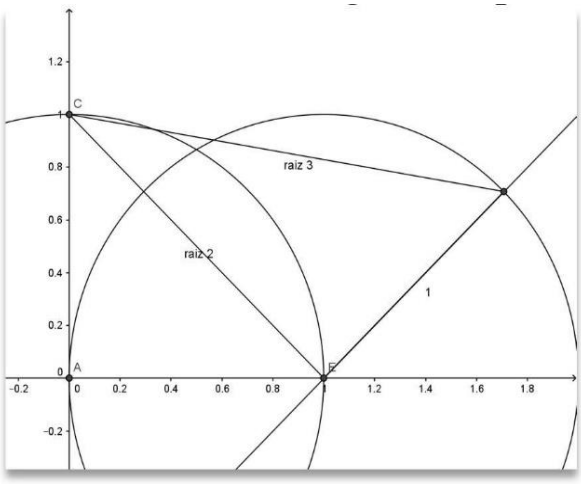

Figure 8. Sqrt(3) is obtained with a right triangle, with sqrt(2) and 1.

The sqrt(3) can be obtained in a segment with the Geogebra computer program.

We know that $\sqrt{2}$ corresponds to the diagonal of a square with sides 1. Therefore, if we build on this diagonal another right triangle with a leg on this diagonal and a leg of measure 1, the hypotenuse will be $\sqrt{3}$

Surely you already knew this geometric representation. Now we will use Euclid's theorem to obtain the reciprocal $\frac{1}{\sqrt{3}}$

I hope to surprise you a little with this idea. The segment $\sqrt{3}$ was used as the leg of a right triangle at F, the other leg of length 1.

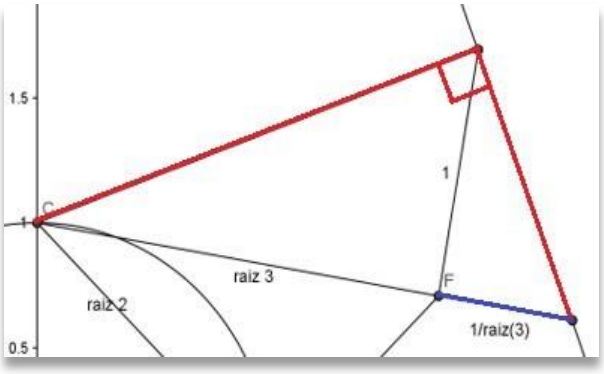

Figure 9. The reciprocal value of the sqrt(3) is obtained by extending the segment and applying Euclid's Theorem.

Then another right triangle with red legs is completed (as shown in the figure). The prolongation of the segment where the root of 3 was, according to Euclid's Theorem corresponds to the reciprocal of the root of 3

If you weren't surprised, maybe with this one you will be. The reciprocal of root of 3 will be a number we will need later, and we require all its decimals to be considered by a large computer. We need, perhaps, more than 1000000 decimals of this number, so you may wonder how we could do this. If we proceed with Euclid's algorithm to approximate with a fraction in this segment we will systematically obtain:

$$\frac{1}{\sqrt{3}} \approx \frac{1}{1+\frac{1}{1+\frac{1}{2}}} = 0.6$$

$$\frac{1}{\sqrt{3}} \approx \frac{1}{1+\frac{1}{1+\frac{1}{2+\frac{1}{1+\frac{1}{2+\frac{1}{1+\frac{1}{2+1}}}}}}} = 0.5773195876$$

We do not need to continue any further, with these iterations we already have its continuous fractional expression.

Wolfram Alpha Computational Platform expresses it as:

$$\frac{1}{\sqrt{3}} \approx 0,577350269189625764509148780501957455647601 75$$

$$\ddots\ 127012687601860232648397767230293334569371539558574952522520871380 5135$$

This is in continuous fractional form $[0; 1, \overline{1,2}]$

In this way and later, we will ask a computer to complete all the required decimals with Euclid's algorithm, doing operations of addition, multiplication and division, controlling in each case the projected decimal continuity. The idea is to do these operations as any schoolchild learning with 4 decimals, but now with the requested extension.

8. Leibniz's proposal to obtain the value of pi

Now with sums instead of products, it is the so-called Leibniz formula deduced in the 17th century by the German mathematician who gives his name to it. The process of Wallis integrals that we did earlier taught us to work with infinite sums, so you should not be surprised by Leibniz's proposal:

$\pi = 4\left(1 - \frac{1}{3} + \frac{1}{5} - \frac{1}{7} + \frac{1}{8} - \frac{1}{11} + \cdots\right)$ or what is the same $\frac{\pi}{4} = \sum_{k=1}^{\infty} \frac{(-1)^{k+1}}{2k-1}$

We can represent this in infinite sums, called alternating series due to their change of sign.

Functions associated with infinite sums.
Before, we can mention that there is a correspondence between some functions with infinite series. For example, we define as geometric series, the one that allows us to add the following numbers:

$$5 + \frac{10}{3} + \frac{20}{9} + \frac{40}{27} + \frac{80}{81} + \frac{160}{243} + \frac{320}{729} = \sum_{k=1}^{7} 5 \cdot \left(\frac{2}{3}\right)^{k-1}$$

It is called geometric sum only because the regularity between the number succeeding the other is formed from the multiplication of $r = \frac{2}{3}$.

You can check that the result of this sum is obtained from the formula:

$$5 \cdot \frac{1 - \left(\frac{2}{3}\right)^{7}}{1 - \frac{2}{3}} = \frac{10295}{729} \approx 14.122$$

Moreover, this example considers 7 terms of the sum, but we can extend this sum to infinite since the multiplicative ratio has the property of being $r = \frac{2}{3} < 1$. That is $\lim_{n\to\infty} \left(\frac{2}{3}\right)^{n} = 0$, is satisfied, then:

$$\sum_{k=1}^{\infty} 5 \cdot \left(\frac{2}{3}\right)^{k-1} = 5 \cdot \frac{1 - \left(\frac{2}{3}\right)^{\infty}}{1 - \frac{2}{3}} = 5 \cdot \frac{1}{1 - \frac{2}{3}} = 15$$

Now if we make some changes, we come to the conclusion that infinite power functions "converge" whenever the value of$r$ is between $-1 < r < 1$.

$$f(r) = 1 + r + r^2 + r^3 + \cdots = \sum_{n=0}^{\infty} r^n = \frac{1}{1-r} \quad \text{as long as } |r| < 1$$

Thus, also, if we replace with $r = -x^2$, we get:

$$\frac{1}{1+x^2} = \sum_{n=0}^{\infty} (-1 \cdot x^2)^n = \sum_{n=0}^{\infty} (-1)^n \cdot x^{2n} \quad \text{provided that } |x| < 1$$

Then, if we integrate the left and right sides, we obtain the so-called Gregory-Leibniz formula:

$$arctan(x) = \sum_{n=0}^{\infty} (-1)^n \cdot \frac{x^{2n+1}}{2n+1}$$

We check that if $x = 1$ is achieved $arctan(1) = \frac{\pi}{4}$ and we obtain Leibniz's formula. However, x = 1 is not within the convergence interval of this series, that is why Leibniz develops other convergence criteria for alternating series. Then, if we change the beginning of n=0 to k=1, i.e. $n = k - 1$, we arrive at Leibniz's expression:

$$\frac{\pi}{4} = \sum_{n=0}^{\infty} (-1)^n \cdot \frac{1}{2n+1} = \sum_{k=1}^{\infty} \frac{(-1)^{k+1}}{2k-1}$$

9. Taylor series and Euler transforms

Taylor series approximations

Power series are infinite sums that approximate functions, the domain of the function is the interval of convergence of the series. Taylor (Frederick Winslow Taylor (1856-1915), industrial engineer by profession, was born in Philadelphia, USA). He defined the power series of any differentiable function f of order n, around $x = a$.

$$F(x) = \sum_{n=0}^{\infty} c_n (x-a)^n \quad \text{then } c_n = \frac{f^{(n)}(a)}{n!}$$

The advantages are enormous, since we can find a polynomial that approximates the function around a convergence interval where the value of$x = a$ is in the center. With this we will make a leap to the models of convergence of the number pi.

For example, if we use the function $f(x) = arctan\,(x)$ and derive it to apply the Taylor series around $x = 0$, we obtain:

$$f(x) = \arctan(x)\,;\ f'(x) = \frac{1}{1+x^2};\ f''(x) = \frac{-2x}{(1+x^2)^2};\ f'''(x) = \frac{6x^2-2}{(1+x^2)^3};$$

$$f^{(4)}(x) = \frac{24x(1-x^2)}{(1+x^2)^4};\ f^{(5)}(x) = \frac{120\,x^4 - 240x^2 + 24}{(1+x^2)^5}$$

$$f(0) = 0; \quad f'(0) = 1; \quad f''(0) = 0; \quad f'''(0) = -2; \quad f^{(4)}(0) = 0; \quad f^{(5)}(0) = 24$$

Consider that when evaluating to zero the even derivatives also result in zero. Thus, we confirm the alternating series for the arctangent, but this time obtained by the Taylor series.

$$\arctan(x) = \frac{0}{0!}x^0 + \frac{1}{1!}x^1 + \frac{0}{2!}x^2 + \frac{-2}{2!\,3}x^3 + \frac{0}{4!}x^4 + \frac{24}{4!\,5}x^5 + \cdots$$

So, then:

$$x - \frac{1}{3}x^3 + \frac{1}{5}x^5 - \cdots = \sum_{n=0}^{\infty} (-1)^n \cdot \frac{x^{2n+1}}{2n+1}$$

This series relates to our theme because $\arctan(1) = \frac{\pi}{4}$

An example of Euler transforms with number series.
The Euler argument demonstrates that the harmonic series, which we know for those who have studied this, the harmonic is divergent and turns out to be convergent when it is alternating and furthermore converges to $ln(2)$ (or the natural logarithm of 2).

$$1-\frac{1}{2}+\frac{1}{3}-\frac{1}{4}+\cdots=\sum_{n=1}^{\infty}\frac{(-1)^{n-1}}{n}=\ln(2)$$

Let us see how this is justified. The sum of terms of the alternating harmonic series can be written as an integral:

$$1-\frac{1}{2}+\frac{1}{3}-\frac{1}{4}+\cdots=\left(x-\frac{x^2}{2}+\frac{x^3}{3}-\frac{x^4}{4}+\cdots\right)\Big|_0^1$$

We can think that it is: $x-\frac{x^2}{2}+\frac{x^3}{3}-\frac{x^4}{4}+\cdots$ and it is the result of an integral, then it is evaluated between 0 and

1 of the definite integral is obtained. But which integral are we talking about?

From this integral $\int_0^1(1-x+x^2-x^3+\cdots)\,dx$. Do you agree?

We said earlier that:

$$1+r+r^2+r^3+\cdots=\frac{1}{1-r}\quad\text{provided that } |r|<1$$

Thus, if we replace$r=-x$ we obtain:

$$\frac{1}{1+x}=\sum_{n=0}^{\infty}(-1\cdot x)^n=\sum_{n=0}^{\infty}(-1)^n\cdot x^n\ =1-x+x^2-x^3+\cdots$$

Then:

$$\int_0^1(1-x+x^2-x^3+\cdots)\,dx=\int_0^1\frac{1}{1+x}dx=\ln(1+x)\Big|_0^1=\ln(2)$$

Great, isn't it?

So, we can approximate numbers by series. Euler has more cards up his sleeve for these things.

Part 2. The secrets

The next part will be devoted to revealing the secrets to obtain an efficient algorithm to reach all decimals of pi. For various reasons these have not been fully revealed, and you may not know them. If you are a computer professional, you will be able to identify the techniques of large number processing. We will discuss integer operations on decimals to solve the problem of representing the floating point in a bounded environment, even if it is over the 100,000th decimal place or larger, if you prefer, of the number pi.

When we want to work with many decimals, we face the problem of numerical representation in computers, first let's go back to the Taylor series and then let's worry about the numerical representation. For all these models it is known, it is better to use fractions than decimal numbers, that is why the algorithms use mixed representations, thus, we only have to solve how to work with decimals that are far away from the floating point of their computational representation.

1. The most successful way with continuous function.

Let's try another arctangent.

The case is $\tan\left(\frac{\pi}{6}\right) = \frac{1}{\sqrt{3}}$. Then $6 \arctan\left(\frac{1}{\sqrt{3}}\right) = \pi$

This time the function will $f(x) = 6 \arctan\left(\frac{1}{\sqrt{3}} - x\right)$ to be evaluated at $x = 0$.

Deriving to obtain the Taylor series, we obtain:

$$6 \arctan\left(\frac{1}{\sqrt{3}} - x\right) = 6\sum_{n=0}^{\infty} \frac{(-1)^n \left(\frac{1}{\sqrt{3}} - x\right)^{2n+1}}{2n+1}$$

$$\text{for } \left|x - \frac{1}{\sqrt{3}}\right| < 1$$

Then, the convergence interval is:

$$-1 < x - \frac{1}{\sqrt{3}} < 1$$

$$-1 + \frac{1}{\sqrt{3}} < x < 1 + \frac{1}{\sqrt{3}}$$

$$-0.4226 < x < 1.577$$

That's fantastic; we've achieved it!
Then there is convergence for x=0.

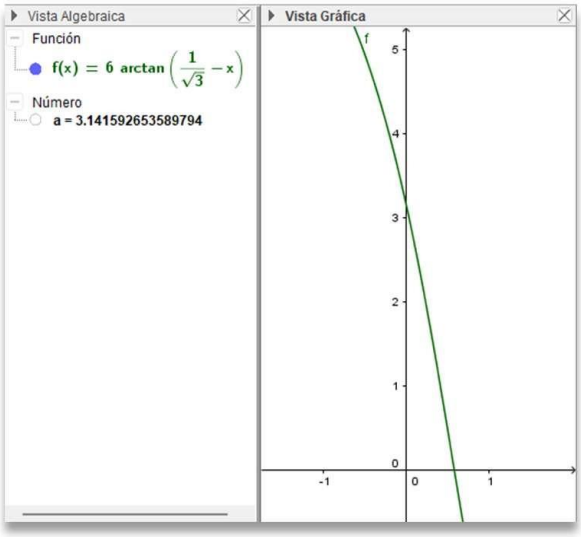

Figure 10. Decreasing curve of the arctangent.

Then, an excellent series would be:

$$6 \arctan\left(\frac{1}{\sqrt{3}}\right) = 6\sum_{n=0}^{\infty} \frac{(-1)^n 3^{-\frac{2n+1}{2}}}{2n+1}$$

Then for n=100

$$6\sum_{n=0}^{100} \frac{(-1)^n 3^{-\frac{2n+1}{2}}}{2n+1} = 3.1415926535897935$$

Thus, we discovered two very good series for our purpose. Both are convergent and systematically add real number terms progressively. The problem here is that, if we use an algorithm like this, we depend on the computer representation of decimals, because of these very small terms that must be added at the end of the series. That is, we cannot be sure that this is the correct result not because we are doing it wrong but because the computer uses a fixed number of decimals, about 15 decimals and when we

must go on and affect those further decimals would be just those that are at the limit of the computer's numerical representation.

2. Newton's algorithm

In 1666 the mathematician and physicist Newton (Isaac Newton who proposed the theory of gravitational attraction) obtained a series to calculate the number pi and concluded it from the trigonometric value:

$$\sin\left(\frac{\pi}{6}\right) = \frac{1}{2} \quad \Rightarrow \quad \frac{\pi}{6} = \arcsin\left(\frac{1}{2}\right)$$

Studying Taylor's series, he finds the series of :

$$f(x) = \frac{\arcsin(2x)}{2x} = \sum_{k=0}^{\infty} \frac{\binom{2k}{k}}{2k+1} x^{2k} \quad \text{donde } f\left(\frac{1}{4}\right) = \frac{\pi/6}{1/2} = \frac{\pi}{3}$$

Then:

$$\sum_{k=0}^{5} \frac{\binom{2k}{k}}{2k+1} \left(\frac{1}{4}\right)^{2k} \approx 1.047192239\cdots$$

Where the correct value of $\frac{\pi}{3} = \mathbf{1.047197}551\cdots$

Thus, increasing the n-value of the summation continued to approximate the remaining decimals [3]. We rate this algorithm as excellent.

3. The Bailey Borwein Plouffe (BBP) algorithm

It is a method that was developed in 1995 to calculate exclusively the number pi, with an infinite series, so that the terms can be calculated independently **[15]**. Simon Plouffe together with David Bailey and Peter Borwein obtained the formula using a computer program called PSLQ that searches for relations between integers and in base 16.

The formula they derived was:

Bailey Borwein Plouffe (BBP) algorithm

$$\pi = \sum_{k=0}^{\infty} \left(\frac{1}{16^k} \left(\frac{4}{8k+1} - \frac{2}{8k+4} - \frac{1}{8k+5} - \frac{1}{8k+6} \right) \right)$$

The five-in-five proof of the summation argument:

$$\sum_{k=0}^{4} \left(\frac{1}{16^k} \left(\frac{4}{8k+1} - \frac{2}{8k+4} - \frac{1}{8k+5} - \frac{1}{8k+6} \right) \right) = \frac{16071212445820879}{5115625817702400}$$

$$\approx \mathbf{3,141592}6545460336319557021222442381831727406617979907186696980654 4\ldots$$

$$\sum_{k=0}^{9} \left(\frac{1}{16^k} \left(\frac{4}{8k+1} - \frac{2}{8k+4} - \frac{1}{8k+5} - \frac{1}{8k+6} \right) \right) = \frac{64251934196540737654784844866951}{20452025861189303550405613977600}$$

$$\approx 3,141592\mathbf{653589}7911463887769659103474147790158884889967725870672423\ldots$$

$$\sum_{k=0}^{14}\left(\frac{1}{16^k}\left(\frac{4}{8k+1}-\frac{2}{8k+4}-\frac{1}{8k+5}-\frac{1}{8k+6}\right)\right)$$

$$=\frac{5176589783112773341415369728859884802804127138772045 31}{16477597046828005199640861488342741777304263055114240 0}$$

$\approx 3.14159265358979\mathbf{323846}17324820379824868000562781430467327805787580917527935134 04$

The computational algorithm uses the numerical base 16 to optimize the calculation when many decimals are used, only then the result of the operation is expressed in decimal base.

4. The Chudnovsky brothers' algorithm

Led by one of the brothers Gregory Chudnovsky, they proposed an algorithm that is based on a Ramanujan formula. The Chudnovsky brothers (Ukrainians naturalized Americans) used their own algorithm to calculate 2.7 billion digits of pi in 2009 where they obtained a world record, and then progressively advanced until in 2011 they get 10 billion decimals of the number pi **[13]**. With this same algorithm, computer scientists Alexander Yee and Shigeru Kondo in 2013 manage to calculate 12.1 billion decimals **[14]**.

The algorithm is based on the generalized hypergeometric series. This being alternating has Leibniz properties regarding its convergence.

$$\frac{1}{\pi}=12\cdot\sum_{k=0}^{\infty}\frac{(-1)^k(6k)!\,(13591409+545140134k)}{(3k)!\,(k!)^3 640320^{3k+3/2}}$$

The trick is to consider approximations by sections so that the result can be controlled in a vector of data that maintains the position of the decimals as if they were whole numbers, and thus to complete each segment where the sum term intervenes.

For example, if we observe the behavior of the algorithm on the first 50 known decimals of pi and from them validate a rule. Let us consider this number of correct decimals of pi.

π≈3.14159265358979323846264338327950288419716939937510582097494459230781640628620 8998628034 825342117068

And we use the algorithm:

Chudnovsky Brothers Algorithm

$$\pi=\frac{1}{12\cdot\sum_{k=0}^{\infty}\frac{(-1)^k(6k)!\,(13591409+545140134k)}{(3k)!\,(k!)^3 640320^{3k+3/2}}}$$

If we calculate the first term of that sum, the one corresponding to $k = 0$, the approximation of pi obtained will be 1 divided by that result, which gives us the following (with sums from wolframalfa.com):

3.14159265358973420766845359157829834076223326091 57

$$\frac{4\,268\,80\sqrt{10\,005}}{13\,591\,409} \approx 3.14159265358973420766845359157829834076223326091 57$$
$$\because 0659089414549873766620940165910806611734746968 9758$$

Let us now calculate the first two terms. The approximation of pi will now be $k = 0,1$ divided by the sum of them.
We get this:

3.14159265358979323846264338**279502884197 16**76788548

$$\frac{27\,243\,597\,425\,235\,335\,774\,827\,985\,240\,064\,000\,000\sqrt{10\,005}}{867\,407\,410\,133\,324\,147\,761\,288\,805\,130\,794\,983\,129} \approx 3.1415926535897932384626$$
$$\because 433832795028841971676788548462879127277903706429773351769587 26$$

As can be seen, the decimals that were already exact with the first term are maintained with this second term, and we add 14 more (they are the ones highlighted in bold). To do one more, let's see that the trend continues with the next term. By calculating 1 divided by the sum of the first three($k = 0,1,2$) terms we get the following approximation of pi:

3.14159265358979323846264338**279502884197 16**76788548

$$\frac{27\,243\,597\,425\,235\,335\,774\,827\,985\,240\,064\,000\,000\sqrt{10\,005}}{867\,407\,410\,133\,324\,147\,761\,288\,805\,130\,794\,983\,129} \approx 3.1415926535897932384626$$
$$\because 433832795028841971676788548462879127277903706429773351769587 26$$

The previous ones are maintained, and 14 new exact decimals are added. And so on.

It is amazing to get sequences of 14 more exact decimal places with each additional term, since with very few terms we get a much closer approximation to the real value. Much better than any algorithm. So, we rate this algorithm as excellent.

5. Silva Selamé Algorithm (ASS)

If you find it incredible how they have been able to find and define these algorithms, now we will be the protagonists. According to the study we have done in this essay, we can think of joining all the considerations of the most outstanding mathematical authors in history and start from the beginning.

Let's develop our own algorithm, starting with:

$$6\arctan\left(\frac{1}{\sqrt{3}}\right) = \pi$$

And we tried with: $f(x) = 6\arctan\left(\frac{1}{\sqrt{3}} - x\right)$ for which arose from the power series Taylor in $x = 0$, $f(0) = \pi$.

$$\pi = 6\sum_{n=0}^{\infty}\frac{(-1)^n\left(\frac{1}{\sqrt{3}}\right)^{2n+1}}{2n+1} = 6\sum_{n=0}^{\infty}\frac{(-1)^n 3^{-\frac{2n+1}{2}}}{2n+1}$$

If we expand to $x \to 0$

$$\arctan\left(\frac{1}{\sqrt{3}} - x\right) = \frac{\pi}{6} - \frac{3x}{4} - \frac{3\sqrt{3}x^2}{16} + \frac{9\sqrt{3}x^4}{128} + \frac{27x^5}{320} + O(x^7)$$

With x=0

$$6\arctan\left(\frac{1}{\sqrt{3}}\right)=6\sum_{n=0}^{\infty}\frac{(-1)^n 3^{-\frac{2n+1}{2}}}{2n+1}$$

Let's work on the sum of terms to get an expression of the algorithm

$$6\left(\sum_{n=0}^{11}\frac{(-1)^n 3^{-\frac{2n+1}{2}}}{2n+1}\right)=6\left(\sum_{n=0}^{11}\frac{(-1)^n\left(\frac{\sqrt{3}}{3}\right)^{2n+1}}{2n+1}\right)=6\cdot\frac{\sqrt{3}}{3}\left(\sum_{n=0}^{11}\frac{(-1)^n\left(\frac{\sqrt{3}}{3}\right)^{2n}}{2n+1}\right)$$

$$=6\cdot\frac{\sqrt{3}}{3}\left(\sum_{n=0}^{11}\frac{(-1)^n\left(\frac{1}{\sqrt{3}}\right)^{2n}}{2n+1}\right)$$

$$=2\sqrt{3}\left(\sum_{n=0}^{11}\frac{(-1)^n}{(2n+1)3^n}\right)=\mathbf{3.141592}4542\cdots$$

$$=2\sqrt{3}\left(\frac{1}{1}-\frac{1}{9}+\frac{1}{45}-\frac{1}{189}+\frac{1}{729}-\frac{1}{2673}+\frac{1}{9477}-\frac{1}{32805}+\frac{1}{111537}-\frac{1}{373977}+\frac{1}{1240029}-\frac{1}{4074381}\right)$$

$$=2\sqrt{3}\left(\left(\frac{1}{1}-\frac{1}{9}\right)+\left(\frac{1}{45}-\frac{1}{189}\right)+\left(\frac{1}{729}-\frac{1}{2673}\right)+\left(\frac{1}{9477}-\frac{1}{32805}\right)+\left(\frac{1}{111537}-\frac{1}{373977}\right)+\left(\frac{1}{1240029}-\frac{1}{4074381}\right)\right)$$

$$=2\sqrt{3}\sum_{k=0}^{5}\left(\frac{1}{(4k+1)3^{2k}}-\frac{1}{(4k+3)3^{2k+1}}\right)$$

$$=2\sqrt{3}\sum_{k=0}^{5}\frac{1}{9^k}\left(\frac{1}{4k+1}-\frac{1}{12k+9}\right)$$

$$=2\sqrt{3}\left(\left[\frac{1}{9^0}\left(\frac{1}{1}-\frac{1}{9}\right)+\frac{1}{9^1}\left(\frac{1}{5}-\frac{1}{21}\right)\right]+\left[\frac{1}{9^2}\left(\frac{1}{9}-\frac{1}{33}\right)+\frac{1}{9^3}\left(\frac{1}{13}-\frac{1}{45}\right)\right]+\left[\frac{1}{9^4}\left(\frac{1}{17}-\frac{1}{57}\right)+\frac{1}{9^5}\left(\frac{1}{21}-\frac{1}{69}\right)\right]\right)$$

$$=\mathbf{3.141592}4542\cdots$$

$$=2\sqrt{3}\sum_{n=0}^{2}\left[\frac{1}{9^{2k}}\left(\frac{1}{8k+1}-\frac{1}{24k+9}\right)+\frac{1}{9^{2k+1}}\left(\frac{1}{8k+5}-\frac{1}{24k+21}\right)\right]$$

Thus, we have a first version of our algorithm:

Silva Selamé Algorithm (ASS)

$$=2\sqrt{3}\sum_{k=0}^{\infty}\frac{1}{81^k}\left[\frac{1}{8k+1}-\frac{1}{24k+9}+\frac{1}{72k+45}-\frac{1}{216k+189}\right]$$

Let's try it five by five, as we did before with the BBP algorithm:

$$=2\sqrt{3}\sum_{k=0}^{4}\frac{1}{81^k}\left[\frac{1}{8k+1}-\frac{1}{24k+9}+\frac{1}{72k+45}-\frac{1}{216k+189}\right]$$

$$\frac{3910931416055305913838 4}{71873649923225953052 25\sqrt{3}}$$

$\approx \mathbf{3.141592653}571403381773710564577918457497083709025588000624503360391109748639673 5$

$\because 41872279003639093245$

$$= 2\sqrt{3}\sum_{k=0}^{9}\frac{1}{81^k}\left[\frac{1}{8k+1}-\frac{1}{24k+9}+\frac{1}{72k+45}-\frac{1}{216k+189}\right]$$

$$\frac{13796631637857654289486674501245033938711680163337 6}{25354938938138034138686381394493163496142563285825\sqrt{3}}$$

$\approx 3.14159265358979323846264338327950288419716939937510582097494459230781640628620899$

$\because 50728600074005410 1$

$$= 2\sqrt{3}\sum_{k=0}^{14}\frac{1}{81^k}\left[\frac{1}{8k+1}-\frac{1}{24k+9}+\frac{1}{72k+45}-\frac{1}{216k+189}\right]$$

$$\frac{14177725678419176989383216040837621457098441999820138432527910152984533089264}{260552994595867405589195393325869696817814112597392141529597948040532535692 5\sqrt{3}}$$

$\approx 3.14159265358979323846264338327950288419716939937510582097494459230781640628620899$

8628034825342117068

6. Computational Algorithm and Memory Management

Programming defines the memory spaces necessary to store all the decimals of the first calculations. It is important to start with a preset length, one billion decimals or more. From that moment on, the calculations can determine rational or irrational, and if all of them the total number of decimals will be considered. It begins then expressing those irrationals that are repeated in the process, will thus have the precision to continue the operations of addition and multiplication. The inverses can be expressed with all decimals and used as multiplication. So far so good if the calculations in the partial sections of the algorithm do not result in decimals that are outside the possible ranges of the floating point computational representation.

For this reason, algorithms must consider computations on truncated decimal operations and treated as integers. Let us discuss the situation about an array of decimals of pi and the storage of surplus operations, when transiting from a specific point, in obtaining a set of decimals of pi.

3	1	4	1	5	9	2	6	5	3	5	8	9	7	9	3	2	3	8	4	5	9	9	8	9	0	4	5	4	5	8	1	5	7	2	3	.	.	.	.
1	2	3	4	5	6	7	8	9	10	11	12	13	14	15	16	17	18	19	20	21	22	23	24	25	26	27	28	29	30	31	32	33	34	35	36	37	38	39	40

In an array (or memory vector) the previously obtained digits and the newly found digits are stored, these are located starting from the previous position and only from that point. The characteristics of the array can give clue of the exact place of the digits from where to continue.

Each set of calculations (summation argument) and with the current programming, can be distributed among different processors, 32 or 64 or more processors can synchronize the calculations and get very fast answers to obtain the billion or more decimal places of the number pi.

Truncated multiplication computes a truncated product, a contiguous subsequence of the digits of the product of 2 integers. Some truncated polynomial multiplication algorithms adapted to integers are presented. They are based on the most used full n-digit multiplication algorithms with a time complexity of $O(n^{\alpha})$, with $1 < \alpha \leq 2$, but a constant 100 times faster **[16]**. For example, products of the least significant half with Karatsuba multiplication need only 80% of the full multiplication time. The faster the multiplication, the less relative time savings can be achieved **[17]**.

7. Code implementation, ASS Algorithm in Python (gmpy2 library)

The Python language has a unique command library for numerical computation in a long-decimal execution environment. The library is called gmpy2 and allows declaring the number of precision decimals. Gmpy2 is an optimized Python extension module coded in C that supports fast multiple-precision arithmetic. It is based on the original gmpy module. **Gmpy2** adds support for true multiple-precision correctly rounded arithmetic (using the MPFR library) and complex arithmetic (using the MPC library). This means that, in particular, the most timeconsuming division operations are controlled and optimized for each command in the library.

Next, I will reveal one of the last secrets of these com algorithms. This algorithm we will code with this Python library and its execution will give answer about the decimals of pi to be counted from decimal n. Just as in Part 1 we learned how it was possible to obtain the Fibonacci number from a specific position, now the coding of the algorithm will give us a set of decimals of pi from the nth position of its decimals. This would allow us to avoid operating on the decimals already found and only solve for the decimals of pi in an environment that is relevant for our purposes.

Coding stages:

$$\sum_{k=0}^{\infty} \frac{2\sqrt{3}}{81^k}\left[\frac{1}{8k+1} - \frac{1}{24k+9} + \frac{1}{72k+45} - \frac{1}{216k+189}\right]$$

We will divide our algorithm into sections, for example, for the first section:

$$s1 = \sum_{k=0}^{N} \frac{2\sqrt{3}}{81^k}\left[\frac{1}{8k+1}\right]$$

Then to optimize an efficient decimal response, we modify this section starting from a value n and then N will be just a little higher, to optimize the precision around the decimal place n.

$$s1 = \left(\sum_{k=0}^{n}\left(\left(\frac{2\sqrt{3}}{81^k}\ mod\ [8k+1]\right)/[8k+1]\right) + \sum_{k=n+1}^{N} \frac{2\sqrt{3}}{81^k}\left[\frac{1}{8k+1}\right]\right)$$

The mod command provides only the integer remainder of the division, then this remainder is divided by [8k+1], thus taking care only of the remaining decimal places counting from position n. Then the sum up to N is added, to ensure precision around decimal place n.

The same is done with the other sums of the terms of the algorithm. For these, it will be necessary to eliminate the integer (before the comma) to control the result SumTotal= s1 - s2+ s3 - s4.

Below, we explain the complete code, which you can run in Google's Colab.

Complete code and execution

Let's go back to the digits of pi. The first case in red, counting from decimal 101 with 17 decimal places of precision. But then, the second case against decimal 901, with more 76 decimal places of precision. Both with 1000 decimal places of precision in the numerical context. Context, GoogleColab memory, no GPU.

```
n=900
gmpy2.get_context().precision=100030
```

- Digits from position 901
- It took less than 2 seconds to obtain the decimal places from 901

Definitive Python code

```
import sys
!{sys.executable} -m pip install gmpy2
!pip install gmpy2 --user # Install the gmpy2
import numpy as np
import math
import gmpy2
n=900
gmpy2.get_context().precision=100030
N=n+4
digitsPi=gmpy2.mpfr(0)
c=2*gmpy2.sqrt(3) # algorithm constants
lug=pow(10,n-1) # decimal position powers
cc=gmpy2.mpfr(c*lug) # position constant calculation
# first processor
pp=[]  # list of partial sum calculations
Suma1a=gmpy2.mpfr(0) # start addition of remainder/divisor
for k in range(0,n+1):
    pp.append(gmpy2.div(gmpy2.mpfr(cc),gmpy2.mpfr(81**k))) # position precision
    divisor1 = gmpy2.mpz(8 * k + 1)
    resto1 = gmpy2.fmod(pp[k],gmpy2.mpfr(divisor1)) # MOD remainder, division whole
    Suma1a = Suma1a + gmpy2.div(gmpy2.mpfr(resto1),gmpy2.mpfr(divisor1)) # save division
Suma1b=gmpy2.mpfr(0) # start additional decimals
for k in range(n+1, N):
    pp.append(gmpy2.div(gmpy2.mpfr(cc),gmpy2.mpfr(81**k))) # position precision
    Suma1b = Suma1b + gmpy2.div(gmpy2.mpfr(pp[k]),gmpy2.mpfr(8 * k + 1))
Suma1 = Suma1a + Suma1b
Suma1 = Suma1 - gmpy2.trunc(Suma1) + 10.0  #Wildcard added for first priority
# second independent processor
```

```
Suma2a=gmpy2.mpfr(0) # start addition of remainder/divisor
for k in range(0,n+1):
    divisor2 = gmpy2.mpz(24 * k + 9)
    resto2 = gmpy2.fmod(pp[k],gmpy2.mpfr(divisor2)) # MOD remainder, division whole
    Suma2a = Suma2a + gmpy2.div(gmpy2.mpfr(resto2),gmpy2.mpfr(divisor2)) # save division
Suma2b=gmpy2.mpfr(0) # start additional decimals
for k in range(n+1, N):
    Suma2b=Suma2b+gmpy2.div(gmpy2.mpfr(pp[k]),gmpy2.mpfr(24 * k + 9))
Suma2 = Suma2a + Suma2b
Suma2 = Suma2 - gmpy2.trunc(Suma2) + 5.0  #Wildcard added for first priority in operation
# third independent processor
Suma3a = gmpy2.mpfr(0)  # start addition of remainder/divisor
for k in range(0,n+1):
    divisor3 = gmpy2.mpz(72 * k + 45)
    resto3 = gmpy2.fmod(pp[k],gmpy2.mpfr(divisor3)) # MOD remainder, division
    Suma3a = Suma3a + gmpy2.div(gmpy2.mpfr(resto3),gmpy2.mpfr(divisor3))
Suma3b=gmpy2.mpfr(0)
for k in range(n+1, N):
   Suma3b = Suma3b + gmpy2.div(gmpy2.mpfr(pp[k]),gmpy2.mpfr(72 * k + 45))
Suma3 = Suma3a + Suma3b
Suma3 = Suma3 - gmpy2.trunc(Suma3) + 2.0 #Wildcard
# fourth independent processor
Suma4a=gmpy2.mpfr(0)
for k in range(0,n+1):
    divisor4 = gmpy2.mpz(216 * k + 189)
    resto4 = gmpy2.fmod(pp[k],gmpy2.mpfr(divisor4))
    Suma4a = Suma4a + gmpy2.div(gmpy2.mpfr(resto4),gmpy2.mpfr(divisor4))
Suma4b = gmpy2.mpfr(0)
for k in range(n+1, N):
    Suma4b = Suma4b + gmpy2.div(gmpy2.mpfr(pp[k]),gmpy2.mpfr(216 * k + 189))
Suma4 = Suma4a + Suma4b
Suma4 = Suma4 - gmpy2.trunc(Suma4)
#Return to the first processor
#The four processes are added to obtain the digits from n+1
digitsPi = Suma1 - Suma2 + Suma3 - Suma4
digitsPi = digitsPi - gmpy2.trunc(digitsPi) #removing wildcards from operation
print("\n Digits for Pi=",10000000000000000*digitsPi)
```

Context, GoogleColab memory, no GPU
n=100000
gmpy2.get_context().precision=100030

- The digits from position 100001
- It took 48 minutes to get the decimals from the decimal of pi, or to count from 100001

35313143701227785.99458341904095222770287823210114292726309849900695389736400900
707866391952699441232008465236203635227972014354931028577071966622 1

8. Conclusion

This paper was an essay that brought together the main motivations of mathematicians in history that lead to this enigmatic number pi. We detail with simplicity the mathematical representations of researchers, from different eras, to answer the original problem of squaring the area of the unit circle, equal to pi.
The contribution of the quadrature of Hippocrates' lunula, highlighted by the mathematician Alhacen, raised the expectations at the time for solving the squaring of the circle. We learned how continuous functions can graph the complex scheme leading to this number. The intervention of the mathematician Euler, which radically changed the scenario, managed to demonstrate that complex numbers could be a better option to understand the original problem. Euler reveals the relationship between the two irrational numbers: $e = 2{,}718281\cdots$ and $\pi = 3{,}141592\cdots$. Nowadays, the convergence techniques of alternating series allowed computer technology to define algorithms that can systematically approximate all decimals of the number pi. We highlight the series method to find our own ASS algorithm (authored by this author) for decimal approximation

We conclude that, with the mathematical exercise of the series, a simple way to obtain computational algorithms to find decimals for this copper number pi, or for any other number, is completed. We were able to help Akira Haraguchi recite the digits of pi and continue with them from 100,001 onwards.

References

[1] First Archimedean algorithm
Arturo Olivares, January 2024. Physios [ISSN 292-684X].
https://www.physios.mx/articulos/arquimedes-y-el-primer-algoritmo-para-calcular-el-numero-p

[2] Numerical approximation by continuous fractions.
Martín González. 2016.
https://riucv.ucv.es/handle/20.500.12466/243

[3] Algorithms to calculate the number pi. Autonomous University of Madrid. Antonio Matín, 2020.
https://repositorio.uam.es/bitstream/handle/10486/693628/martin_masuda_antonio_tfg.pdf?sequence=1

[4] History of square roots and properties.
https://es.wikipedia.org/wiki/Ra%C3%ADz_cuadrada

[5] Study of strings circumference. String (geometry) - Wikipedia, free encyclopedia
https://es.wikipedia.org/wiki/Cuerda_(geometr%C3%ADa)

[6] Calculation of Pi by Archimedes.
https://www.microsiervos.com/archivo/ciencia/ingenioso-metodo-arquimedes-calcular-numero-pi.html

[7] Video. Marcos Chicot.
Formula to find pi with roots of 2.
https://www.youtube.com/watch?v=DuxYZPtiz0s

[8] Important formulas of quantum mechanics that contain the number pi.
https://www.europapress.es/ciencia/laboratorio/noticia-numero-pi-vincula-fisica-cuantica-matematica-pura-20151110175027.html

[9] Last record memorizing digits of the number pi.
https://iesvirgendelpilar.com/numero-pi-%CF%80-nuevo-record-del-instituto/#:~:text=El%20r%C3%A9cord%20actual%20est%C3%A1%20en,memorizado%20sin%20ometer%20ning%C3%BAn%20error.

[10] Solidigm.com datacenter.
https://www.solidigm.com/products/data-center.html
https://www.livescience.com/physics-mathematics/mathematics/pi-calculated-to-105-trillion-digits-smashing-world-record
https://www.numberworld.org/y-cruncher/

[11] Wolfram Alpha. Computational Intelligence [https://www.wolframalpha.com/]

[12] Metal numbers.
https://matematicasiesoja.wordpress.com/wp-content/uploads/2013/09/numeros_metalicos_1.pdf

[13] Methods to obtain decimals of pi.
https://matematicascercanas.com/2017/01/28/metodos-decimales-pi

[14] Gaussian hypergeometric model.
https://www.gaussianos.com/el-algoritmo-de-chudnovsky-o-como-se-calculan-los-decimales-de-pi-en-el-siglo-xxi/#google_vignette.

[15] BBP algorithm formula
https://www.coursehero.com/file/213769209/F%C3%B3rmula-de-Bailey-Borwein-Plouffepdf/

[16] Binary computing. F. Bellard, “A new formula to compute the nth binary digit of a numbers” January 1997. https://nyjm.albany.edu/j/2010/16-14v.pdf

[17] D. Takahashi, “Computation of the 100 quadrillionth hexadecimal digit of on a cluster of intel Xeon phi processors.”, Parallel Computing, vol. 75, pp. 1–10, 2018.
https://dl.acm.org/doi/10.1007/11545262_16

[18] Beckmann P. (1971) Publishes “A History of Pi.St.” Martin's Press.
https://archive.org/details/historyofpipi0000beck_g8t1/mode/1up

Properties of Celtic knot design of $p \times q$ square grid and $p \times q$ honeycomb grid

Yukari Funakoshi
yukarifunakoshi@gifu.shotoku.ac.jp
Faculty of Education, Gifu Shotoku Gakuen University, 501-6194, Japan

Megumi Hashizume
megumihashizume@math.akita-u.ac.jp
Faculty of Integrated science and Engineering for Environments,
Akita University, 010-8502, Japan

Abstract

Fisher-Mellor defined knotwork design as a type of alternating link diagram related to Celtic knots ([3]). In this paper, we define Celtic knot design (CKD) induced from $p \times q$ square grid and $p \times q$ honeycomb grid as a generalized knotwork design. We show the geometric properties of CKDs from these grids and present how these structures can be mathematically described and classified. These concepts and results support mathematics education by deepening understanding of geometric structures and work well with technology-enhanced instructional design ([4]).This multidisciplinary approach, integrating mathematics, art, culture, and technology, offers potential applications in STEAM education.

1 Introduction

The Celtic knot is a traditional geometric symbol of the Celtic peoples of ancient Britain, Scotland, and Ireland. It appears in [7] and in cultural works such as the Book of Kells, a bible manuscript decorated with many Celtic knots. P. R. Cromwell introduced the Celtic knot into knot theory ([1, 2]). In 2004, G. Fisher and B. Mellor showed results for "Celtic knot design induced from $p \times q$ square grid" ([3]). Our study presents results for *Celtic knot design* (*CKD*) induced from both $p \times q$ *square grid* and $p \times q$ *honeycomb grid*. Specifically, while Fisher and Mellor focused on the number of components in square grid-based designs, our study provides new results on the number of crossings, diagram shapes, component classification, and geometric properties of CKDs such as decomposition into substructures. We extend our results for the CKD induced from a $p \times q$ square grid by introducing CKD derived from $p \times q$ honeycomb grid.

In Section 2, we introduce basic definitions of knot theory and give key definitions of CKD, $p \times q$ square grid, $p \times q$ honeycomb grid, spur, track, etc. We also show known results and some of our own. In Section 3, we show main results of the CKD induced from a $p \times q$ square grid and a $p \times q$

honeycomb grid (Proposition 3.2, Theorem 3.14, Theorem 3.15, Theorem 3.16, Proposition 3.21, Theorem 3.22, Corollary 3.23, Theorem 3.28, and Proposition 3.29). Results of the CKD induced from a $p \times q$ honeycomb grid correspond to results of the CKD induced from a $p \times q$ square grid. For example, results on the number of components of the links represented by CKDs are shown in Theorem 2.9 ([3]) and Theorem 3.15, and results on the shape of CKDs are shown in Proposition 3.1, Proposition 3.2, Theorem 3.22, Corollary 3.23, and Proposition 3.24.

Programming education has become more popular around the world in recent years. As of 2024, about two-thirds of countries offer some form of computing education in their school curricula, growing fast in Africa, Asia, and Latin America [10]. In this context, Japan introduced mandatory programming education in elementary schools in 2020. The animations developed by Y. Funakoshi [4] for constructing Celtic knot projections based on $p \times q$ square and honeycomb grids not only support mathematical education, but also serve as effective tools for programming education. These constructions can be implemented algorithmically, allowing students to engage with computational logic, geometric reasoning, and visual creativity. By integrating mathematical structure, algorithmic thinking, and artistic design, CKDs provide a rich interdisciplinary platform for STEAM education. These visual constructions enable exploration of symmetry, pattern generation, and cultural narratives, which align closely with its educational, creative, and integrative goals [11].

2 Preliminaries

2.1 Terminologies in Knot Theory

Definition 2.1 (component, link, knot)**.** An *r-component link* is a union of r disjoint smooth embeddings of S^1 into $\mathbb{R}^3$. Each image of S^1 is called a *component* of the link. A 1-component link is called a *knot*.

Definition 2.2 (projection, diagram, component segment set, crossing, trivial)**.** Let $p : \mathbb{R}^3 \to \mathbb{R}^2$ be a projection and L be a link in $\mathbb{R}^3$. If all multiple points of $p(L)$ are transverse double points, then $p(L)$ is called a *projection* of L. A *diagram* of L is a projection with over/under information at each double point. A diagram of a knot is called a *knot diagram*. The union of segments composing a diagram that corresponding to a component of L is called the *component segment set*. A point in a diagram of L corresponding to the double point in $p(L)$ is called a *crossing*. A *self crossing* is a crossing on a single component. A knot is *trivial* if it admits a diagram with no crossings.

On the other hand, a projection may be regarded as obtained from a diagram by ignoring the over/under information of the crossings.

Definition 2.3 (alternating)**.** Fix a base point on each component segment set of a diagram of a link and travel along it. The diagram is *alternating* if the crossings alternate over and under along each component segment set. A link is *alternating* if it admits an alternating diagram.

Definition 2.4 (plane ambient isotopy)**.** For a projection of a link, an ambient isotopy in $\mathbb{R}^2$ is called *plane ambient isotopy*. For projections P_1, P_2 of a link, suppose that P_1 is plane ambient isotopic to P_2. Moreover, for diagrams D_1, D_2 of the link, if P_1 (P_2 respectively) is obtained from D_1 (D_2 respectively), then we say that D_1 is plane ambient isotopic to D_2 as in Figure 1.

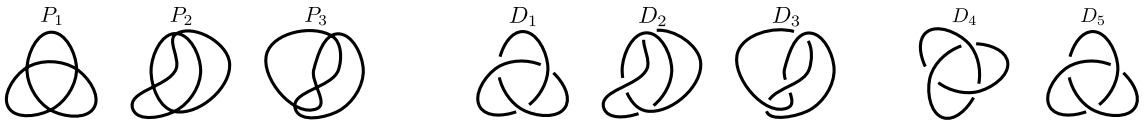

Figure 1: P_1 is plane ambient isotopic to P_2, and D_1 is plane ambient isotopic to D_2, D_4, and D_5. However, P_1 is not plane ambient isotopic to P_3, nor is D_1 to D_3.

For diagrams A, B, if B is obtained from A by parallel translation in $\mathbb{R}^2$, then we denote $A \parallel B$. For example, $D_1 \parallel D_5$ and $D_1 \nparallel D_i$ $(i = 2, 3, 4)$ as in Figure 1. For the definitions of other standard terms in knot theory, we refer to "A Survey of Knot Theory" ([6]).

2.2 Definition of Celtic knot design and its known results

Definition 2.5 (grid)**.** A closed subset of a tiled $\mathbb{R}^2$ whose boundary consisting of some edges of the polygons is called a *grid*. For a grid G, the boundary of G is denoted by ∂G.

Definition 2.6 (Celtic knot projection, Celtic knot design)**.** Draw a new polygon inscribed at the midpoints of the edges for any polygon forming a grid. Then the union of the new polygons is considered a projection of a link. The projection is called *Celtic knot projection* (*CKP*). A diagram obtained from the CKP by adding alternating over/under information for each double point is called *Celtic knot design* (*CKD*).

Note that a CKD may represent either a knot or a multi-component link. In this paper, we use the term CKD to denote diagrams representing the corresponding link. To align with our definitions, we redefine $p \times q$ *knotwork panel* ([3]) as follows:

Definition 2.7 ($p \times q$ square grid)**.** Let $p, q \in \mathbb{N}$ with $p \leq q$. We say that a grid is the $p \times q$ *square grid* if the grid is arranged by $p \times q$ squares vertically and horizontally on an orthogonal coordinate system, where the length of a square composing the grid is 1 as (a) in Figure 4.

In general, a diagram is obtained from a link. In this paper, a CKD defines the link. A CKD varies depending on how it is added over/under information for any double point of a CKP.

Remark 2.8. Any grid has two CKDs.

These two CKDs are mirror images of each other as (a) or (b) in Figure 2. In this paper, we fix the over/under information for any crossing as in Figure 3.

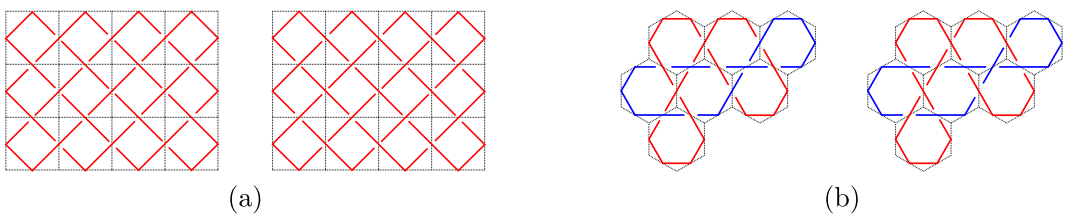

Figure 2: There are two CKDs for each grid.

Figure 3: The over/under information of the crossing on an edge of a polygon of a grid

Let G be a $p \times q$ square grid and D be the CKD induced from G as (b) in Figure 4. For any component segment set of D, a knot diagram is obtained by ignoring the over/under information of the crossings except for the self crossings. Then, $\mathcal{K}_D^\sharp$ denotes the set of the knot diagrams. In this paper, each component segment set is colored by one color, and two different component segment sets are colored by different colors. The element of $\mathcal{K}_D^\sharp$ formed from a component segment set is colored to match the set. Let $r = gcd(p, q)$, $p' = \frac{p}{r}$, and $q' = \frac{q}{r}$.

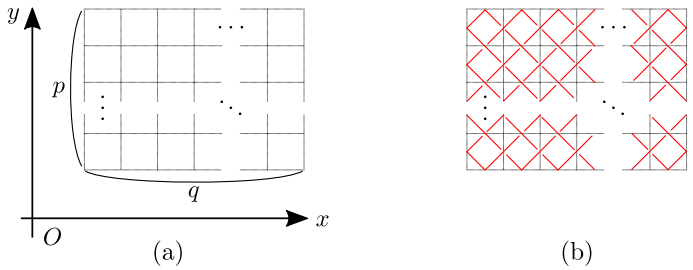

Figure 4: The $p \times q$ square grid and the CKD induced from the grid

Theorem 2.9 ([3]). *A CKD induced from a $p \times q$ square grid represents an r-component link.*

Since p' and q' are relatively prime numbers, we have;

Corollary 2.10. *The CKD induced from the $p' \times q'$ square grid is a knot diagram.*

Let P be a projection obtained from an element of $\mathcal{K}_D^\sharp$. Then, P consists of the line segments, where each line segment has slope 1 or -1 on the orthogonal coordinate system and the end points of each line segment are on ∂G.

Claim 2.11. *The projection P intersects on the left and the right sides of ∂G at p' points each, and P intersects on the upper and the lower sides of ∂G at q' points each.*

Proof. Let the base point be the top intersection of P and the left side of ∂G. We travel on P clockwise from the base point to the same point. Let $k, \ell \in \mathbb{N}$ be the numbers of vertical and horizontal roundtrips, respectively. Based on the slopes of the segments and the shape of G, $2pk = 2q\ell$ holds. Let $(k, \ell) \in \mathbb{N}^2$ be the minimal solution to the equation. Then, $pk = q\ell = lcm(p, q)$ holds. Furthermore, this fact together with $pq = lcm(p, q)gcd(p, q) = lcm(p, q)r$ shows that $\ell = \frac{p}{r} = p'$, $k = \frac{q}{r} = q'$. Hence, P intersects on the left and the right sides of ∂G at p' points each, and P intersects on the upper and the lower sides of ∂G at q' points each. □

Moreover, Fisher and Mellor claimed that any element of $\mathcal{K}_D^\sharp$ is plane ambient isotopic to the CKD induced from the $p' \times q'$ square grid ([3]). We show own proof of this claim as Theorem 3.5 in Section 3.1.

Example 2.12. Let D be the CKD induced from the 6×9 square grid. $K_i \in \mathcal{K}_D^\sharp$ $(i = 1, 2, 3)$ is plane ambient isotopic to the CKD induced from the $\frac{6}{3} \times \frac{9}{3}$ square grid in Figure 5.

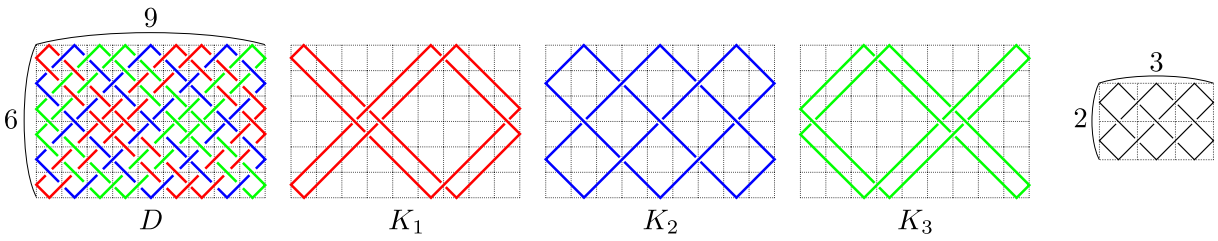

Figure 5: A relationship between the CKDs induced from the 6×9 and the 2×3 square grid

2.3 Celtic knot design of $p \times q$ honeycomb grid

Definition 2.13 ($p \times q$ honeycomb grid)**.** Let $p, q \in \mathbb{N}$ with $p \leq q$. We consider an oblique coordinate system with an angle of $\frac{\pi}{3}$ rad on the plane. Let $A = \{(x, y) \in \mathbb{R}^2 | 1 \leq x \leq q, 1 \leq y \leq p, x, y \in \mathbb{N}\}$. For any $(x, y) \in A$, draw a regular hexagon centered at (x, y) with side length $\frac{1}{\sqrt{3}}$ as in Figure 6. The union of the $p \times q$ regular hexagons is called the $p \times q$ *honeycomb grid*, and each hexagon with central coordinate (x, y) is simply denoted by (x, y).

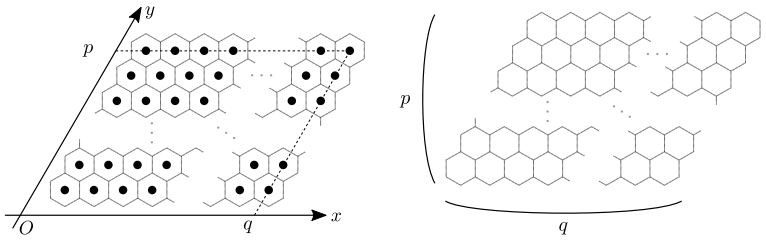

Figure 6: A black dot in the left figure represents the point $(x, y) \in A$ as the center of a regular hexagon that contains itself, and the right figure represents the $p \times q$ honeycomb grid.

Let G be a $p \times q$ honeycomb grid and D be the CKD induced from G. For a hexagon (m, n) composing G, let $(m, n)_1, \ldots, (m, n)_6$ be the midpoints of the edges of (m, n) ordered as in Figure 7. We may express to "the spur passes through $(1, n)_1$ ($(m, 1)_4$, $(q, n)_4$, $(m, p)_1$ respectively)" as "the spur passes through the regular hexagon in the leftmost column (the bottom row, the rightmost column, top row respectively) of G".

For any component segment set of D, a knot diagram is obtained by ignoring the over/under information of non-self crossings. Then, $\mathcal{K}_D^*$ denotes the set of the knot diagrams.

Definition 2.14 (spur)**.** We say that an element of $\mathcal{K}_D^*$ is the *spur* of D if the element passes through the point $(1, p)_1$.

Definition 2.15 (track)**.** The set of elements of $\mathcal{K}_D^*$ other than the spur is called the *track* of D.

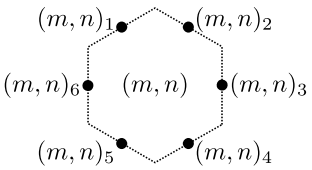

Figure 7: The black dots represent the midpoints of the edges of (m,n).

Example 2.16. Let D be the CKD induced from the 7×11 honeycomb grid. The spur and the elements of the track of D are as in Figure 8.

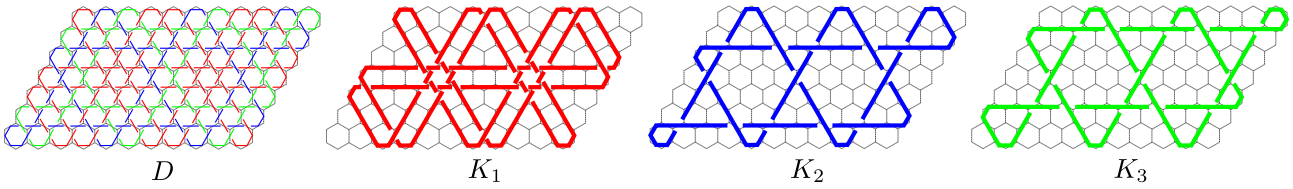

Figure 8: K_1 is the spur of D and K_2, K_3 are the elements of the track of D.

In this paper, each component segment set is colored by one color, and two different component segment sets are colored by different colors. The element of $\mathcal{K}_D^*$ formed by a component segment set is colored the same color as the component segment set. In particular, the spur is depicted in red.

Fact 2.17. *For any $p \times q$ honeycomb grid G, the spur bends only at ∂G as in Figure 9.*

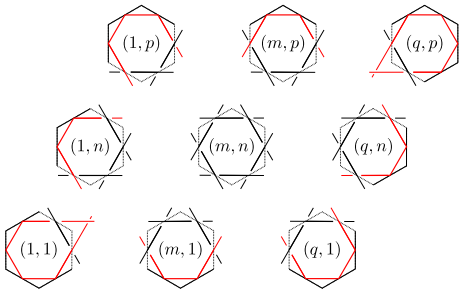

Figure 9: $m \neq 1, q$ and $n \neq 1, p$.

Let the base point O be the point of the spur at $(1,p)_1$ as in Figure 10. We travel on the spur clockwise from O.

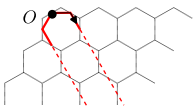

Figure 10: The travel on the spur from the base point O

Theorem 2.18. *The spur of D passes through $(q,1)_4$.*

Proof. We begin traveling clockwise on the spur from O, move toward the lower right, and return to O in the direction toward the upper left. Let $m', n' \in \mathbb{N}$ with $2 \leq m' \leq q$, $1 \leq n' \leq p-1$. By Fact 2.17, it is only at $(m',1)_4$, $(q,n')_4$ that the spur may bend toward the upper left direction. Before we pass through $(m',1)_4$, $(q,n')_4$ ($m' \neq q$, $n' \neq 1$) toward the upper left direction, the direction of this travel changes toward upper left at least once. Then, the direction of the travel changes to upper left for the first time at $(q,1)_4$. Hence, the spur passes through $(q,1)_4$ as in Figure 11.

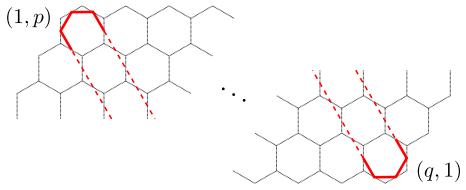

Figure 11: The spur of D passes through $(q,1)_4$.

□

3 Main results

3.1 Results of Celtic knot design of $p \times q$ square grid

Let G be a $p \times q$ square grid and D be the CKD induced from G. Let $\mathcal{K}^\sharp_D$ be as in Section 2.2. Let $r = gcd(p,q)$, $p' = \frac{p}{r}$ and $q' = \frac{q}{r}$. For $1 \leq i \leq p'$, $1 \leq j \leq q'$, let $G(i,j)$ be a closure of a piece of G obtained by dividing G into $p'q'$ pieces where the closure is the $r \times r$ square grid and the closure is located i-th from the top and j-th from the left on G.

Proposition 3.1. *The crossings of D on $\partial G(i,j)$s are the self crossings.*

The proof of Proposition 3.1 is given together with that of Proposition 3.2.

For any i, j, take a small disk at any crossing on $\partial G(i,j)$, and let $D(i,j)$ be the diagram on $G(i,j)$ obtained by replacing the small disks as in Figure 12. Then, any $D(i,j)$ is alternating by Definition 2.6. Thus, any $D(i,j)$ is regarded as the CKD induced from $G(i,j)$.

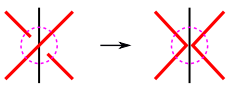

Figure 12: The deformation for obtaining $D(i,j)$s from D

For $1 \leq k \leq r$, let $e_k \in \mathcal{K}^\sharp_{D(1,1)}$ that has the k-th intersection from the top on the left side of $\partial G(1,1)$. Let $D(1,1)^{\frac{\pi}{2}}$ be the image of $D(1,1)$ rotated by $\frac{\pi}{2}$ rad on $G(1,1)$. Then, e_k is transformed into the k-th element from the left that passes through the lower side of $\partial G(1,1)$.

Proposition 3.2. *If $i+j$ is even, then $D(i,j) \parallel D(1,1)$. If $i+j$ is odd, then $D(i,j) \parallel D(1,1)^{\frac{\pi}{2}}$.*

Proof. Let P be a projection obtained from an element of $\mathcal{K}_D^\sharp$. P has at least one intersection with each side of ∂G by Claim 2.11. Let the base point be the top intersection on the left side of ∂G. We travel on P clockwise from the base point to the same point. For simplicity, we may call the travel P.

First, we divide P into the parts from the left side to the right side of ∂G and from the right side to the left side of ∂G.

bL-R: The part of P that starts from the base point on the left side of ∂G and reaches the right side of ∂G

The base point of P is on $G(h,1)$ where $1 \leq h \leq p'$. Let $k \in \mathbb{N}$ such that P starts from the base point in the k-th square from the top left square of $G(h,1)$ as in Figure 13, where $1 \leq k \leq r$. If $h=1$, P is reflected by the upper side of $\partial G(1,1)$. If $1<h$, P passes through the upper side of $\partial G(h,1)$. Then, the intersections of $\partial G(i,j)$ and P as in Figures 14 and 15 are determined by the slopes of the line segments composing P. (a)$^{\mathrm{b}}$ ((e)$^{\mathrm{b}}$ respectively) in Figure 13 corresponds to (a) ((e) respectively) in Figure 14. Thus, the part bL-R starts from (a) or (e).

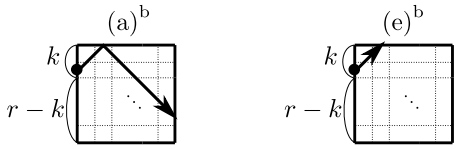

Figure 13: Each dot represents the base point on $G(h,1)$, and each arrow represents the line segments with the direction of the travel on $G(h,1)$.

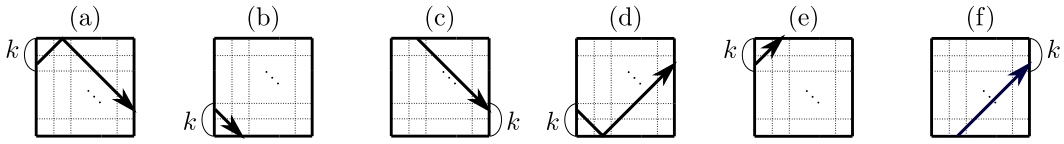

Figure 14: The part bL-R or a part L-R consists of the arrows, where each arrow represents the line segments with the direction of the travel on $G(i,j)$.

case (a): P passes through (a) in Figure 14

Step 1. If P reaches the right side of ∂G by (a), the part bL-R is finished. If P goes straight after (a), then P repeats (b), (c) in this order, P goes into (d) after repeating (b), (c), or P goes into (d) directly. When P reaches the right side of ∂G via (c), the part bL-R is finished. When P is reflected by the lower side of ∂G via (d), we go to Step 2.

Step 2. If P reaches the right side of ∂G via (d), the part bL-R is finished. If P goes straight after (d), then P repeats (e), (f) in this order, P goes into (a) after repeating (e), (f), or P goes into (a) directly. When P reaches the right side of ∂G via (f), the part bL-R is finished. When P is reflected by the upper side of ∂G via (a), we go to Step 1.

case (e): P passes through (e) in Figure 14

P is reflected by the upper side of ∂G via (a) after repeating (e), (f) in this order since $p' \leq q'$. We go to Step 1 in case (a).

Hence, the part bL-R is finished at (a), (c), (d) or (f) in Figure 14. Then, a part R-L starts from (g), (h), (j) or (k) in Figure 15.

R-L: A part of P that starts from the right side of ∂G and reaches the left side of ∂G

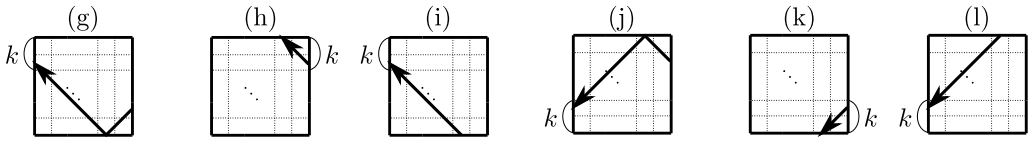

Figure 15: A part R-L consists of the arrows, where each arrow represents the line segments with the direction of the travel on $G(i, j)$.

By similar arguments of the part bL-R, a part R-L is finished at (g), (i), (j) or (l) in Figure 15. If a part R-L is finished at $G(h, 1)$, P is finished at (g) or (i). Otherwise, a part L-R starts from (a), (b), (d) or (e) in Figure 14.

L-R: A part of P that starts from the left side of ∂G and reaches the right side of ∂G

By similar arguments of the part bL-R, a part L-R is finished at (a), (c), (d) or (f) in Figure 14. Then, a part R-L starts again.

By the above argument, the connections obtained from the travel on P between the figures in Figure 14 and Figure 15 are illustrated by the arrows as in Figure 16.

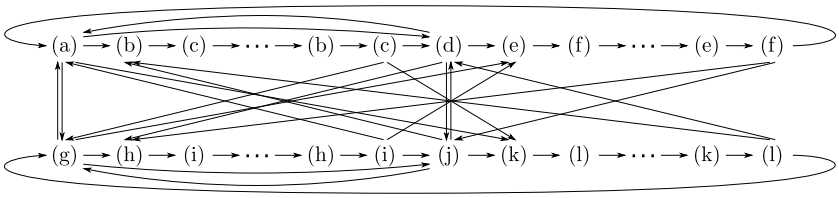

Figure 16: (a) $\to$ (b) represents that P passes through $G(i, j)$ by (b) after (a).

Next, for any $G(i, j)$ that P passes through, we consider the parity of $i + j$. P passes through $G(i - 1, j)$, $G(i + 1, j)$, $G(i, j - 1)$ or $G(i, j + 1)$ after $G(i, j)$. For i, j, the numbers $(i - 1) + j$, $(i + 1) + j$, $i + (j - 1)$ and $i + (j - 1)$ have the same parity, and have the different parity from $i + j$. This fact together with the connections between the figures in Figure 14 and Figure 15 shows that a connected pair of one of (a)-(f) and one of (g)-(l) in Figure 16 has the same parity. Moreover, a connected pair of (a)-(f) or a connected pair of (g)-(l) in Figure 16 has the different parities. Hence, (a)-(f) and (g)-(l) are classified into two sets based on the parity of $i + j$: (a), (c), (e), (g), (i), and (k) belong to one set, while (b), (d), (f), (h), (j), and (l) belong to the other set.

Finally, we focus on the shape of the union of the line segments composing P on any $G(i, j)$ which P passes through. By the previous argument, for $1 \leq i \leq p', 1 \leq j \leq q'$, the union on $G(i, j)$ consists of figures belonging to one of the two classified sets. Then, the union is a subset of the rectangle. The perimeter of the rectangle is $2\sqrt{2}r$. On the other hand, recall that the length of P is $2\sqrt{2}p'q'r$ by Claim 2.11, and G is divided into $p'q'$ $G(i, j)$s. Thus, the union is the rectangle.

Any double point of P is on $\bigcup \partial G(i,j)$. Hence, any crossing of an element of $\mathcal{K}_D^\sharp$ is on $\bigcup \partial G(i,j)$s. Therefore, Proposition 3.1 is proved. Since Theorem 2.9 and the fact that the union of the line segments composing P is the rectangle on any $G(i,j)$, there are r rectangles on any $G(i,j)$, where any two rectangles on $G(i,j)$ are formed by two projections obtained from mutually different elements of $\mathcal{K}_D^\sharp$. Then, for any pair of i,j, the union of the rectangles on $G(i,j)$ is regarded as the CKP obtained from $G(i,j)$. On the other hand, the rectangles formed by P on $G(i,j)$ with even and odd values of $i+j$ are $\frac{\pi}{2}$-rotationally symmetric to each other. Then, the CKPs obtained from $G(i,j)$ with even and odd values of $i+j$ are also $\frac{\pi}{2}$-rotationally symmetric. Hence, $D(i,j)$s with even and odd values of $i+j$ are also $\frac{\pi}{2}$-rotationally symmetric, by Definition 2.6. Then, Proposition 3.2 holds by the parity of $1+1$. □

Corollary 3.3. *The number of $D(i,j)$s with $D(i,j) \parallel D(1,1)$ is $\lceil \frac{p'}{2} \rceil \lceil \frac{q'}{2} \rceil + \lfloor \frac{p'}{2} \rfloor \lfloor \frac{q'}{2} \rfloor$, and the number of $D(i,j)$s with $D(i,j) \parallel D(1,1)^{\frac{\pi}{2}}$ is $\lceil \frac{p'}{2} \rceil \lfloor \frac{q'}{2} \rfloor + \lfloor \frac{p'}{2} \rfloor \lceil \frac{q'}{2} \rceil$.*

Example 3.4. Let $D_{6\times 9}$ be the CKD induced from the 6×9 square grid. The number of $D(i,j)$s with $D(i,j) \parallel D(1,1)$ is 3, and $D(i,j)$s with $D(i,j) \parallel D(1,1)^{\frac{\pi}{2}}$ is 3 as in Figure 17.

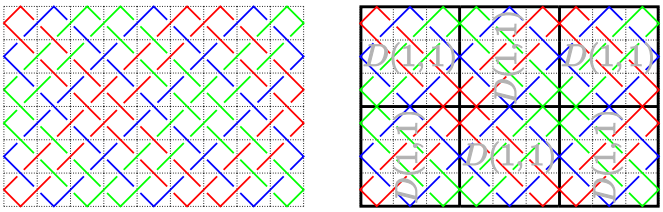

Figure 17: $D_{6\times 9}$ and the arrangement of $D(1,1)$s and $D(1,1)^{\frac{\pi}{2}}$s on $D_{6\times 9}$

We provide our own proof of the claim by Fisher and Mellor, which was mentioned in Section 2.2.

Theorem 3.5 ([3])**.** *Any element of $\mathcal{K}_D^\sharp$ is plane ambient isotopic to the CKD induced from the $p' \times q'$ square grid.*

Proof. First, we compare P obtained from an element of $\mathcal{K}_D^\sharp$ and the CKP obtained from the $p' \times q'$ square grid. Each of the left and right sides (the upper and lower sides respectively) of ∂G is divided into p' (q' respectively) equal parts of length r. Then, take the midpoint for any part. Connect each midpoint on the left or lower (left or upper respectively) sides of ∂G to the midpoint on the right or upper (right or lower respectively) sides of ∂G by the line segment of slope 1 (-1 respectively). The union of the line segments is regarded as a projection of a link, since each midpoint is connected by line segments of slopes 1 and -1. The projection, denoted by P', is the enlarged r times figure of the CKP obtained from the $p' \times q'$ square grid. By the above argument and Proposition 3.2, each of $2(p'+q')$ equal parts of ∂G contains one point of P and one point of P'. The line segments connected to each midpoint are kept fixed with the slopes preserved, while each point of P' is moved to coincide with the corresponding point of P. Then, P' and P coincide as projections. Hence P is plane ambient isotopic to the CKP obtained from the $p' \times q'$ square grid.

Next, we focus on the over/under information of a crossing. Let $K \in \mathcal{K}_D^\sharp$ that obtains P. P divides G into rectangles and triangles. For any polygon of P, each vertex on ∂G doesn't correspond

to a crossing of K, and each vertex on the interior of G corresponds to a crossing of K. Take the checkerboard coloring for K where the top crossing of K on a shaded region is on a horizontal edge of G. Then, regions of K corresponding to some rectangles of P are shaded, and a region of K corresponding to any triangle of P is not shaded. By the following mention of Remark 2.8, the coloring at a neighborhood of any crossing of K is as in Figure 18. On the other hand, for the CKD induced from the $p' \times q'$ square grid, take the same checkerboard coloring as the above. By the same argument as the above, the coloring at a neighborhood of any crossing of the CKD induced from the $p' \times q'$ square grid is as in Figure 18. Since P is plane ambient isotopic to the CKP obtained from the $p' \times q'$ square grid, over/under information of the top or bottom (the left or right respectively) crossing on a shaded region of K and the top or bottom (the left or right respectively) crossing on a shaded region of the CKD induced from the $p' \times q'$ square grid are the same. Therefore, any element of $\mathcal{K}_D^\sharp$ is plane ambient isotopic to the CKD induced from the $p' \times q'$ square grid. □

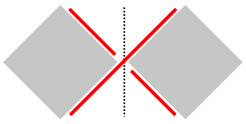

Figure 18: The over/under information of the crossing on an edge of a polygon of G, and the checkerboard coloring of a neighborhood of the crossing

Corollary 3.6. *Any element of $\mathcal{K}_D^\sharp$ is alternating.*

In general, *the crossing number* of a link is defined as the minimum number of crossings among all possible diagrams of the link. On the other hand, Lemma 3.7 and Proposition 3.8 present results for the number of crossings in a specific diagram, which is different from the crossing number.

Lemma 3.7. *D has $2pq - p - q$ crossings.*

Proof. By Definition 2.7, the cardinality of the set of the sides of the squares composing G without ∂G is $2pq - p - q$. Moreover, for any element of the set, there exists a crossing of D on the midpoint of the element by Definition 2.6. Hence, D has $2pq - p - q$ crossings. □

Proposition 3.8. *Any element of $\mathcal{K}_D^\sharp$ has $2p'q' - p' - q'$ crossings.*

Proof. It follows from Theorem 3.5 and Lemma 3.7. □

Remark 3.9. Kauffman, Murasugi and Thistlethwaite showed that if a link L admits an alternating, irreducible diagram of m crossings, then L cannot be projected with fewer than m crossings ([5, 8, 9]). This fact together with Proposition 3.8 shows that the minimal number of the crossings of any diagram of the knot represented any element of $\mathcal{K}_D^\sharp$ is $2p'q' - p' - q'$ except for the CKD induced from a $p \times np$ square grid.

3.2 Results of Celtic knot design of $p \times q$ honeycomb grid

For a $p \times q$ honeycomb grid G, let (m, n), $(m, n)_i$ $(i = 1, 2 \ldots, 6)$, D, $\mathcal{K}_D^*$ and O be as in Section 2.3. The spur of D passes through at least one reglar hexagon in the rightmost column of G by Theorem 2.18. Let (q, s) be the top regular hexagon that the spur passes through in the rightmost column of G as in Figure 19, and let $r := p - s + 1$.

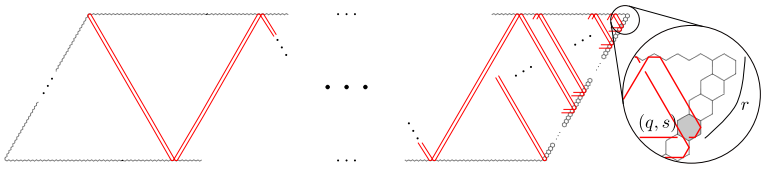

Figure 19: The shaded hexagon represents (q, s).

For $r \geq 2$, $k \in \mathbb{N}$ $(1 \leq k \leq r - 1)$, let $T_k \in \mathcal{K}_D^*$ passing through $(q, p - r + 1 + k)_4$ and $L := \{\text{the spur}, T_k\}$.

Lemma 3.10. *Any pair of elements of L are different elements of $\mathcal{K}_D^*$.*

Proof. Since the spur passes through $(q, p - r + 1)_4$, if $r \geq 2$, then T_k is not the spur. Let $i, j \in \mathbb{N}$ where $1 \leq i \leq \frac{q+1}{r+1}$, $1 \leq j \leq \frac{p+1}{r+1}$. We travel on all of T_k simultaneously counterclockwise from $(q, p - r + 1 + k)_4$. By Definitions 2.6 and 2.13, for any i, j, all of T_k simultaneously pass through $(1, (j-1)(r+1)+k)_1$ on ∂G. Similarly, all of T_k simultaneously pass through $((i-1)(r+1)+k, 1)_4$, $(q, (j-1)(r+1)+1+k)_4$, $((i-1)(r+1)+1+k, p)_1$ on ∂G. Then, the mutual positional relation of any pair of T_k is not deviated during the travels. Hence, all of T_k are different elements. Therefore, any pair of elements of L are different elements. □

By the definition of r and Lemma 3.10, Proposition 3.11 holds.

Proposition 3.11. *For $p \in \mathbb{N}$, if $q = p$, then the spur of D has no self crossing and each element of the track of D has one self crossing.*

We travel clockwise from O to O via $(q, 1)_4$ on G by Theorem 2.18. The travel from O to $(q, 1)_4$ is called the first half travel. The travel from $(q, 1)_4$ to O is called the second half travel. Let S_1 (S_2 respectively) be the subset of the projection obtained from the spur corresponding to the first half travel (the second half travel respectively), with over/under information added to the crossings that are passed through twice during the half travel.

Lemma 3.12. *If the spur traverses $(q, 1)$ clockwise, then S_2 passes through the regular hexagons left or lower adjacent to the regular hexagons which S_1 passes through.*

Proof. We consider the travel on S_1 that starts from O clockwise, and the travel on S_2 that starts from O counterclockwise simultaneously. Note that, the direction of the travel in this proof on S_2 is opposite of the direction of the second half travel. Let $i, j \in \mathbb{N}$ where $1 \leq i \leq \frac{q+1}{r+1}$, $1 \leq j \leq \frac{p+1}{r+1}$. By a similar argument of the proof of Lemma 3.10, S_1 passes through $(1, j(r + 1))_1$ and S_2 passes through $(1, j(r + 1) - 1)_1$ simultaneously. If $j = \frac{p+1}{r+1}$, $(1, j(r + 1))_1$ is not defined. In this case,

S_1 passes through $(1,p)_1$. S_1 passes through $(i(r+1),1)_4$ and S_2 passes through $(i(r+1)-1,1)_4$ simultaneously. If $i=\frac{q+1}{r+1}$, $(i(r+1),1)_4$ is not defined. In this case, S_1 passes through $(q,1)_4$. S_1 passes through $(q,(j-1)(r+1)+1)_4$ and S_2 passes through $(q,(j-1)(r+1))_4$ simultaneously. If $j=1$, $(q,(j-1)(r+1))_4$ is not defined. In this case, S_2 passes through $(q,1)_4$. S_1 passes through $((i-1)(r+1)+1,p)_1$ and S_2 passes through $((i-1)(r+1),p)_1$ simultaneously. If $i=1$, $((i-1)(r+1),p)_1$ is not defined. In this case, S_2 passes through $(1,p)_1$. Then, S_1 and S_2 are parallel during the travels except for $(1,p)$ and $(q,1)$ since S_1 and S_2 are closed at $(1,p)_1$ and $(q,1)_4$. □

Definition 3.13 (broken segment, length of a broken segment)**.** Let P_K be a projection obtained from $K\in\mathcal{K}_D^*$. A subset of a line segment composing P_K which has just two points intersecting with ∂G is called a *broken segment (of K)*. The *length of a broken segment* is the distance between the two intersections.

Theorem 3.14. *If the spur of D traverses $(q,1)$ counterclockwise, then D is a knot diagram.*

Proof. Let (m_e,p) be the e-th regular hexagon in the top row of G which the spur passes through during the travel from O to O. By $O=(1,p)_1$, $(m_1,p)=(1,p)$ holds. Let b_e be the number of the regular hexagons in the top row of G from (q,p) to (m_e,p). If $e=1$, then $b_1=q\geq p$. Thus, $1\leq b_e\leq q$ and $m_e=q-b_e+1$ hold. Then, there are three cases.

Assume $b_1=q=p$. The spur traverses $(q,1)=(p,1)$ clockwise by Proposition 3.11.

Assume $b_1=q=p+1$. The spur traverses $(q,1)=(p+1,1)$ counterclockwise. Then, S_2 passes through p hexagons in the top row of G $(2,p),\ldots,(p+1,p)$ in this order, that is, $b_e=p-e+2$, $(e=2,3,\ldots,p+1)$.

Assume $b_1=q\geq p+2$. Then $b_2=b_1-p-1$ holds. Moreover, suppose that $e\geq 2$. If $b_e\geq p+2$, then $b_{e+1}=b_e-p-1$. If $b_e=p+1$, then the spur traverses $(q,1)$ counterclockwise. If $b_e=p$, then the spur traverses $(q,1)$ clockwise. If $b_e\leq p-1$, then $b_{e+1}=q-p+b_e$. Hence, it is enough to consider this case $b_e=p+1$.

We may suppose that the spur passes through $(1,p)_1$ ($(q,1)_4$ respectively) in S_1 (S_2 respectively). Let u_1 (u_2 respectively) be the number of the regular hexagons in the top row of G that S_1 (S_2 respectively) passes through. Let v_1 (v_2 respectively) be the number of the regular hexagons in the rightmost column of G that S_1 (S_2 respectively) passes through. Recall that G is on the oblique coordinate. By Definition 3.13, S_1 and S_2 consist of broken segments. Focus on the broken segments with the directions composing the first half travel S_1 such that the direction of each broken segment corresponds to the positive direction of the x-axis. By the sum of the lengths of the broken segments, $(p+1)u_1-v_1=q(v_1+1)\Leftrightarrow -(p+1)u_1+(q+1)(v_1+1)=1\Leftrightarrow u_1=\frac{(q+1)(v_1+1)-1}{p+1}$ holds. Since $u_1,v_1\in\mathbb{N}$, $gcd(p+1,q+1)=1$ holds. Focus on the broken segments with the directions composing the second half travel S_2 such that the direction of each broken segment corresponds to the negative direction of the x-axis. By the sum of the lengths of the broken segments, $(p+1)(u_2+1)-(v_2+1)=qv_2$ $\Leftrightarrow u_2+1=\frac{(q+1)(v_1+v_2+1)}{p+1}-\frac{(q+1)(v_1+1)-1}{p+1}\Leftrightarrow u_2+1=\frac{(q+1)(v_1+v_2+1)}{p+1}-u_1$ holds. Since $u_2+1\in\mathbb{N}$ and $u_1\in\mathbb{N}$, $\frac{(q+1)(v_1+v_2+1)}{p+1}\in\mathbb{N}$ holds. By these arguments, since $gcd(p+1,q+1)=1$ and $v_1+v_2\leq p$, $\frac{(q+1)(v_1+v_2+1)}{p+1}\in\mathbb{N}\Leftrightarrow v_1+v_2=p$ holds. Suppose that the track is not empty. There is at least one regular hexagon that an element of the track passes through in the leftmost column of G by Definitions 2.6, 2.13 and a similar argument of the proof of Theorem 2.18. The same is true for regular hexagons in the bottom row, the rightmost column and the top row of G. This fact together

with the above argument shows that if the spur of D traverses $(q, 1)$ counterclockwise, then D is a knot diagram. □

Theorem 3.15. *D represents an r-component link.*

Proof. We prove $L = \mathcal{K}_D^*$ by dividing r into two cases.
Case 1: $r \geq 2$
There is at least one element of $\mathcal{K}_D^*$ which is not the spur. Let $i, j, k \in \mathbb{N}$ where $1 \leq i \leq \frac{q+1}{r+1}$, $1 \leq j \leq \frac{p+1}{r+1}, 1 \leq k \leq r-1$. By arguments of the proofs of Lemmas 3.10 and 3.12, any regular hexagon in the leftmost column of G is passed through by an element of L. The same is true for the regular hexagons in the bottom row, the rightmost column and the top row of G. Then, $L = \mathcal{K}_D^*$ holds for $r \geq 2$. We showed Theorem 3.15 in the case of $r \geq 2$.

Case 2: $r = 1$
$L = \{\text{the spur}\}$ holds. By Theorem 2.18, the spur passes through $(q, 1)_4$. If the spur passes around counterclockwise at $(q, 1)_4$, then $L = \mathcal{K}_D^*$ by Theorem 3.14. Assume that the spur passes around clockwise at $(q, 1)_4$. We show that there are no elements of $\mathcal{K}_D^* \setminus L$. We assume that there exists an element of $\mathcal{K}_D^* \setminus L$, denoted by T. By a similar argument of the proof of Theorem 2.18, T passes through at least one regular hexagon which has an intersection point of T and each side of ∂G. Let $(q, n_1)_4$ be a point which T passes through. Since the spur passes through $(q, 1)_4$, we see that $1 < n_1$. Let $(q, n_2)_4$ be the point which the spur passes through where $n_2 < n_1$ and $n_1 - n_2$ is minimum. For any point $(q, n_2')_4$ which the spur passes through, there exists the point $(q, n_1')_4$ which T passes through such that $n_1' - n_2' = n_1 - n_2$ by similar arguments of the proof of Lemma 3.10 and 3.12. Hence, the fact contradicts $r = 1$. Thus, there are no elements of $\mathcal{K}_D^* \setminus L$, i.e., $L = \mathcal{K}_D^*$ holds.

Therefore, D represents an r-component link. □

Theorem 3.16. *If $gcd(p+1, q+1) = 1$, then $r = 1$ and the spur traverses $(q, 1)$ counterclockwise. If $gcd(p+1, q+1) \neq 1$, then $r = gcd(p+1, q+1) - 1$ and the spur traverses $(q, 1)$ clockwise.*

Proof. Focus on the set of the broken segments composing the first half travel S_1 whose directions corresponds to the positive x-axis. Let u (v respectively) be the number of the regular hexagons that S_1 passes through in the top row (the rightmost column respectively) of G, i.e. $u, v \in \mathbb{N}$, $1 \leq u \leq q$, $1 \leq v \leq p$. Since the spur traverses $(q, 1)$ clockwise, by the sum of the lengths of the elements in the set, $(p+1)u - v = qv$ holds. Hence, $(p+1)u = (q+1)v$ holds. We note that $(u, v) \in \mathbb{N}^2$ is the minimal solution to the equation. Then, $(p+1)u = (q+1)v = lcm(p+1, q+1)$ holds. Furthermore, this fact together with $(p+1)(q+1) = lcm(p+1, q+1)gcd(p+1, q+1)$ shows that $gcd(p+1, q+1) = \frac{p+1}{v}$, $gcd(p+1, q+1) = \frac{q+1}{u}$. On the other hand, by an argument of the proof of Lemma 3.12, the regular hexagons in the leftmost column of G that S_1 passes through are located per distance of $r+1$. The same is true for regular hexagons in the bottom row, the rightmost column and the top row of G. Then, $\frac{p+1}{v} = \frac{q+1}{u} = r+1$ holds. These facts show that $r+1 = gcd(p+1, q+1)$ holds. Since $r \geq 1$, if $gcd(p+1, q+1) \neq 1$, then $r+1 = gcd(p+1, q+1)$ holds. Then, $gcd(p+1, q+1)$ is divided into the following two cases for the remainder of the proof of Theorem 3.16.

We assume $gcd(p+1, q+1) \neq 1$. Then, $r = gcd(p+1, q+1) - 1$ holds. If the spur traverses $(q, 1)$ counterclockwise, then $gcd(p+1, q+1) = 1$ holds by the proof of Theorem 3.14. Hence, if $gcd(p+1, q+1) \neq 1$, then $r = gcd(p+1, q+1) - 1$ and the spur traverses $(q, 1)$ clockwise.

We assume $gcd(p+1, q+1) = 1$. If the spur traverses $(q, 1)$ clockwise, then $(p+1)u = (q+1)v$ holds by the previous argument. Since $1 \leq v \leq p$, $gcd(p+1, q+1) \neq 1$ holds. This fact contradicts $gcd(p+1, q+1) = 1$. Then the spur on G traverses $(q, 1)$ counterclockwise. Hence, the CKD induced from G is a knot diagram by Theorem 3.14. This fact together with the definition of r shows that if $gcd(p+1, q+1) = 1$, then $r = 1$ and the spur traverses $(q, 1)$ counterclockwise. □

Example 3.17. For a CKD induced from a $5 \times q$ honeycomb grid, if $q = 5$, then $r = 5$; if $q = 6$, then $r = 1$; if $q = 8$, then $r = 2$; and if $q = 11$, then $r = 5$ as in Figure 20.

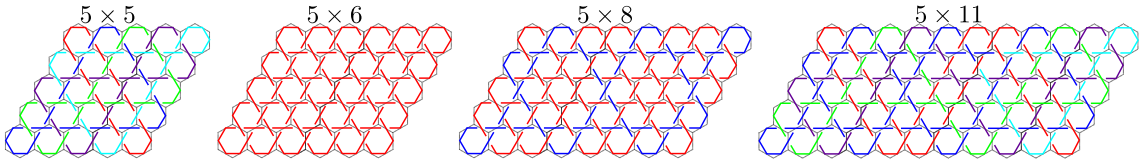

Figure 20: CKDs induced from $5 \times q$ honeycomb grids

Corollary 3.18. *If $p + 1$ is a prime number, then $r = 1$ or $r = p$.*

Corollary 3.19. *Suppose that $p = 1$, then $r = 1$. Moreover, if q is even, then the spur traverses $(q, 1)$ counterclockwise, otherwise it traverses $(q, 1)$ clockwise.*

Corollary 3.20. *For $h \in \mathbb{N}$, if $q = h(p + 1) - 1$, then $r = p$ and D represents a p-component link.*

We consider the opposite side of Corollary 3.20.

Proposition 3.21. *If $p \neq 1$ and D represents a p-component link, then $q \in \{h(p + 1) - 1 \mid h \in \mathbb{N}\}$.*

Proof. By Theorem 3.15 and the assumption of Proposition 3.21, $r = p \geq 2$ holds. Then, by Theorem 3.14 and $r \geq 2$, the spur traverses $(q, 1)$ clockwise. Moreover, by the definition of T_k, T_k passes through $(q, k+1)_4$ $(1 \leq k \leq p-1)$. Let $(S_1, T_1, \ldots, T_{p-1})$ and $(S_2, S_1, T_1, \ldots, T_{p-1})$ be ordered sets. By Definition 2.14 and arguments of the proofs of Lemmas 3.10 and 3.12, the elements of $\mathcal{K}_D^*$ are lined up at the upper side of ∂G as follows: just $(S_1, T_1, \ldots, T_{p-1})$, or the sequence $(S_1, T_1, \ldots, T_{p-1})$, $(S_2, S_1, T_1, \ldots, T_{p-1}), \ldots, (S_2, S_1, T_1, \ldots, T_{p-1})$. Hence, $q \in \{h(p + 1) - 1 \mid h \in \mathbb{N}\}$ holds. □

We assume $\gcd(p + 1, q + 1) \neq 1$. Then, $r = \gcd(p + 1, q + 1) - 1$ by Theorem 3.16. Let $1 \leq i' \leq \frac{q+1}{r+1} - 1$, $1 \leq j' \leq \frac{p+1}{r+1} - 1$, $1 \leq m \leq p$, $1 \leq n \leq q$. The closure of $G \setminus \bigcup ((i'(r + 1), m) \cup (n, j'(r + 1)))$ is the union of $r \times r$ honeycomb grids on G where the number of $r \times r$ honeycomb grids is $\frac{p+1}{r+1} \times \frac{q+1}{r+1}$. Let $1 \leq i \leq \frac{q+1}{r+1}$, $1 \leq j \leq \frac{p+1}{r+1}$. Let $G(i, j)$ be the $r \times r$ honeycomb grid composing the union located i-th from the left and j-th from the bottom on G. The broken segments of the spur of D of slope 0 and length q, and the broken segments of the spur of slope ∞ and length p divide G into $G(i, j)$ by Definition 2.14 and a similar argument of the proof of Lemma 3.12.

We extend deformations of a CKD in Figure 12 by applying the following Step 1 and Step 2. In Figures 21-23, $\partial G(i, j)$ is black, the interior of $G(i, j)$ shaded, and the replacing disks pink. Since the spur of D divides G into $G(i, j)$s, each crossing of D on $\partial G(i, j)$ involves the spur. Thus, the crossing is either a self crossing or a crossing of the spur and an element of the track of D. For

$k \in \mathbb{N}$ $(1 \leq k \leq r-1)$, let $T_k \in \mathcal{K}_D^*$ passing through the intersections of the regular hexagon $(q, p-r+1+k)$ and the right side of ∂G. By considering the shape of each element of $\mathcal{K}_D^*$ and the arrangement of $G(i,j)$, there exist two types of arrangements of crossings of D on $\partial G(i,j)$: one self crossing of the spur of D as (a) in Figure 21 and two adjacent crossings of the spur and T_k as (b) in Figure 21. Note that an arrangement (a) (an arrangement (b) respectively) in Figure 22 is composed of a combination of two copies of an arrangement (a) (an arrangement (b) respectively) in Figure 21. Then, the crossings in the exterior of $G(i,j)$ are self crossings as in Figures 21, 22 . Hence, for the two types of arrangements as in Figure 21, we define extensions of deformations of Figure 12 as Step 1 and Step 2. Moreover let $D(i,j)$ be the diagram on $G(i,j)$ obtained by Step 1 and Step 2.

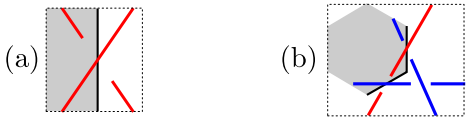

Figure 21: The two types of arrangements of crossings of D on $\partial G(i,j)$

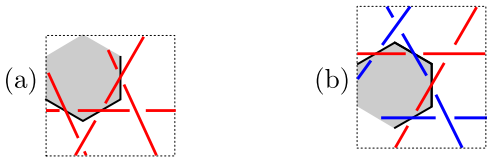

Figure 22: Arrangements are composed of figures in Figure 21.

Step 1 For any self crossing of the spur of D on $\partial G(i,j)$, take a small disk, and replace it with a new small disk as (a) in Figure 23.

Step 2 For any k, we focus on two adjacent crossings of the spur of D and T_k on $\partial G(i,j)$. Take a small disk including the crossings, and replace it with a new small disk as (b) in Figure 23.

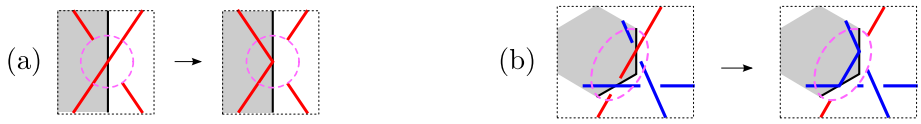

Figure 23: Deformations of a self crossing of the spur and two crossings of the spur and T_k

The diagram $D(i,j)$ is regarded as a CKD induced from $G(i,j)$ by the over/under information of the crossings of D. For any i, j, k, let $t_k^{D(i,j)} \in \mathcal{K}_{D(i,j)}^*$ passing through the intersection of the regular hexagon $(i(r+1)-1, (j-1)(r+1)+1+k)$ and the right side of $\partial G(i,j)$. By Step 1, Step 2 and the shapes of the elements of $\mathcal{K}_D^*$, the following theorem holds.

Theorem 3.22. *For any i, j, k, the spur of $D(i,j)$ ($t_k^{D(i,j)}$ respectively) corresponds to the spur of D (T_k respectively).*

The color of an element of $\mathcal{K}^*_{D(i,j)}$ obtained by Step 1, Step 2 coincides the color of the corresponding element of $\mathcal{K}^*_D$.

Corollary 3.23. $D(i,j) \parallel D(\frac{q+1}{r+1}, \frac{p+1}{r+1})$.

Proposition 3.24. *Any crossing of D on $G \setminus \bigcup G(i,j)$ is a self crossing.*

Example 3.25. Let D be the CKD induced from the 7×11 honeycomb grid. Then $r = 3, 1 \leq i \leq \frac{11+1}{3+1}$, $1 \leq j \leq \frac{7+1}{3+1}$, $1 \leq k \leq 3-1$. The spur of $D(i,j)$ ($t_k^{D(i,j)}$ respectively) corresponds to the spur of D (T_k respectively) as in Figure 24. Any crossing of D on $G \setminus \bigcup G(i,j)$ is a self crossing.

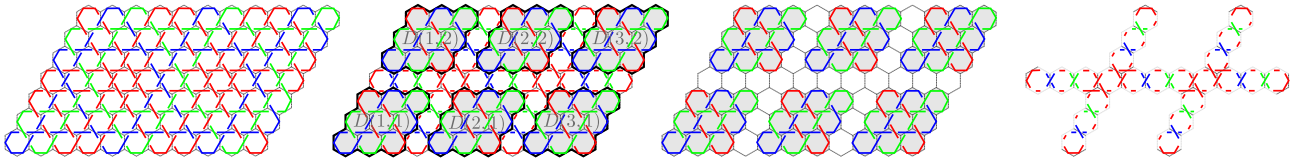

Figure 24: From left to right - D; the figure obtained from D by applying Step 1 and Step 2; $\bigcup D(i,j)$ on G; D on $G \setminus \bigcup G(i,j)$.

Corollary 3.26. *The number of the self crossings of the spur of D is* $12(\frac{p+1}{r+1}-1)(\frac{q+1}{r+1}-1) + 2(\frac{p+1}{r+1}-1) + 2(\frac{q+1}{r+1}-1)$. *The number of the self crossings of each element of the track of D is* $\frac{p+1}{r+1}\cdot\frac{q+1}{r+1} + (\frac{p+1}{r+1}-1)\frac{q+1}{r+1} + \frac{p+1}{r+1}(\frac{q+1}{r+1}-1)$.

Proposition 3.27. *For $h \in \mathbb{N}$, if $q = h(p+1)-1$, then $r = p$ and each element of $\mathcal{K}^*_D$ is the diagram of a trivial knot.*

Proof. By Corollary 3.20 and the assumption of Proposition 3.27, $r = p$. Hence we have $j = 1$ by $1 \leq j \leq \frac{p+1}{r+1}$. This fact together with Propositions 3.11, 3.24 and Corollary 3.23 shows that any crossing of any element of $\mathcal{K}^*_D$ is nugatory. Then, Proposition 3.27 holds. □

Theorem 3.28. *Any element of the track of D is uniquely determined up to plane ambient isotopy.*

Proof. Let $D_{p\times p}$ be the CKD induced from a $p \times p$ honeycomb grid. The number of the elements of $\mathcal{K}^*_{D_{p\times p}}$ is p by Theorems 3.15 and 3.16. By Proposition 3.11, each element of the track of $D_{p\times p}$ has one self crossing. The crossing of each element of the track consists of two line segments of slopes 0 and ∞. Thus, the over/under information of the crossing is uniquely determined. Hence, each element of the track of $D_{p\times p}$ is unique up to plane ambient isotopy.

For any $i,j,k \in \mathbb{N}$, the above argument and preliminaries of Theorem 3.22 show that $t_k^{D(i,j)}$ and $t_{k+1}^{D(i,j)}$ obtained from D is unique up to plane ambient isotopy, where $1 \leq i \leq \frac{q+1}{r+1}$, $1 \leq j \leq \frac{p+1}{r+1}$, $1 \leq k \leq r-1$. Moreover, for any $i',j,k \in \mathbb{N}$, by Theorem 3.22 and Proposition 3.24, $t_k^{D(i',j)}$ and $t_k^{D(i'+1,j)}$ are connected by a self crossing of T_k, where $1 \leq i' \leq \frac{q+1}{r+1}-1$. The crossing consists of two line segments of slopes -1 and 0. Then, the over/under information of the crossing is uniquely determined. Similarly, for any $i,j',k \in \mathbb{N}$, $t_k^{D(i,j')}$ and $t_k^{D(i,j'+1)}$ are connected by a self crossing of T_k, where $1 \leq j' \leq \frac{p+1}{r+1}-1$. The crossing consists of two line segments of slopes -1 and ∞. Then, the over/under information of the crossing is uniquely determined. Therefore, any element of the track of D is uniquely determined up to plane ambient isotopy. □

Proposition 3.29. *Any element of $\mathcal{K}_D^*$ is alternating.*

Proof. If $p = 1$ ($gcd(p+1, q+1) = 1$ respectively), D is a knot diagram by Corollaly 3.19 (Theorems 3.15 and 3.16 respectively). Thus, Proposition 3.29 holds. If $p \geq 2$, $gcd(p+1, q+1) \neq 1$ and $q = h(p+1)-1$ ($h \in \mathbb{N}$), then any element of $\mathcal{K}_D^*$ is alternating by Corollary 3.23, Propositions 3.11 and 3.24. In the remainder of this proof, suppose that $p \geq 2$, $gcd(p+1, q+1) \neq 1$ and $q \neq h(p+1)-1$ ($h \in \mathbb{N}$). Let P_K be a projection obtained from $K \in \mathcal{K}_D^*$.

First, we show that P_K has equilateral triangles (i.e. a triangle whose three sides are equal in length) and hexagons on the interior of G. Then, K consists of the broken segments each with slope -1, 0 or ∞. For any broken segment, take the straight line that includes itself.

Assume K is an element of the track. The distance between any pair of parallel and adjacent broken segments of K with length greater than $\frac{1}{2}$ on G is $r+1$ by an argument of the proof of Lemma 3.10. Fix a broken segment of K of slope 0 (∞, -1, respectively) and length greater than $\frac{1}{2}$, and let X_t (Y_t, Z_t, respectively) be the set of infinite parallel straight lines which are arranged per distance of $r+1$ on the plane, where the set includes the straight line obtained from the broken segment. Three lines - one from each of X_s, Y_t, and Z_t - form an equilateral triangle. Six lines - two from each set - form a hexagon. Hence, $X_t \cup Y_t \cup Z_t$ divides the plane into the equilateral triangles and the hexagons. Then, P_K has the equilateral triangles and the hexagons on the interior of G.

Assume K is the spur. The parallel and adjacent straight lines obtained from broken segments of K alternate between distance of r and 1 by an argument of the proof of Lemma 3.12. Fix a broken segment of $S_1 \subset K$ with length greater than $\frac{1}{2}$. The image on G obtained from the fixed broken segment of S_1 of slope 0 (∞, -1, respectively) by the parallel translation of -1 along the y-axis (x-axis, x-axis respectively) is the broken segment of $S_2 \subset K$ by Lemma 3.12. Let X_s (Y_s, Z_s, respectively) be the set of infinite parallel straight lines which are arranged per distance of $r+1$ on the plane, where the set includes the straight line obtained from the fixed broken segment of slope 0 (∞, -1, respectively). Let X_s' (Y_s', Z_s' respectively) be the set obtained by translating X_s (Y_s, Z_s respectively) by -1 along the y-axis (x-axis, x-axis respectively). Hence, $X_s \cup X_s' \cup Y_s \cup Y_s' \cup Z_s \cup Z_s'$ divides the plane into the equilateral triangles and the hexagons as in Figure 25. Then, P_K has the equilateral triangles and the hexagons on the interior of G.

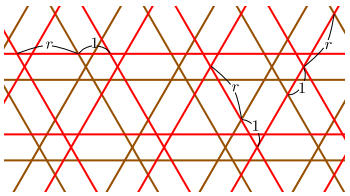

Figure 25: Elements of $X_s \cup Y_s \cup Z_s$ ($X_s' \cup Y_s' \cup Z_s'$ respectively) are depicted in red (brown respectively)

Second, we show that any crossing of K corresponds to a vertex of the polygons on the interior of G. Assume K is an element of the track. The shape of K is recognized by Corollaries 3.23, 3.26, Theorem 3.22 and Proposition 3.24. Recall that there exists just one crossing of $t_k^{D(i,j)}$ on $G(i,j)$ for $1 \leq i \leq \frac{q+1}{r+1}$, $1 \leq j \leq \frac{p+1}{r+1}$. For any $D(i,j)$ ($(i,j) \neq (1, \frac{p+1}{r+1}), (\frac{q+1}{r+1}, 1)$) and k, the crossing of $t_k^{D(i,j)}$ corresponds to the vertex of at least one equilateral triangle on the interior of G. We checked $\frac{p+1}{r+1} \cdot \frac{q+1}{r+1} - 2$ crossings. The self crossings on $G \setminus \bigcup G(i,j)$ correspond to the remaining vertices of

the equilateral triangle. We checked $(\frac{p+1}{r+1}-1)\frac{q+1}{r+1}+\frac{p+1}{r+1}(\frac{q+1}{r+1}-1)$ crossings. By the assumption of p and q, there are two or more broken segments of K of slope -1 and length greater than $\frac{1}{2}$ on G. The same is true for broken segments of slope 0 or ∞ and length greater than $\frac{1}{2}$ on G. Recall that the distance between any pair of parallel and adjacent broken segments of K with length greater than $\frac{1}{2}$ on G is $r+1$. Then, for $(i,j)=(1,\frac{p+1}{r+1}),(\frac{q+1}{r+1},1)$, K has two broken segments that passes through $G(i,j)$ of slope -1, and $t_k^{D(i,j)}$ has two broken segments of slopes 0 and ∞ and length greater than $\frac{1}{2}$ by the shape of $D(i,j)$. The crossing of $t_k^{D(i,j)}$ corresponds to the crossing of K consisting of the broken segments of slopes 0 and ∞ by Theorem 3.22 and Corollary 3.23. By the assumption of p and q, there exists the broken segment of K of slope 0 and length greater than $\frac{1}{2}$ on G at a distance of $r+1$ from the broken segment of K of slope 0. The same is true for the broken segment of slope ∞ on G. The straight lines including these six broken segments form a hexagon on the interior of G. Thus, for $(i,j)=(1,\frac{p+1}{r+1}),(\frac{q+1}{r+1},1)$, the crossing of $t_k^{D(i,j)}$ corresponds to the vertex of the hexagon on the interior of G. We checked two crossings. Then, we checked all crossings of K by Corollary 3.26. Hence, any crossing of K corresponds to a vertex of the equilateral triangles or a vertex of the hexagons on the interior of G in this case.

Assume K is the spur. The shape of K is recognized by Corollaries 3.23, 3.26, Theorem 3.22 and Proposition 3.24. Any crossing of K is in the closure of $G\setminus\bigcup G(i,j)$ by Proposition 3.11 and Corollary 3.23. Any $G(i,j)$ is obtained by dividing G by the broken segments of K of slope 0 and length q, and the broken segments of K of slope ∞ and length p. Then, the union of the straight lines obtained from the broken segments of K of slope -1 and the straight lines obtained from the broken segments that divide G forms the equilateral triangles and the regular hexagons with side length $\frac{1}{2}$ on the interior of G. Let A be the set of the crossings of K each of which is corresponding to a vertex of the equilateral triangles. We checked $12(\frac{p+1}{r+1}-1)(\frac{q+1}{r+1}-1)$ crossings. Let B be the set of the crossings of K not in A. Since any element of B is not in A and on $\partial G(i,j)$ having an intersection with ∂G, any element of B corresponds to a vertex of the equilateral triangles with side length $r-\frac{1}{2}$ on the interior of G. We checked $2(\frac{p+1}{r+1}-1)+2(\frac{q+1}{r+1}-1)$ crossings. Then, we checked all crossings of K by Corollary 3.26. Hence, any crossing of K corresponds to a vertex of the equilateral triangles on the interior of G in this case.

Finally, we show that the crossings of K corresponding to the vertices of a polygon on the interior of G are "locally alternating", in order to show that K is alternating. Take a compact region intersecting with a diagram of a link on the plane. The intersection points of the boundary of the region and the diagram are transverse double points. The intersection of the region and the diagram is called *the restricted diagram by the region*. We say that the restricted diagram by the region is *locally alternating* if the over/under information of the crossings on every segment in the restricted diagram appears alternately. For any polygon of P_K on the interior of G, take a neighborhood of the polygon that is not including a vertex of another polygon. The neighborhood corresponds to the compact region intersecting K. If the restricted diagrams by the neighborhoods are locally alternating, then K is alternating because any crossing of K corresponds to a vertex of the polygons on the interior of G. Hence, the restricted diagram by the neighborhood is locally alternating because the over/under information of the crossings on every segment in the restricted diagram by the neighborhood appears alternately by the slopes of the broken segments of K. Therefore, K is alternating.

In all cases, any element of $\mathcal{K}_D^*$ is alternating. □

Example 3.30. Let D be the CKD induced from the 7×11 honeycomb grid as in Figure 8. Then,

the spur passes through $(11, 1)$. Moreover, the elements of the track ($K_2, K_3 \in \mathcal{K}_D^*$) are unique up to plane ambient isotopy. Any element of $\mathcal{K}_D^*$ is alternating.

Acknowledgment

We sincerely thank the anonymous referee for their careful reading and helpful comments, which greatly improved this manuscript.

References

[1] P. R. Cromwell, "Celtic knotwork: mathematical art", *Math. Intelligencer, 15 no 1* (1993), 36-47.

[2] P. R. Cromwell, "The distribution of knot types in Celtic interlaced ornament", *J. Mathematics and the Arts 2* (2008), 61-68.

[3] G. Fisher & B. Mellor, "On the Topology of Celtic Knot Designs", *Bridges Mathematical Connections in Art, Music, and Science* (2004), 37-44.

[4] Y. Funakoshi, "Animations based on knot theory for drawing Celtic knot projection of $p \times q$ square grid and $p \times q$ honeycomb grid", *The annals of Gifu Shotoku Gakuen University. Faculty of Education, 63 (2024)*, 21-40, Japanese.

[5] L. H. Kauffman, "State Models and the Jones Polynomial", *Topology 26* (1987), 395-407.

[6] A. Kawauchi, *A Survey of Knot Theory*, Birkhäuser, Basel (1996).

[7] A. Meehan, *Celtic Design, Knotwork, The Secret Method of the Scribes*, Thames and Hudson (1991).

[8] K. Murasugi, "The Jones Polynomial and Classical Conjectures in Knot Theory", *Topology 26* (1987), 187-194.

[9] M. B. Thistlethwaite, "A Spanning Tree Expansion of the Jones Polynomial", *Topology 26* (1987), 297-309.

[10] Code.org, CSTA, and ECEP Alliance. *2024 State of Computer Science Education*. Code.org Advocacy Coalition, 2024.

[11] Perales, F. J., & Aróstegui, J. L. (2024). The STEAM approach: Implementation and educational, social and economic consequences. *Arts Education Policy Review*, 125(2), 59-67.

Geometry as a Computational Engine for Continued Fractions of Transcendental Logarithms

Narinder Kumar Wadhawan,
e-mail: narinderkw@gmail.com
Civil Servant, Indian Administrative Service, Now Retired,
Haryana, India

Abstract

The purpose of this paper is to introduce a geometric method using a straightedge and compass for representing the exponent x of an equation, equivalently expressed as x=ln(a)/ln(b), in the form of a continued fraction, thereby enabling its computation. Although analogous to the Euclidean algorithm, this method operates on exponents, with division carried out geometrically rather than symbolically. The exponent of the equation is determined by locating the two perpendiculars between which the magnitude b lies. In the geometric construction, perpendiculars are drawn on the hypotenuse AC and base BC of a right-angled triangle ABC with the right angle at B, where AB=1 and cos(C)=a with a<1. Since the exponent, being transcendental, is not an integer, the process must be repeated for the remainder. The reciprocal of the remainder, treated geometrically, again produces a new remainder, thus continuing the geometric process. This method opens the door to using geometry as a computational tool, rather than restricting it to its traditional illustrative or grammatical role.

1. Introduction

Going back to our school days, when simplifying fractions was part of the curriculum, we encountered many operations—addition, subtraction, multiplication, and division—each requiring careful execution according to a memorised priority rule. This rule was often remembered by the acronym BADMAS, which determined the order of arithmetic operations: first Brackets (BA), followed by Division (D), then Multiplication (M), then Addition (A), and finally Subtraction (S). The combination BA + D + M + A + S formed the word BADMAS (in Hindi बदमाश), which literally means a 'rogue' or 'villain', and this amusing association helped students memorise the order of operations. In contrast, continued fractions involve a single operational priority: computation proceeds from the last term to the first. A simple fraction can be written $a = r/q$ where r and q are real positive integers. But a fraction can also continue as:

$$a = a_0 + \cfrac{a_1}{a_2 + \cfrac{a_3}{a_4 + \cfrac{a_5}{a_6 + \cdots}}}$$

This expansion may involve a finite number of terms (for rational numbers) or an infinite sequence (for irrational or transcendental numbers), where $a, a_0, a_1, a_2, \ldots$ are positive integers. Euclid, in his Elements (c. 300 BCE), introduced an algorithm for computing the greatest common divisor (GCD or HCF) of two numbers [3, 7]. This algorithm forms the backbone of continued fraction construction for a ratio a/b.

Briefly stating, the method finds the GCD of r/q by dividing r by q, yielding quotient a_0 and remainder r_1. Then q is divided by the remainder r_1, yielding quotient a_1 and remainder r_2 and the process continues until the remainder vanishes or the division continues indefinitely. The fraction p/q is then expressed as

$$a_0 + \cfrac{a_1}{a_2 + \cfrac{a_3}{a_{4+\frac{a_5}{\ddots}}}}.$$

For example, $375/147$ is written as a continued fraction using the Euclidean algorithm:

$$2+\cfrac{1}{1+\cfrac{1}{1+\cfrac{1}{4+\cfrac{1}{2+\frac{1}{2}}}}}.$$

In published literature, continued fractions have been visualised geometrically to interpret their properties, their connection to integer lattices, their algorithmic structure, the Farey sequence, and hyperbolic geometry. However, geometry has not been used to extract continued fractions; rather, it has served to analyse the fractions derived from the Euclidean algorithms. These visual interpretations find applications in Diophantine approximation, rational approximation, symmetries, and pattern analysis [5].

Very little work has explored geometry as a *semantic engine for computational purposes*. Foundational contributions in this direction were made by the great geometer René Descartes, who used geometry to solve algebraic problems. In particular, he considered the problem of generating a sequence of lengths between two points a and b such that the ratio of two consecutive terms is constant. To achieve this, he proposed a mechanism involving *movable perpendicular linkages* along the base BC and movable rulers on the hypotenuse AC of a right triangle ABC. This device, now known as *Descartes's Logarithm Machine*, was designed to trace logarithmic curves [1, 2]. The concept was later implemented using dynamic geometry software [1]. More recently, independent semantic constructive approaches, aligned with Descartes' vision, have appeared in published work [8]. The method presented in this paper, developed independently, extends this lineage by using iterative *perpendicular constructions* within a *fixed* triangle to compute the *continued fraction expansion* of the transcendental exponent x in $a^x = b$ —a goal not previously pursued.

In this paper, the geometry using a straightedge and compass is utilised as a computational tool to generate

I. indefinitely continuing fractions of x given by the equation $a^x = b$, where a and b are algebraic and $\neq 0, 1$ or $\pm\infty$ and x is not real rational, and
II. prove the ratio of two transcendental, i.e. $ln(a)/ln(b)$ is transcendental when a and b are algebraic and are $\neq 0, 1$ or $\pm\infty$ and x is not real rational.

1.1 Proof Notations and Definitions

Letters like $A, B, C, ..., A', B', C', \ldots,$ or $A'', B'', C'', ...$ while referring to the geometric Figures 1, 2 and 3, denote points. Two alphabets without gap like AB, BC, GH ,.., $A'B', B'C', G'H', ...$ $A''B'', B''C'', G''H'', ...$, $D_1D_2, A_3E_4,\ BD_1$ ... denote a line or its segment. Three alphabets without gap like $ABC,\ DEF$ ..., $A'B'C', D'E'F', ..., A''B''C'', D''E''F'', ...$, denote a triangle. Geometric signs $\perp$, $\angle$, Δ, denote a perpendicular, an angle, and a triangle, respectively. Alphabet p_m, P_m denote the magnitude of the mth perpendicular corresponding to $cos^m(C)$ and the magnitude of the mth perpendicular corresponding to $1/cos^m(C)$, respectively

Mathematical signs ∞, $\rightarrow$, $>$, $<$, $=$, $\geq$, $\leq$, denote infinity, tending to (approaching), more than, less than, equal to, equal to or more than, equal to or less than, respectively. Letters $a, b, c, \ldots, x, y, z, ..$, denote real quantities. Real quantities r_i, q_i where $i = 0, 1, 2, 3, ...$ denote positive integers. $Cos\ (C)$ is the trigonometric ratio of the base to the hypotenuse of a right-angled triangle that has angle C (in radians) opposite to the angle $\pi/2$.

2. Construction and Operation

2.1. Construction of The Right-Angled Triangle ABC with ∠C=a radian

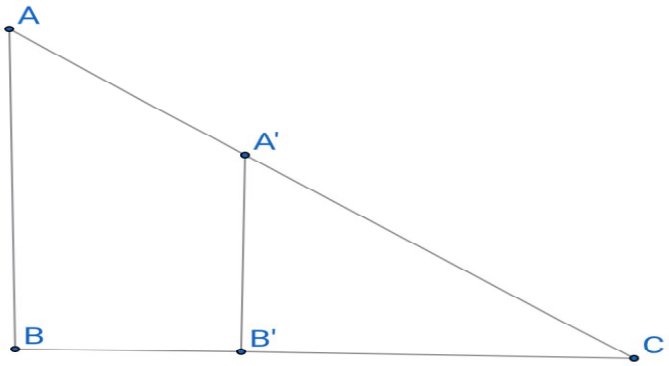

Figure 1 Construction of the right-angled triangle ABC with a line segment $AB = 1$, and ∠C= a radians

When $0 < a < 1$, draw a horizontal line $B'C = a$ unit and construct a perpendicular $A'B'$. With the compass centre at C and opening it equal to 1 unit, draw an arc intersecting A'B' at A' so that CA'=1 unit. Extend CA' to A such that segment AB, perpendicular to CB', meets it at B and equals 1 unit. Now the right-angled Δ ABC has cos(C)= a unit, ∠ABC=π/2 and perpendicular segment AB=1 unit.

When $a > 1$, write the equation $(1/a)^x = 1/b$, and construct the right-angled Δ ABC, assuming a as $1/a$ and following the steps as already explained.

2.2. Construction of $(a)^x = b$

For extracting x in the equation $a^x = b$, equivalently $x = ln(b)/ln(a)$, a and b must be nonzero positive real quantities. If a and b both are less than 1, the right-angled triangle for extracting x is constructible. If a and b both are more than 1; the equation can be written as $(1/a)^x = 1/b$ and the right-angled triangle for extracting x is constructible. If $a < 1$ and $b > 1$, then x will be negative from $ln(b)/ln(a)$, and the substitution $x = -X$ and $B = 1/b$ transforms the equation to $a^X = B$. Similarly, if $a > 1$ and $b < 1$. Then the substitution $A = 1/a$ and $X = -x$ transforms the equation to $A^X = b$. In both cases, the right-angled triangle for extracting X $(-x)$ is constructible.

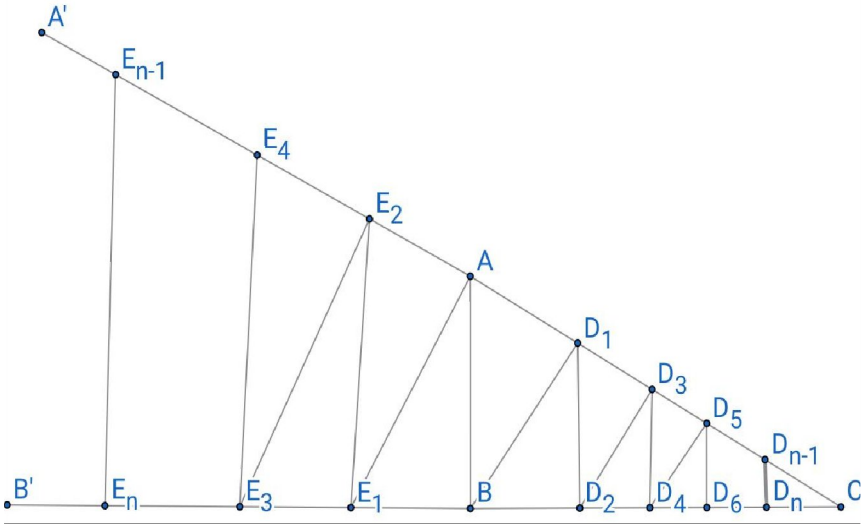

Figure 2 Displaying the construction of $cos^{-n}\ (C)$ to $cos^{n}\ (C)$

Given: Segment lengths a, b, and a unit segment.
Construction: To express x geometrically using a straightedge and compass as given by the equation $a^x = b$, where given $0 < a < 1$ and both a and b are algebraic numbers and $\neq 0, 1$ or $\pm\infty$ and x is not rational, the geometric construction in Figure 2 is drawn as follows:

i. Construct Δ ABC, with base BC, $\angle ABC = \pi/2$, perpendicular segment $AB = 1$. Let $cos(\angle ACB) = a$ or simply $cos(C) = a$ as explained in section 2.1.

ii. Construct segment $BD_1 \perp$ line AC meeting it at D_1. Construct segment $D_1D_2 \perp$ line BC meeting it at D_2. Construct segment $D_2D_3 \perp$ line AC meeting it at D_3. Continue this alternating construction of perpendiculars on lines BC and AC. Let the final segment be $D_{n-1}D_n \perp$ line BC meeting it at D_n. Denote the perpendicular segments BD_1, D_1D_2, D_2D_3,…, $D_{n-1}D_n$ by $p_1, p_2, p_3, \ldots, p_n$.

iii. Similarly, construct a segment $AE_1 \perp$ line CB (extension of line CB) meeting it at E_1. Construct segment $E_1E_2 \perp$ line CA (extension of line CA), meeting it at E_2. Continue constructing perpendiculars alternately on CB' and CA'. Let the final segment be $E_{n-1}E_n$. Denote the perpendicular segment AE_1, E_1E_2, E_2E_3,…, $E_{n-1}E_n$ by $P_1, P_2, P_3, \ldots, P_n$.

iv. Let the m_0th perpendicular be such that $p_{m_0} > b$ and the $(m_0 + 1)$th perpendicular satisfies $p_{m_0+1} < b$.

v. A new relation emerges: $(a)^{\frac{r_0}{q_0}} = \frac{b}{p_{m_0}}$ or $\left(\frac{b}{p_{m_0}}\right)^{\frac{q_0}{r_0}} = a$, where r_0, q_0 are rational quantities such that $r_0 < q_0$. Lengths of b and a are given and the length of the perpendicular p_{m_0} can be measured by a compass.

vi. Repeat the construction of Figure 2 using this new triangle Δ A'B'C' with $cos(\angle A'C'B') = (b/p_{m_0})$, $A'B' = 1$, right angle at B'. Apply the same perpendicular-dropping procedure to extract the next quotient m_1.

vii. Let the m_1th perpendicular be such that $p_{m_1} > a$ and the $(m_1 + 1)$th perpendicular satisfies $p_{m_1+1} < a$.

viii. This yields a new relation $\left(\frac{b}{p_{m_0}}\right)^{\frac{r_1}{q_1}} = \frac{a}{p_{m_1}}$ or $\left(\frac{a}{p_{m_1}}\right)^{\frac{q_1}{r_1}} = \left(\frac{b}{p_{m_0}}\right)$ where r_1, q_1 are rational quantities such that $r_1 < q_1$.

ix. Let the m_2th perpendicular be such that $p_{m_2} > \left(\frac{b}{p_{m_0}}\right)$ and the $(m_2 + 1)$th perpendicular satisfies $p_{m_2+1} < \left(\frac{b}{p_{m_2}}\right)$.

x. The process will continue ad infinitum and

$$x = m_0 + \cfrac{1}{m_1 + \cfrac{1}{m_2 + \cfrac{1}{m_3 + \cdots}}}$$

where $m_0, m_2, m_3, .,$ are positive integers [8].

If $a \to 0$ or $a \to 1$, then the $\angle C \to \pi/2$ or $\angle C \to 0$ and it becomes difficult to draw Δ ABC and perpendiculars on base BC and the hypotenuse. In such cases, write the equation $a^x = b$ as $(a)^{-x} = 1/b$ and locate m_0 so that $P_{m_0+1} > 1/b > P_{m_0}$. Proceed as explained in steps v to x.

2.3. Proof

In Δ ABD_1, $\angle ABD_1 = \angle C$, line segment $AB = 1$, therefore, line segment $BD_1 = \cos(C)$. In

$\Delta BD_1D_2, \angle BD_1D_2 = \angle C$, therefore, line segment $D_1D_2 = BD_1cos(C) = cos^2(C)$. Similarly, line segment $D_2D_3 = cos^3(C)$, line segment $D_3D_4 = cos^4(C),..,$ line segment $D_{n-1}D_n = cos^n(C)$. In the same way, line segment $AE_1 = cos^{-1}(C)$, line segment $E_1E_2 = cos^{-2}(C)$, line segment $E_2D_3 = cos^{-3}(C),..,$ line segment $E_{n-1}E_n = cos^{-n}(C)$.

If we consider cos(C) in our continued fractions, then the length of the first perpendicular BD_1 pertains to power 1 of cos(C), length of second perpendicular D_1D_2 to power 2 of cos(C), length of third perpendicular D_2D_3 to power 3 of cos(C) and in this way, the length of the nth perpendicular $D_{n-1}D_n$ to power n of cos(C).

Similarly, if we consider, $1/cos(C)$ in our continued fractions, then the length of the first perpendicular AE_1 pertains to power 1 of $1/cos(C)$, length of the second perpendicular E_1E_2 to power 2 of 1/cos(C), length of third perpendicular E_2E_3 to power 3 of 1/cos(C) and in this way, length of the nth perpendicular $E_{n-1}E_n$ to power n of 1/cos(C).

If $0 < a < 1$, then according to the construction $a = cos(C)$ otherwise $1/a = cos(C)$. When $p_{m_0} > b$ and $p_{m_0+1} < b$, then b corresponds to the length between p_{m_0} and p_{m_0+1}. In other words, it is a fraction r_0/q_0 more than m_0 where $r_0/q_0 < 1$ so that $x = m_0 + r_0/q_0$ and $a^{m_0+r_0/q_0} = b$ and that yields $a^{r_0/q_0} = b/a^{m_0} = b/p_{m_0}$ or $\left(b/p_{m_0}\right)^{q_0/p_0} = a$ which is again an equation same in structure as $a^x = b$.

Figure 2 is reconstructed but with $cos(C) = b/p_{m_0}$. For this equation also, there are perpendicular segments such that $p_{m_1} > a$ and $p_{m_1+1} < a$. Now $q_0/r_0 = m_1 + r_1/q_1$ resulting in an equation $\left(a/p_{m_1}\right)^{q_1/r_1} = b/p_{m_0}$. The process will continue ad infinitum resulting in continued fractions.

2.3 Explanation and Numerical Illustration

In $a^x = b$, let $0 < a < 1$. In geometric language, referring to Figure 2, which shows successive perpendiculars in a triangle ABC with a right angle at B and base BC, $cos(C) = a$ —Which perpendicular has its length equal to b? If x is an integer, which is easily identifiable by comparing the length $\underline{b}$ with that perpendicular. If x is not an integer, we can always find m_0th and $(m_0 + 1)$the perpendicular such that the length of the xth perpendicular lies between them from the inequalities $p_{m_0} > b$ and $p_{m_0+1} < b$, where p_{m_0} and p_{m_0+1} are lengths of m_0th and $(m_0 + 1)$th perpendiculars. Let r_0/q_0 be such that

$$(a)^{m_0+r_0/q_0} = (b), \tag{2.1}$$

where $r_0/q_0 < 1$ and r_0 and q_0 are positive integers and

$$x = m_0 + \frac{r_0}{q_0}. \tag{2.2}$$

In Equation (2.1), m_0 has already been extracted and r_0/q_0 needs extraction but the perpendicular corresponding to $r_0/q_0 < 1$ does not correspond to a nonzero perpendicular. But q_0/r_0 being more than 1 does correspond to a nonzero perpendicular, hence Equation (2,2) is written

$$x = m_0 + \frac{1}{\frac{q_0}{r_0}}. \tag{2.3}$$

This highlights the continued fraction form leading to the extraction of q_0/r_0 by rewriting Equation (2.1) in exponent q_0/r_0 :

$$f^{\frac{q_0}{r_0}} = g,$$

where $f = b/p_{m_0}$, $g = a$, $p_{m_0} = a^{m_0}$ and values of $\underline{b}$ and a are given, thus facilitating the construction of a right-angled triangle $A'B'C'$ with $cos(C') = f = b/p_{m_0}$ (base p_{m_0} and hypotenuse b). Let m_1th and $(m_1 + 1)$th perpendicular such that the magnitude of the (q_0/r_0)th perpendicular lies between them from the inequalities $p_{m_1} > g$ and $p_{m_1+1} < g$, where p_{m_1} and p_{m_1+1} are lengths of m_1th and $(m_1 + 1)$th perpendiculars. Let r_1/q_1 be such that

$$(f)^{m_1+r_1/q_1} = (g), \quad (2.4)$$

where $r_1/q_1 < 1$ and r_1 and q_1 are positive integers. Thus, the value of an integer m_1 is extracted and the value of $q_1/r_1 > 1$ needs extraction. Consequently, the equation (2.4) takes the form

$$x = m_0 + \frac{1}{m_1 + \frac{1}{\frac{q_1}{r_1}}}.$$

Proceeding in this manner, $m_2, m_3, \ldots, m_j$ can be extracted, yielding

$$x = m_0 + \frac{1}{m_1 + \frac{1}{m_2 + \frac{1}{m_3 + \cdots}}},$$

and the larger the value of j, the more precise the result becomes.

2.3.1 Numerical Illustration

Let the given equation be $2^x = 5$. This can be written $(1/2)^x = (1/5)$ so that we may construct a triangle ABC with base BC, $AB = 1$, angle $B = \pi/2$ and $cos(C) = 1/2$. From geometry, x lies between the 2nd and the third perpendicular, and that makes $m_0 = 2$ and $(1/2)^{2+r_0/q_0} = 1/5$ or

$$x = 2 + \frac{r_0}{q_0} = 2 + \frac{1}{\frac{q_0}{r_0}},$$

since $r_0/q_0 < 1$ and does not correspond to any perpendicular 1, 2, 3,…That needs the extraction of $q_0/r_0 > 1$ and writing $(1/2)^{2+r_0/q_0} = 5$ in terms of the exponent of r_0/q_0 :

$$\left(\frac{1}{5p_2}\right)^{\frac{q_0}{r_0}} = \frac{1}{2},$$

where the magnitude of p_2 is known from the construction. From the comparison of lengths of perpendiculars, it is found that ½ lies between the 3rd and 4th perpendiculars in the triangle with $cos(C') = 1/5p_2$ and that extracts $m_1 = 3$. That yields

$$x = 2 + \frac{1}{3 + \frac{1}{\frac{q_1}{r_1}}},$$

leading to the equation $(1/5p_2)^{3+r_1/q_1} = 1/2$ or

$$\left(\frac{1}{2p_3'}\right)^{q_1/r_1} = \frac{1}{5p_2},$$

where p_3' is the magnitude of the third perpendicular. From the comparison of lengths of perpendiculars, it is found that $1/5p_2$ lies between the 9th and 10th perpendiculars in the triangle with $cos(C'') = 1/5p_2$ and that extracts $m_2 = 9$. That yields

$$x = 2 + \frac{1}{3 + \frac{1}{9 + \frac{1}{\frac{q_2}{r_2}}}}.$$

Stopping at the third stage and neglecting r_2/q_2, x calculates as 2.321428571 whereas the actual x is 2.321928095 within .021 percent. That demonstrates the validity of the method.

2.4. Computation and Construction of $e^x = b$ by Geometric Construction

2.4.1. Computation and Construction of Euler Number e

Euler number is transcendental and not constructible by using a straight edge and compass. However, it can be approximated geometrically using the formula e equals, limit $n \to \infty$, $(1 + 1/n)^n$ or n $\to \infty$, $e = \{n/(1+n)\}^{-n}$. Set $cos(C) = n/(n+1)$ a right-angled triangle ABC can be constructed with base $BC = n$ and hypotenuse $AC = n + 1$ with ∠ACB $\to 0$. Although n $\to \infty$, is not practically feasible; an approximation can be obtained by choosing n as large as permitted by the size of the drawing sheet or the precision of the computing device (if implemented in software).

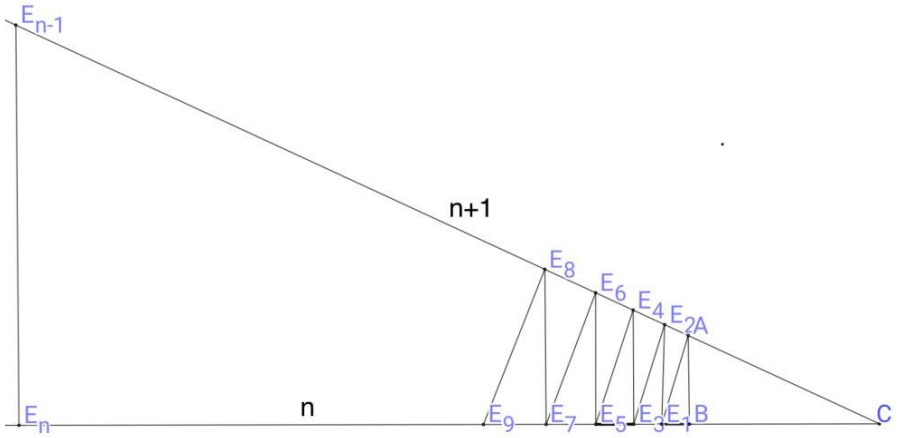

Figure 3 Displaying construction and computation of e

A brief description of the construction is as follows: Referring to Figure 3, construct triangle ABC with $cos(\angle ACB) = n/(n+1)$. From A, drop a perpendicular AE_1 to CB extended, meeting it at E_1. From E_1, drop a perpendicular E_1E_2 to CA extended, meeting it at E_2. From E_2, drop a perpendicular E_2E_3 to CB extended, meeting it at E_3. Continue this process alternately until the nth perpendicular $E_{n-1}E_n$ from E_{n-1} meets CB extended at E_n. From similar triangles ABC, ABE_1, $E_1E_2E_3$ so on, line segment $AE_1 = cos^{-1}(C)$, $E_1E_2 = cos^{-2}(C)$, $E_2E_3 = cos^{-3}(C)$, ..., $E_{n-1}E_n = cos^{-n}(C)$, since line segment $AB = 1$. Therefore, $E_{n-1}E_n = cos^{-n}(C) \approx \{n/(n+1)\}^{-n}$.

2.4.2. Computation and Construction of $e^x = b$

The geometric construction and computation of $e^x = b$ follow the same procedure as that for $a^x = b$ (Sections 2.2 and 2.4), with the following substitutions:

- Replace a by $1/e$,
- Set $cos(\angle ACB) = 1/e$.

Repeating the full details here would duplicate Sections 2.2 and 2.3 in toto and is therefore omitted. For the geometric construction and approximation of Euler's number e, refer to Section 2.4.1 and Figure 3.

3. Comparison With the Euclidean Algorithm

3.1 Euclidean Algorithm

i. The Euclidean algorithm is a general method applicable to fractions r/q where the process of division of q by r is possible and q, r are positive integers.

ii. It divides q by r so that $\frac{q}{r} = m_0 + \frac{r_1}{r} = m_0 + \frac{1}{\frac{r}{r_1}}$. Now r_1 divides r so that $\frac{r}{r_1} = m_1 + \frac{r_2}{r_1} = m_1 + \frac{1}{\frac{r_1}{r_2}}$, thus $\frac{p}{q} = m_0 + \frac{1}{m_1 + \frac{1}{\frac{r_1}{r_2}}}$. Continuing the process, $\frac{q}{r}$ can be written

$$m_0 + \cfrac{1}{m_1 + \cfrac{1}{m_2 + \cfrac{1}{m_3 + \cdots}}},$$

where $m_0, m_2, m_3, ..,$ are positive integers.

iii. The algorithm's applicability is limited to real rational quantities and polynomials. It can be made applicable to other functions when written in polynomials or in numerical values.

3.2 Geometric Method

i. The geometric method is a special method for continued fraction for obtaining the continued fraction of x in the equation $a^x = b$ or equivalently $x = ln(b)/ln(a)$.

ii. It uses the theory that in a right-angled Δ ABC with base BC, $\angle ABC = \pi/2$, perpendicular segment AB=1 if from point B, a perpendicular BD_1 is drawn on line AC, D_1D_2 on BC, D_2D_3 on AC, then $BD_1 = cos(C), D_1D_2 = cos^2(C),\ D_2D_3 = cos^2(C), .., D_{n-1}D_n = cos^n(C)$. Thus, a perpendicular segment denotes to a specific value of k in $cos^k(C)$.The given value of b can then be found to exist between two perpendicular say m_0 and $m_0 + 1$ where $b = m_0 + r_0/q_0$.

iii. Thus b which is a fraction with integer m_0 (quotient) and as r_0/q_0 remainder. It is tantamount to the division of the numerator by the denominator (of b).

iv. Quotient (m_1) and reminder (r_1/q_1) of fraction q_0/r_0 are extracted geometrically by constructing a right-angled triangle with an angle $\angle C$ corresponding to $cos(C) = b/p_{m_0}$. The process is continued.

v. The geometric method is the same in spirit as the Euclidean algorithm, with the difference that it involves exponents and the division takes place geometrically rather than symbolically.

4. Nature of x in $a^x = b$ and $e^x = b$

Lemma 4.1*: (Classical corollary of the Gelfond–Schneider theorem): If x in $a^x = b$ or equivalently $x = ln(b)/ln(a)$, is not rational, and $a > 0$ and $b > 0$ are algebraic with $a \neq 1$, and $b \neq 1$. Then x is transcendental.*

Proof: The following proof is a direct application of the classical Gelfond–Schneider theorem (proved independently by A. O. Gelfond in 1934 and T. Schneider in 1935 [4]. If x is not rational, then there are two remaining possibilities, either x is algebraic, irrational, or transcendental.
Case 1: x is algebraic irrational.

By the Gelfond–Schneider theorem, if a is algebraic with a $\neq 0, 1$ and x is algebraic irrational, then a^x is transcendental [4]. But we are given that b is algebraic, so $a^x = b$ cannot be transcendental. This contradiction shows x cannot be algebraically irrational.

Also x is not rational according to the given condition. Therefore, x must be transcendental. This proves lemma 4.1.

Clarifying remark

The status of results obtained from general operations (addition, subtraction, multiplication, division) on two different transcendental numbers cannot be uniformly determined. However, the imposition of specific conditions that x in $a^x = b$ is not rational, and $a > 0$ and $b > 0$ are algebraic with $a \neq 1$, and $b \neq 1$ makes *x* transcendental as a corollary of Gelfond–Schneider theorem [4].

Lemma 4.2: *Using an unmarked straightedge and compass, let* Δ *ABC be a right triangle with* $\angle ABC = \pi/2$*, base BC, and perpendicular AB = 1. From point B , drop a perpendicular* BD_1 *to hypotenuse AC meeting it at* D_1*. Then, from* D_1*, drop a perpendicular* D_1D_2 *to BC meeting it at* D_2 *; from* D_2*, drop a perpendicular* D_2D_3 *to AC meeting it at* D_3*; and continue this process alternately. Then, for any integers* $n > m > 3$ *and* $p > q > 3$*, the ratio of two transcendental logarithms satisfies*

$$\frac{ln\left(\frac{D_{n-1}D_{n-3}}{D_{m-1}D_{m-3}}\right)}{ln\left(\frac{D_{p-1}D_{p-3}}{D_{q-1}D_{q-3}}\right)} = \frac{n-m}{p-q},$$

Proof: Referring to Figure 2, the segment lengths on the hypotenuse AC are given by:

$$D_{n-1}D_{n-3} = D_{n-2}D_{n-3}sin(C) = sin(C)cos^{n-2}(C),$$

$$D_{m-1}D_{n-3} = D_{m-2}D_{m-3}sin(C) = sin(C)cos^{m-2}(C),$$

Thus,

$$\frac{D_{n-1}D_{n-3}}{D_{m-1}D_{n-3}} = cos^{n-m}(C),$$

Taking the natural logarithm yields:

$$n - m = \frac{1}{ln(cos\, C)} ln\left(\frac{D_{n-1}D_{n-3}}{D_{m-1}D_{n-3}}\right). \quad (4.1)$$

$$p - q = \frac{1}{ln(cos\, C)} ln\left(\frac{D_{p-1}D_{p-3}}{D_{m-1}D_{n-3}}\right). \quad (4.2)$$

Dividing (4.1) by (4.2), we obtain

$$\frac{n-m}{p-q} = \frac{ln\left(\frac{D_{n-1}D_{n-3}}{D_{m-1}D_{m-3}}\right)}{ln\left(\frac{D_{p-1}D_{p-3}}{D_{q-1}D_{q-3}}\right)}, \quad (4.3)$$

although the numerator and denominator of the right-hand side of Equation (4.3) are both transcendental. That proves *Lemma 4.2.*

Remark: By Lemma 4.1, when $x = ln(b)/ln(a)$, is not rational, and a > 0 and b > 0 are algebraic with a $\neq 1$, and b $\neq 1$, then x is transcendental. However, in the present construction, the bases are geometrically related via $a = b^k$ for some integer k , due to the uniform scaling by $cos\, C$. This structural constraint forces the ratio of two transcendental logarithms to be rational — a non-trivial consequence of the geometry. *This rational equality arises purely by construction: the iterative perpendicular process imposes algebraic dependence among the bases via uniform scaling by cos C, independent of general transcendence theory.*

Lemma 4.3 *(Classical corollary of the Lindemann–Weierstrass theorem): If algebraic $b > 0$ is a real algebraic number with $b \neq 1$, then x in $e^x = b$, is transcendental.*
Proof:
The following proof is a direct application of the classical Lindemann–Weierstrass theorem (proved by F. Lindemann in 1882 and generalised by K. Weierstrass in 1885): If α is a non-zero algebraic number, then e^{α} is transcendental.

Suppose x is rational, then $b = e^x$ is transcendental, contradicting to the given statement that b is algebraic. Thus, x can not be rational.

Suppose x is algebraic, since x is a non-zero algebraic number, $e^x$is transcendental (by the Lindemann–Weierstrass theorem), again contradicting that b is algebraic. Thus, x cannot be algebraic. The only remaining possibility is that x is transcendental. This proves Lemma 4.3.

5. Convergence and the Rate of Convergence

It is proved in Section 3 that the continued fraction generated by the geometric method is the standard simple continued fraction of the transcendental number $x = \log_a b$. Since x is irrational (in fact, transcendental by Lemma 4.1), classical theory guarantees that:

i. The value of the continued fraction generated by the extracted quotients converges to *x*. (see [6]).
ii. The error after n steps is less than $1/k_n^2$, where k_n is the denominator (see [6]).
iii. The denominators grow at least exponentially with n, ensuring rapid convergence (see [6]).

These are well-known properties of continued fractions for any irrational number. The novelty of this work lies not in discovering new convergence behaviour, but in constructing the partial quotients geometrically — using only compass and straightedge within a single right triangle. Where the Euclidean algorithm divides numbers symbolically, this method divides exponential scales geometrically, achieving the same mathematical outcome through pure construction.

6. Results and conclusions

The exponentiation of a real quantity a when $0 < a < 1$ i.e. a^x, for $-\infty < x < +\infty$ can be expressed geometrically in the form of $\cos^x(C)$ using a straightedge and a compass. Construct a right-angled Δ ABC, with base BC, $\angle ABC = \pi/2$, and perpendicular line segment AB=1. Let $\cos(ACB) = a$. Successive perpendiculars are drawn on base BC and hypotenuse AC. Denote $BD_1, D_1D_2, D_2D_3, ..$, as first, second, third perpendicular... with lengths $p_1, p_2, p_3, ...$, then $cos^x(C) = a^x = p_x$.

If x is not an integer, suppose it lies between m_0, and $m_0 + 1$ where m_0 is an integer. This can be detected when the magnitude of b in the equation $a^x = b$ satisfies $p_{m_0} < b < p_{m_0+1}$. This identifies m_0. Now consider $x = m_0 + r_0/q_0$, where the fraction $r_0/q_0 < 1$. Then $a^{m_0+r_0/q_0}=b$ or

$$(p_{m_0} a^{r_0/q_0}) = b$$

or

$$\left(b/p_{m_0}\right)^{q_0/r_0} = a.$$

This equation is analogous to $a^x = b$. The integer m_1 in the equation $q_0/r_0 = m_1 + r_1/q_1$ can be found using the same process as for m_0. Similarly, m_2, m_3, m_4 can be extracted, resulting in transcendental

$$x = m_0 + \cfrac{1}{m_1 + \cfrac{1}{m_2 + \cfrac{1}{m_3 + \cdots}}},$$

where $m_0, m_1, m_2, ..$ are positive integers including zero. This continued fraction is infinite and non-terminating [8]. Therefore, the value of the transcendental x can only be approximated by truncating the fraction at a finite number of terms, according to the desired precision. Thus, the geometric construction extracts the terms of the continued fraction and approximates the transcendental value but fails to yield its exact value. Like all other methods, it is a method of approximation.

We demonstrate how approximation is done in [S1]. In summary, for determining *x* by continued fraction, both *a* and *b* are assumed to satisfy $0 < a < 1$ and $0 < b < 1$. The interactive figure displays the values of m_0, m_1 and m_2 for the continued fraction $x = m_0 + \frac{1}{m_1 + \frac{1}{m_2 + \ddots}}$, where $x = \frac{ln(b)}{ln(a)}$. Writing $x_0 = m_0, x_1 = m_0 + \frac{1}{m_1}$, $x_2 = m_0 + \frac{1}{m_1 + \frac{1}{m_2}}$, and letting $k_0 = 1$ the denominator of x_0, $k_1 = m_1$ the denominator of x_1, and $k_2 = m_1 m_2 + 1$ the denominator of x_2 and actual $x = \frac{ln(b)}{ln(a)}$, it can be observed numerically from the interactive figure, in agreement with the known bounds for continued fractions, that $|x - x_0| < \frac{1}{k_0^2}$, $|x - x_1| < \frac{1}{k_1^2}$ and $|x - x_2| < \frac{1}{k_2^2}$. It can further be observed that k_n grows exponentially with n, ensuring rapid convergence of the continued-fraction approximation.

The interactive file not only provides continued fractions approximations for $a^x = b$ (equivalently $x = \ln(b)/\ln(a)$, but also stimulates curiosity and a sense of wonder, showing how calculations that normally require logarithmic tables or calculators can be performed geometrically using right-angled triangles and perpendiculars. Observing this simple yet revealing method encourages one to explore whether the same approach can be applied to other problems, thereby planting the seed for further investigation and research.

7. Supplementary Electronic Material

[S1] An interactive HTML file.

8. References

[1] Dennis, D., Cinfrey, J.: Deriving logarithmic and exponential curves with the computer software Geometer's Sketchpad: A method inspired by historical sources. In: King, J., Schattschneider, D. (eds.) Geometry Turned On: Dynamic Software in Learning, Teaching and Research, pp. 147–156. Mathematical Association of America, Washington D.C. 1997.

[2] Descartes, R.: The Geometry of René Descartes. Translated by Smith, D.E., Latham, M.L. Open Court Publishing Company, Chicago, 1925.

[3] Dummit, D.S., Foote, R.M.: Abstract Algebra, 3rd edn. Wiley, New York, 2004, pp. 270–271. ISBN: 978-0-471-43334-7.

[4] Gelfond, A.O.: Transcendental and Algebraic Numbers. Dover Publications, New York

[5] Karpenkov, O.N.: Geometry of Continued Fractions. Springer, Cham, 2022. https://doi.org/10.1007/978-3-030-95266-4.

[6] Khinchin, A.Ya.: Continued Fractions, 3rd edn. University of Chicago Press, Chicago, IL 1964. Translated from the Russian by Scripta Technica, Inc.

[7] Knuth, D.E.: The Art of Computer Programming, Volume 2: Seminumerical Algorithms, 3rd edn. Addison–Wesley, Boston,1997. ISBN: 0-201-89684-2.
[8] Wadhawan, N.K.: Scientific Calculator with the Aid of Geometry and Based upon it a Mechanical Calculator. In: Science and Technology Journal, vol. 11, no. 2, pp. 1–13. 2023. [DOI: 10.22232/stj.2023.11.02.02.